La Relatività Generale per la dinamica galattica e confronto con gli approcci (L)CDM e MOND attraverso l'astrometria di alta accuratezza della missione Gaia

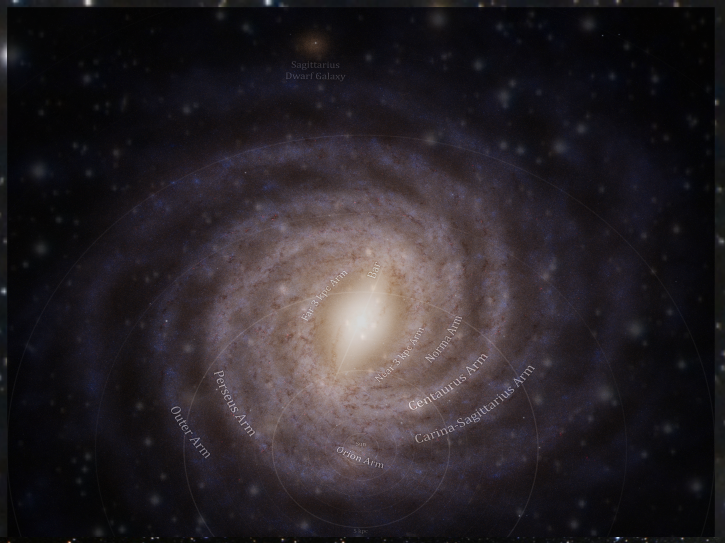

Giornata di Studi sulla Gravità
10 Ottobre 2025
LNSG

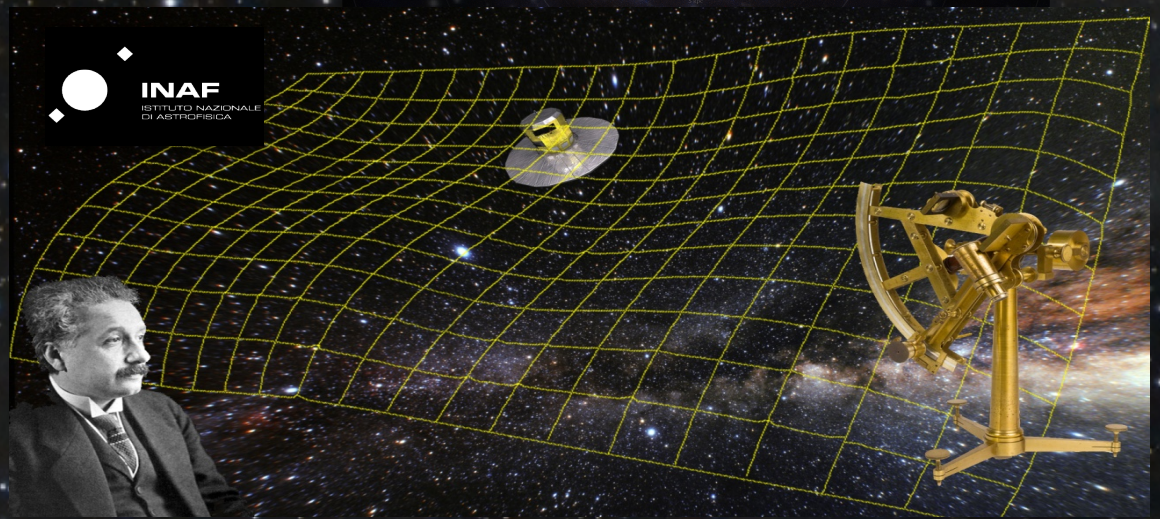

Mariateresa Crosta, INAF-OATo

Collaborators:

W.Beordo, B. Bucciarelli, Mario G. Lattanzi, P. Re Fiorentin, A. Spagna, E. Poggio (INAF-OATo)
V. Akhmetov (INAF-OATo, Kharkiv Obs.), M. Bruni (Portsmouth University), S. Cacciatori (Uninsubria)

Talk outline

Background

- Motivation: Astrometry from Hipparcus to Einstein, Gaia
- Relativistic/Gravitational Astrometry

Challenging the Galactic Models with Milky Way stars

- Local cosmology as ΛCDM laboratory
- Testing General Relativity/Gravity @MilkyWay scale
- Dark Matter interpretation in GR
- Simulations of ΛCDM model predictions @MilkyWay scale

Talk outline

Background

- Motivation: Astrometry from Hipparcus to Einstein, Gaia
- Relativistic/Gravitational Astrometry

Challenging the Galactic Models with Milky Way stars

- Local cosmology as ΛDCM laboratory
- Testing General Relativity/Gravity @MilkyWay scale
- Dark Matter interpretation in GR
- Simulations of ΛCDM model predictions @MilkyWay scale

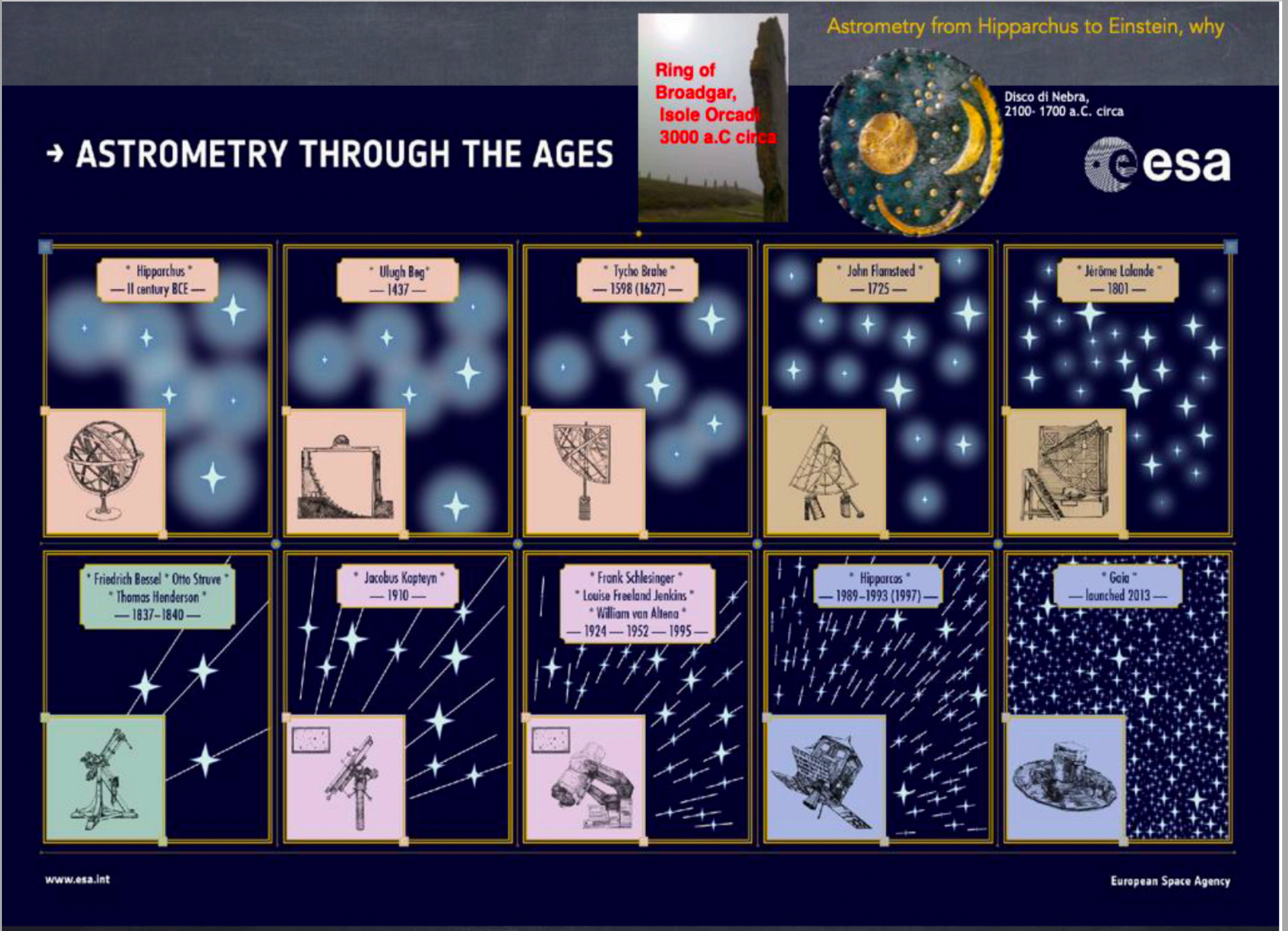

Astrometry is the ancient branch of Astronomy dedicated to the fundamental question: What is our place in the Universe?

-> measurements of the star positions and their movements in the Universe.

It acquires knowledge through the analysis of photons received over time from all sorts of celestial sources at the observer location.

Gaia measures at L2 of the Earth-Sun system position (direction and distance) and velocity of almost 2 billion objects with an accuracy of up to 1 microarcsecond

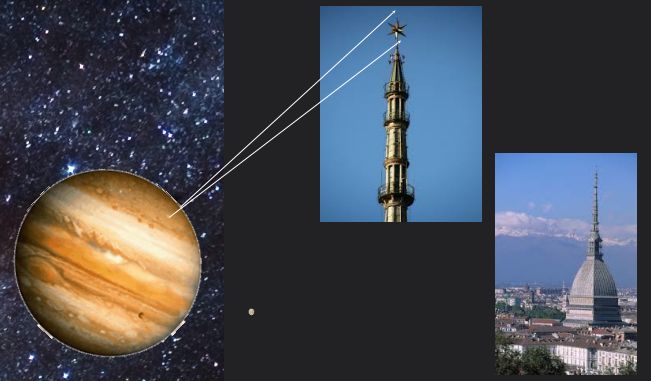

0”,000001 = micro(μ) arc sec

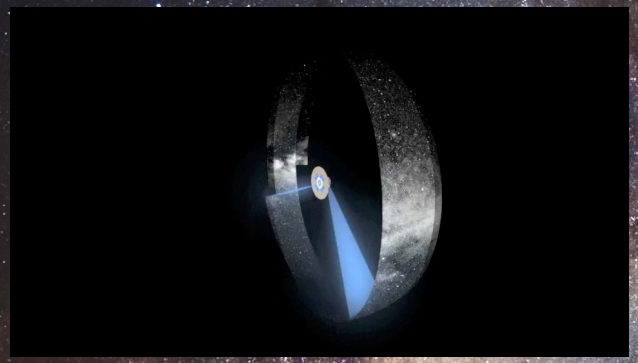

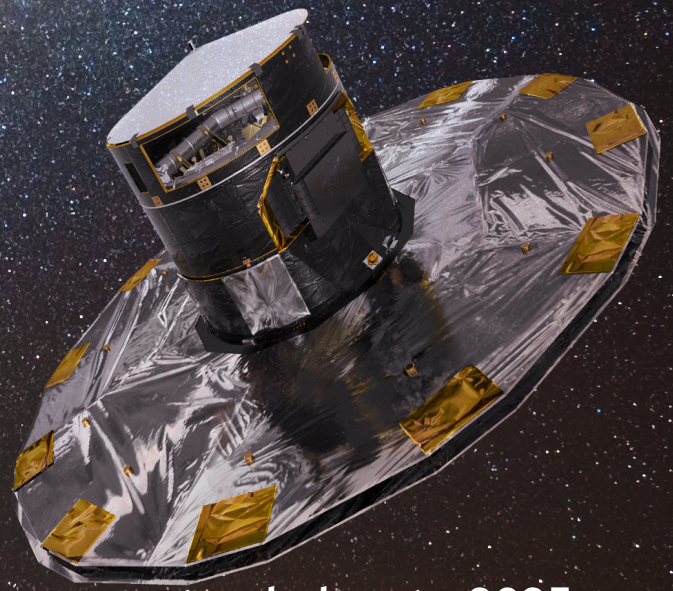

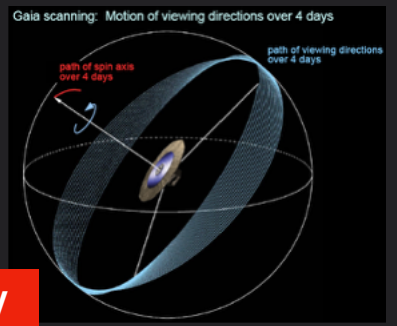

2FOV

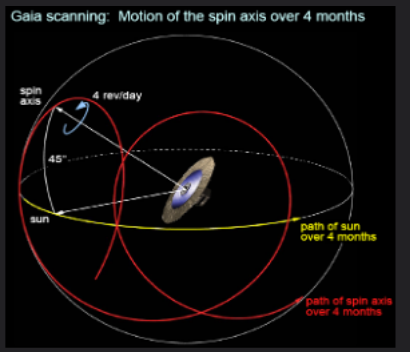

sky coverage with precession at fixed angle to the Sun

ESA mission launched in 2013, nominal lifetime 5 years, extended up to 2025

The location of an object in astrometry is considered reliable if its relative error is less 10%

parallax $\pi(\text{arcsec}) \approx 1(\text{UA})/\text{d}^*(\text{pc})$

Hipparcos $\sigma_\pi = 1 \text{ mas} = 10^{-3}\text{arcsec}$

Gaia $\sigma_\pi = 10\ \mu\text{as} = 10^{-5}\text{arcsec}$

$\pi \approx \sigma_\pi \cdot 10$

d* = 100 pc

d*= 10 kpc

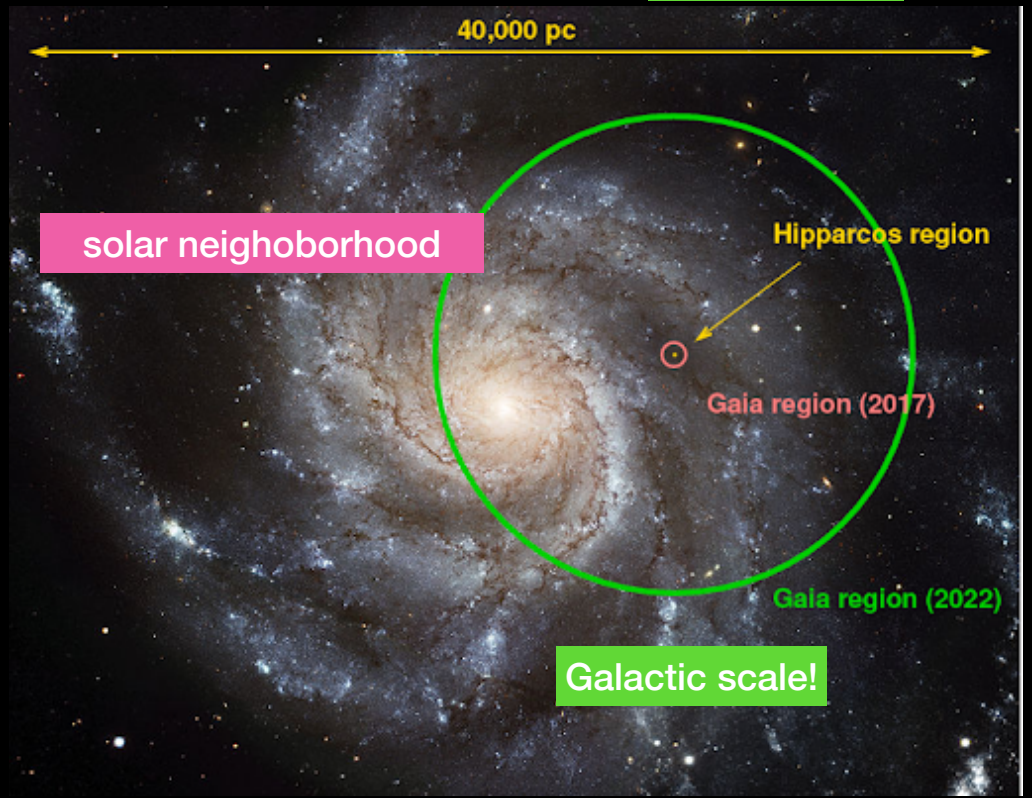

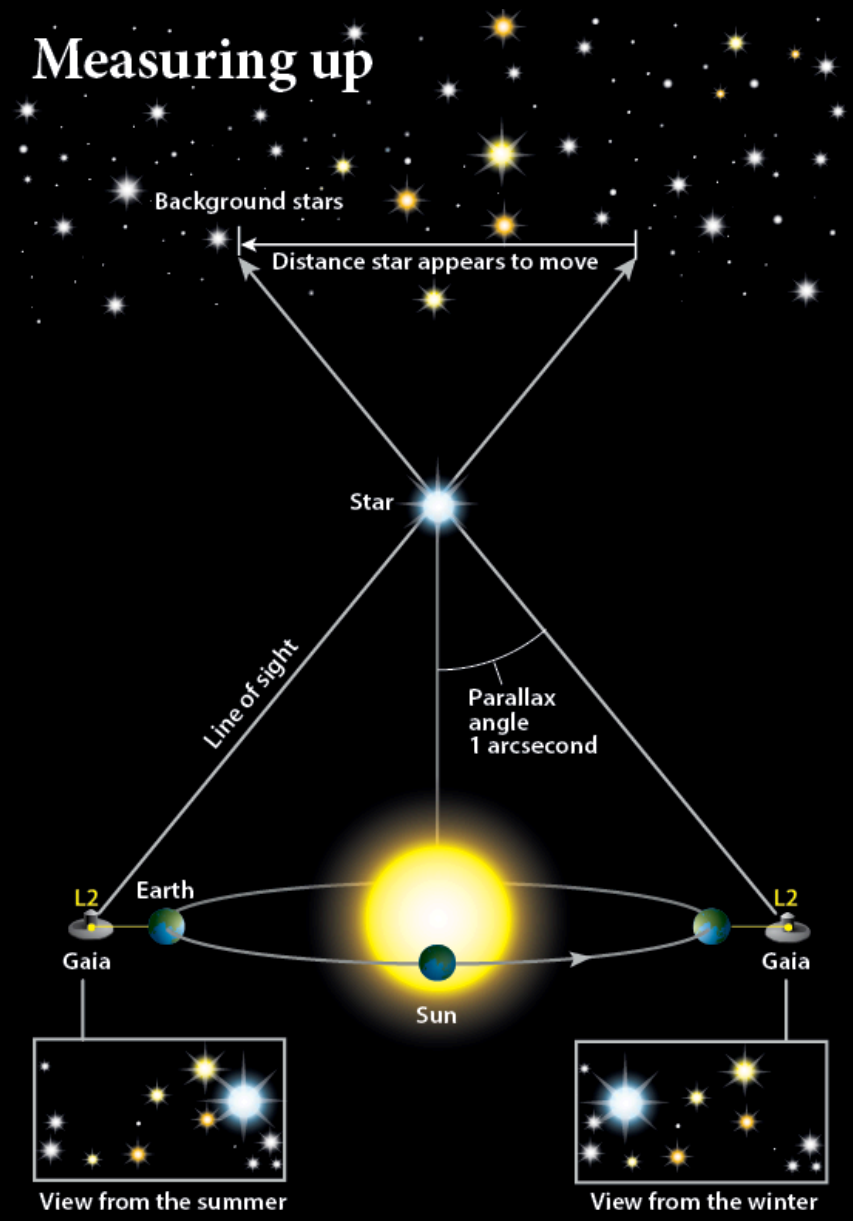

To understand the distances between stars, astronomers rely on a method called parallax. By measuring the distances stars appear to move relative to other stars, astronomers can gauge how far away they are from us and from each other. ASTRONOMY: ROEN KELLY

esa

→ GAIA: THE GALACTIC CENSUS TAKES SHAPE

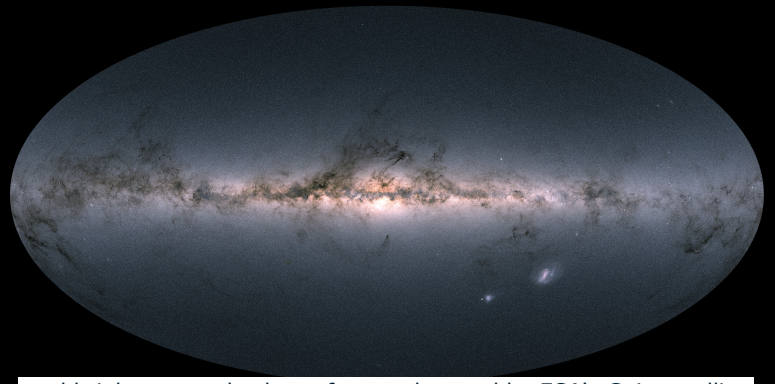

total brightness and colour of stars observed by ESA's Gaia satellite

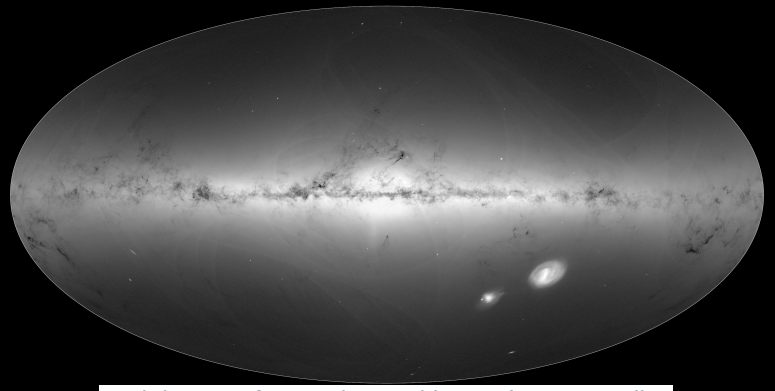

total density of stars observed by ESA's Gaia satellite

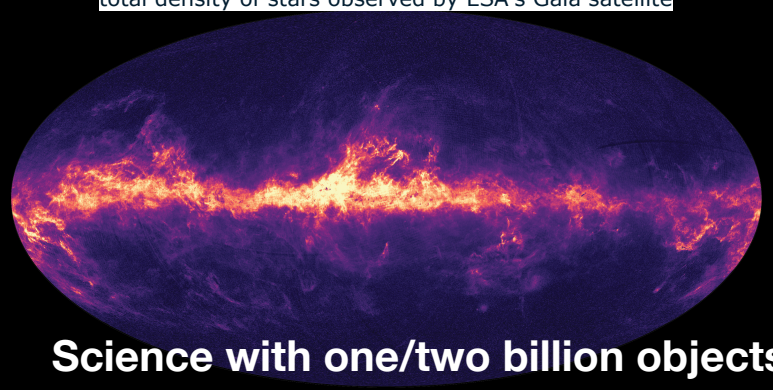

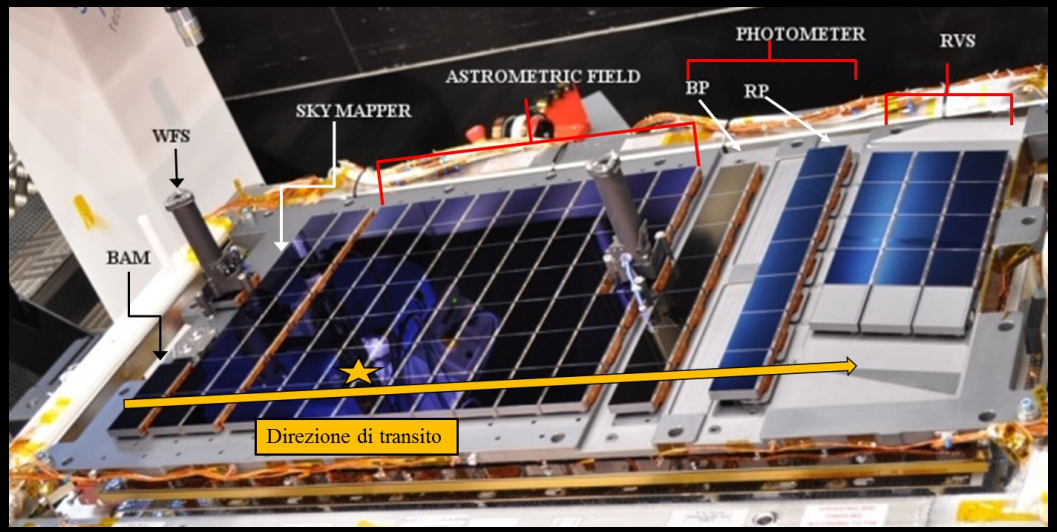

Astrometry
positions
proper motions
parallaxes

end-of-mission astrometric accuracies better than 5-10μas (brighter stars)
130-600μas (faint targets)

Photometry
spectral classification
photometric distances
brightness
temperature
mass
age
chemical composition

G < 20.7 mag

Spectrometry
radial velocity
chemical abundances

G_RVS= 16.2

Science with one/two billion objects in 3D, from structure and evolution of the Milky Way to GR tests

Gaia’s first look into the Milky Way, DR1

observations collected during the first 14 months of Gaia's routine operational phase

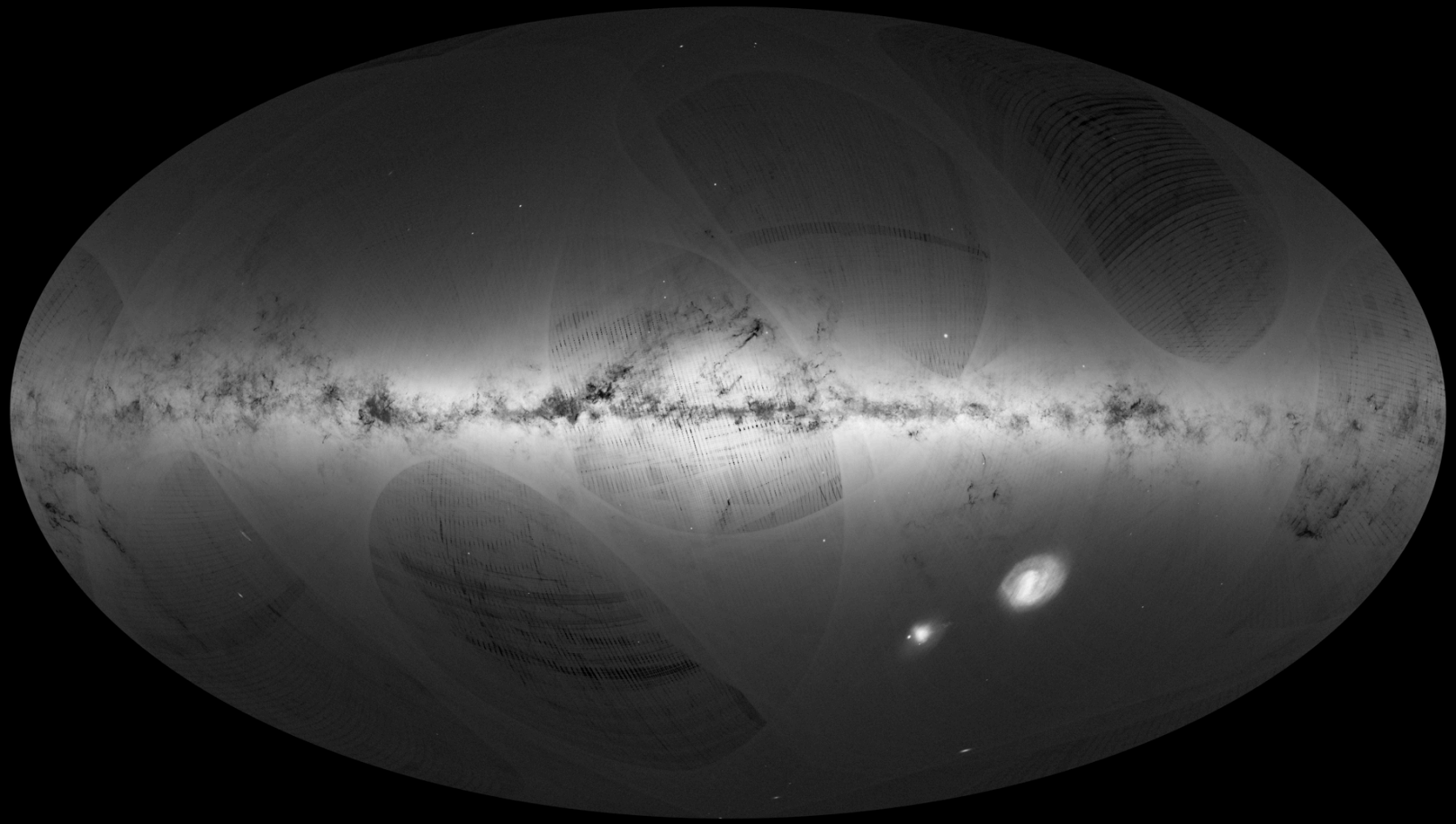

http://www.cosmos.esa.int/web/gaia/science

THE HERTZSPRUNG-RUSSELL DIAGRAM

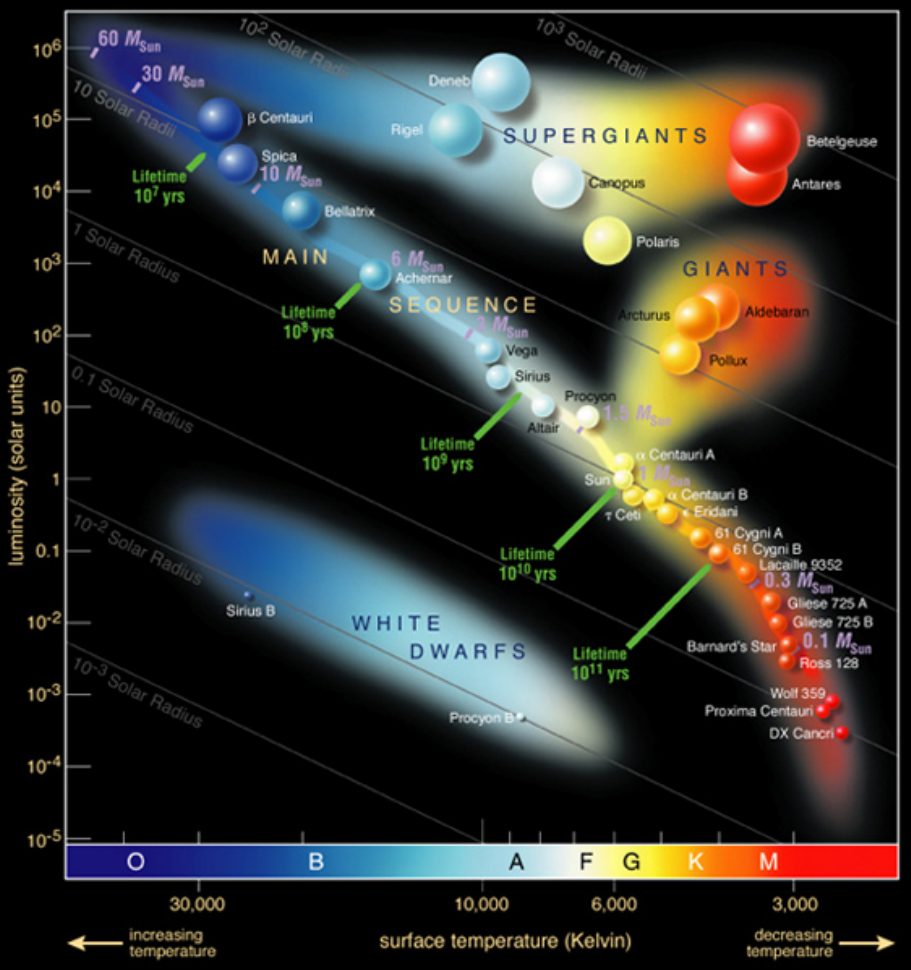

Hipparcos HRD (10^5 stars to 0.1 kpc)

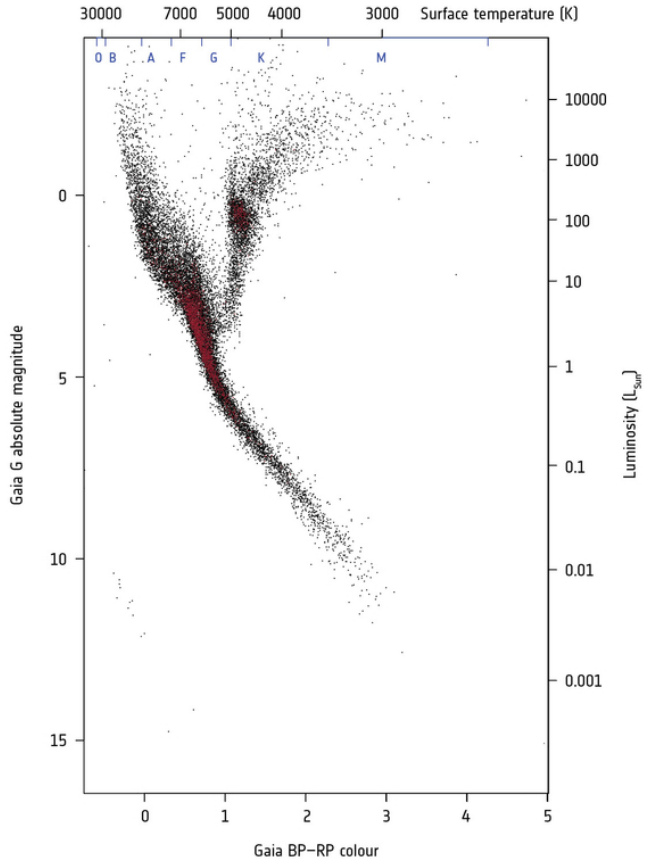

→ GAIA'S HERTZSPRUNG-RUSSELL DIAGRAM

(5 10^6 stars to 1.5 kpc)

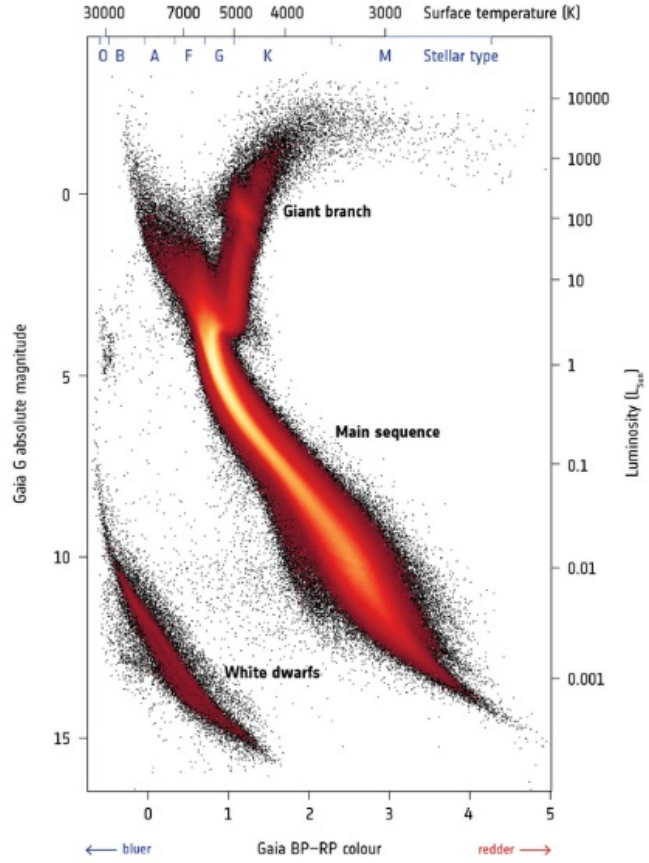

(GDR2)

Stellar density from the full Gaia DR3

based on data collected between 25 July 2014 and 28 May 2017, spanning a period of 34 months

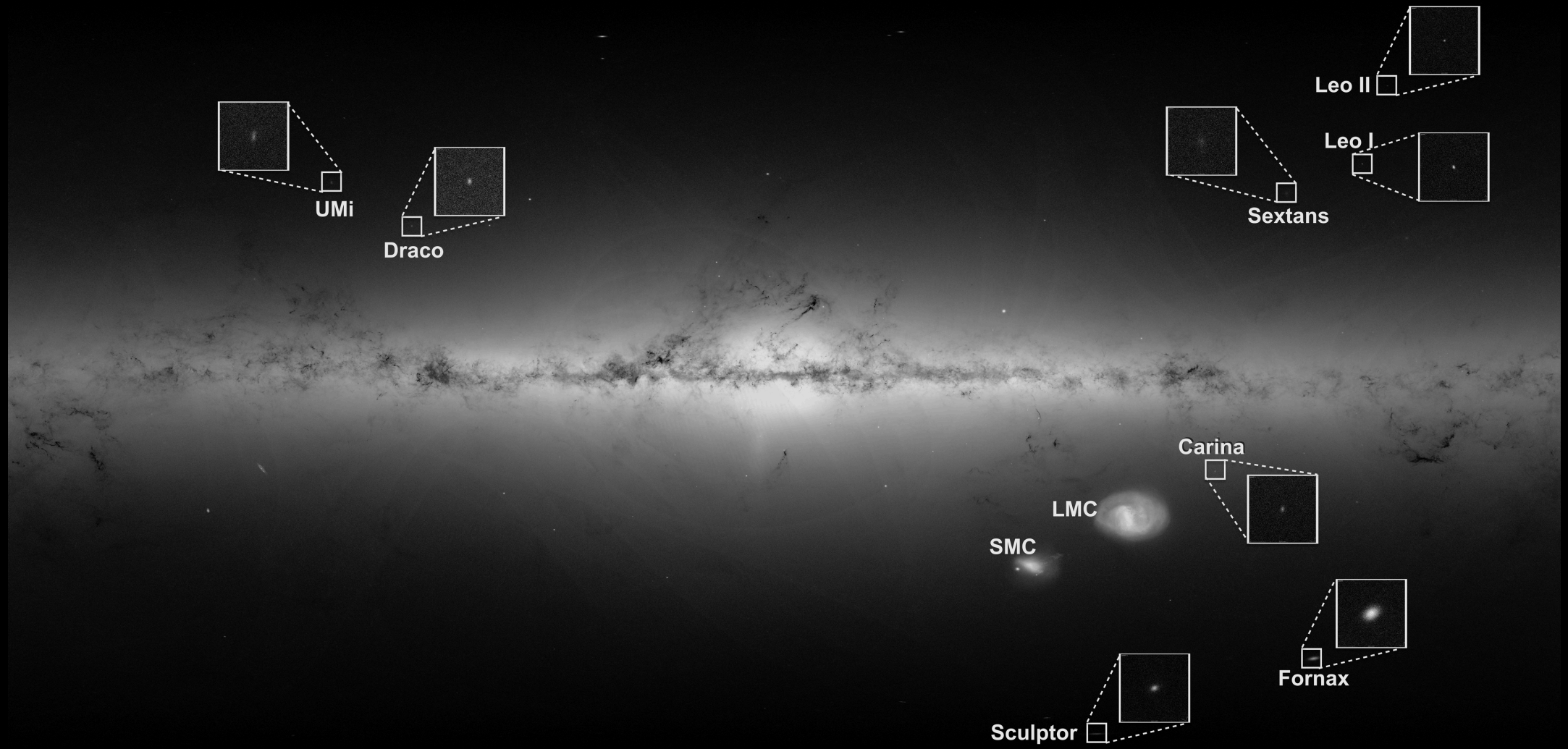

Source count maps based on the Gaia DR3 data.
Image credit: ESA/Gaia/DPAC
Image license: CC BY-SA 3.0 IGO

Acknowledgement: Images were created by André Moitinho and Márcia Barros, University of Lisbon, Portugal

https://www.esa.int/Science_Exploration/Space_Science/Gaia

Credit: ESA/Gaia/
DPAC, CC BY-SA
3.0 IGO.

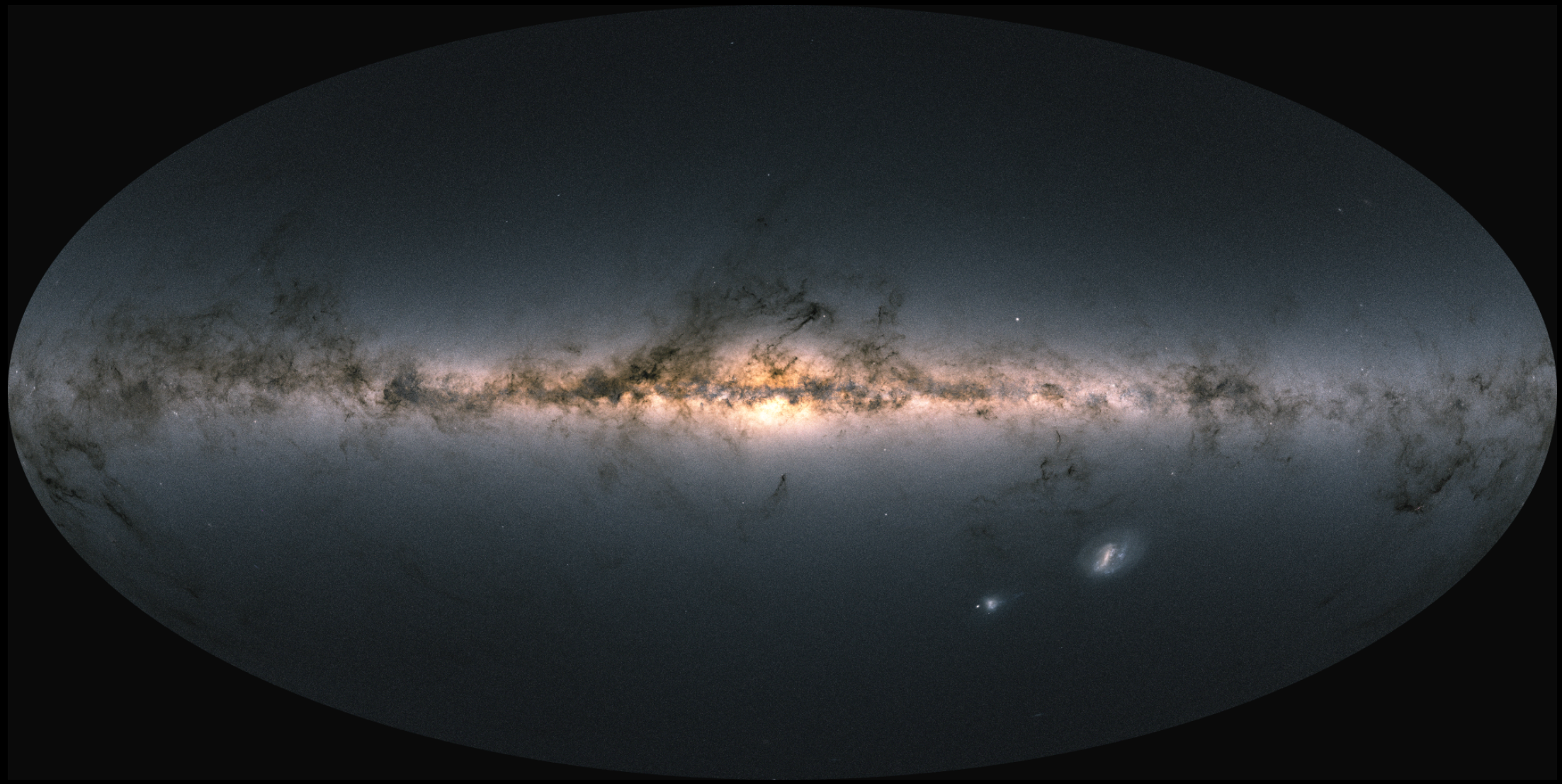

Gaia Data Release 3

https://www.cosmos.esa.int/web/gaia/data-release-3

OUTSIDE OUR GALAXY

esa

Unlike other missions that target specific objects, ESA's Gaia is a survey mission. This means that while surveying the entire sky multiple times, it is bound to see objects outside the Milky Way as well, such as quasars and other galaxies. Gaia's data release 3 provides astronomers with details on a few million extragalactic objects.

1.9 million quasars

Supermassive black holes accreting matter

Redshift | Brightness | Colour

Host galaxy detected for 60 thousand quasars

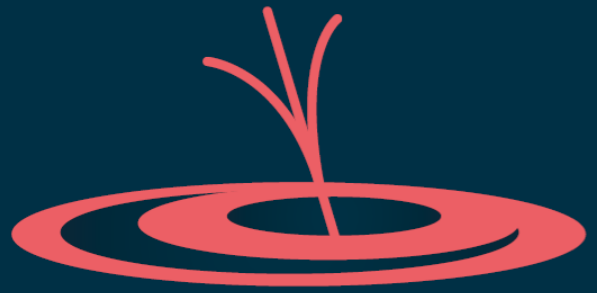

2.9 million galaxies

Brightness | Colour

Star formation history | Shape

Next Gaia DR4 (based on 66 months of data) by the end of 2026 will be consisting of:

- Full astrometric, photometric, and radial-velocity catalogues
- All available variable-star and non-single-star solutions
- Source classifications (probabilities) plus multiple astrophysical parameters (derived from BP/RP, RVS, and astrometry) for stars, unresolved binaries, galaxies, and quasars
- An exoplanet list
- **All epoch and transit data for all sources**!

Gaia DR5 (based on all mission data) not before the end of 2030 will be consisting of **Complete Gaia Legacy Archive of all data**

Data Release Scenario http://www.cosmos.esa.int/web/gaia/release

SKY-SCANNING COMPLETE FOR ESA'S MILKY WAY MAPPER GAIA

From 24 July 2014 to 15 January 2025, Gaia made more than three trillion observations of two billion stars and other objects, which revolutionised the view of our home galaxy and cosmic neighbourhood.

3 TRILLION
Observations

2 BILLION
Stars & other objects observed

938 MILLION
Camera pixels on board

15 300
Spacecraft 'pirouettes'

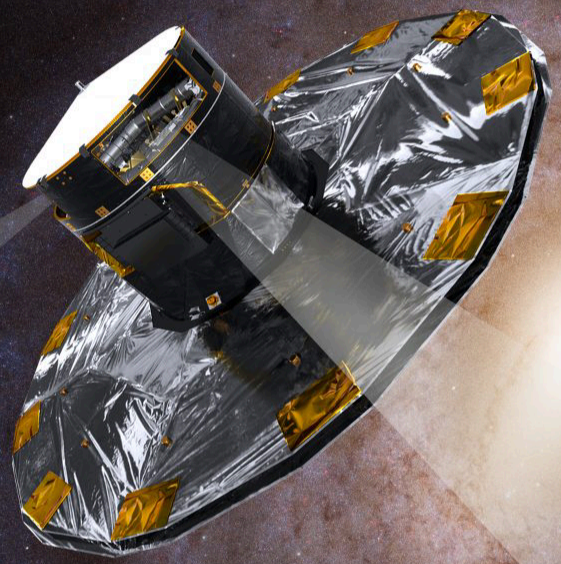

580 MILLION
Accesses of Gaia catalogue so far

13 000
Refereed scientific publications so far

2.8 MILLION
Commands sent to spacecraft

142 TB
Downlinked data (compressed)

500 TB
Volume of data release 4
(5.5 years of observations)

55 KG
Cold nitrogen gas consumed

3827
Days in science operations

50 000 HOURS
Ground station time used

Crosta - LNGS- 10 Ottobre

RELATIVISTIC MODEL OF THE OBSERVER AND THE OBSERVABLES

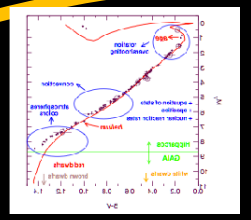

High accurate calibration for all spectral classes the most important of the HR diagram; tens thousands of brown and white dwarfs

Distance scale

2,000 fully reconstructed systems (orbits and masses) around FGK stars; expected new planets around M dwarfs

Cosmology at zero redshift

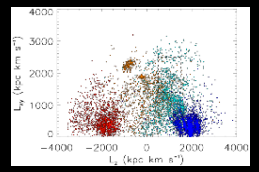

The structure of the halo

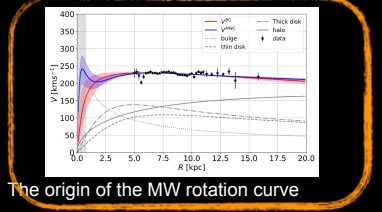

The origin of the MW rotation curve

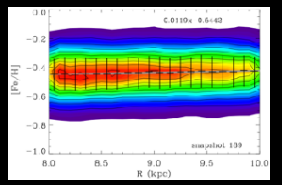

Gradients of cosmological origin in the thick disk

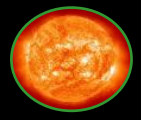

< 650 ly

< 70 UA

Comparison of simulations (L) CDM on the scale of the Milky Way with the data of Gaia

Distance from the Sun

<33,000 ly

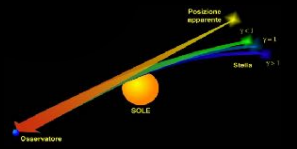

Testing light bending properties of matter

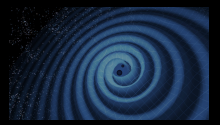

Gravitational waves

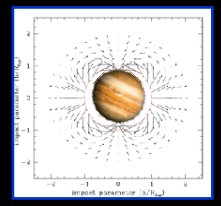

Challenge to Einstein's theory and the standard cosmological model

Beyond General Relativity

✓GR tests from Solar System to Milky Way scales

From Relativistic Astrometry to Gravitational Astrometry:
data interpretation, the impact of GR models for Fundamental Physics/ Local Cosmology

Talk outline

Background

- Motivation: Astrometry from Hipparcus to Einstein, Gaia
- Relativistic/Gravitational Astrometry

Challenging the Galactic Models with Milky Way stars

- Local cosmology as L-DCM laboratory
- Testing General Relativity/Gravity @MilkyWay scale
- Dark Matter interpretation in GR
- Simulations of ΛCDM model predictions @MilkyWay scale

Astrometry nowadays is dominated by Einstein's theory

Stars belong to the architecture of spacetime which is dictated by the Einstein equations

Classical Astrometry

$\alpha,\delta,\mu_\alpha,\mu_\delta,\pi,\ldots$

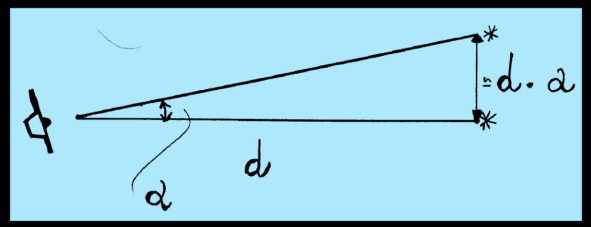

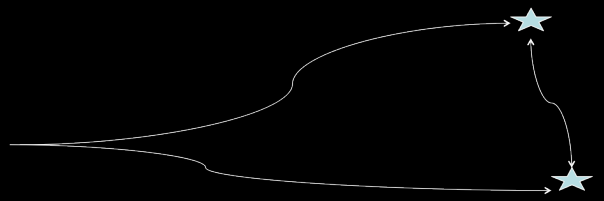

increasingly accurate astronomical data

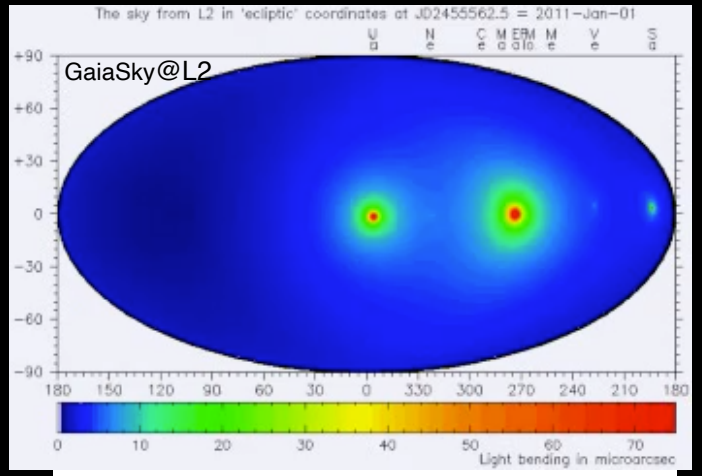

micro-arcsecond accuracy + Solar System gravitational fields => relativistic models for the light-ray propagation, from the observer to the star

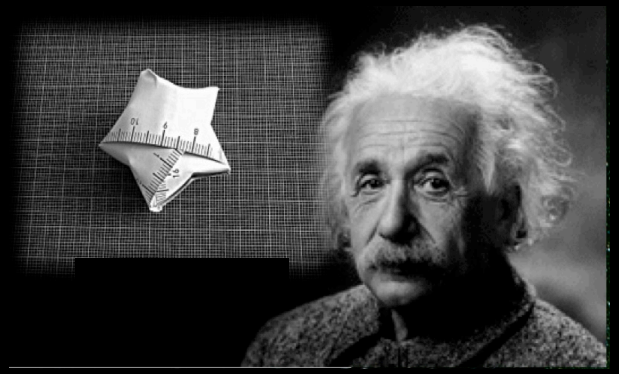

Relativistic Astrometry

theoretical, analytical and/or numerical models, completely based on General Relativity and relativistic attitude (satellite or ground based observers)

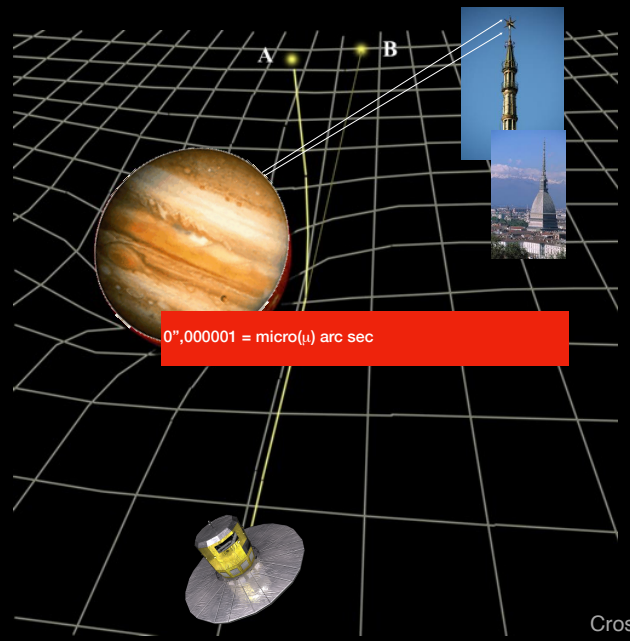

Gaia: the Era of Relativistic Astrometry

the trajectories of photons emitted by the stars
- null geodesics -

should be as fundamental as
the equation of stellar evolution!

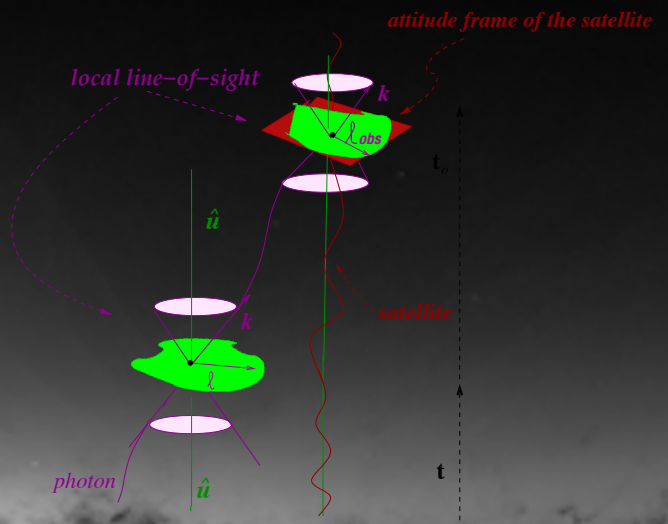

Source count maps based on the Gaia DR3 data.
Image credit: ESA/Gaia/DPAC
Image license: CC BY-SA 3.0 IGO

Acknowledgement: Images were created by André Moitinho and Márcia Barros, University of Lisbon, Portugal

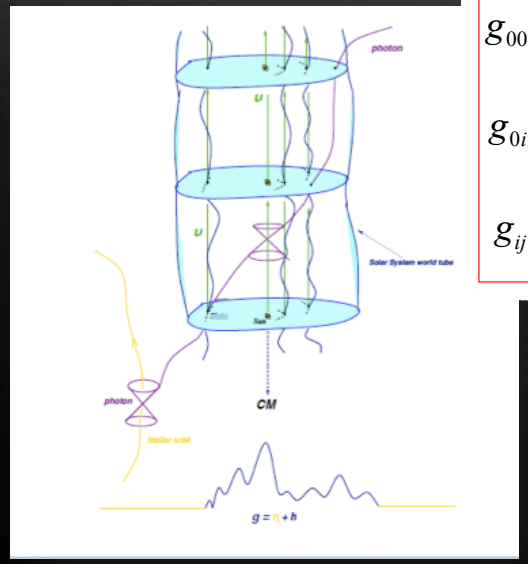

$$g_{00} = -1 + \frac{2}{c^2} w(t,\boldsymbol{x}) - \frac{2}{c^4} w^2(t,\boldsymbol{x}) ,$$

$$g_{0i} = -\frac{4}{c^3} w^i(t,\boldsymbol{x}) ,$$

$$g_{ij} = \delta_{ij} \left(1 + \frac{2}{c^2} w(t,\boldsymbol{x}) \right) .$$

Ephemeris **Relativistic Astrometry**

Used to describe the motion of celestial bodies and the light propagation

IAU metric for the definition of the Celestial Coordinate Systems (BCRS)

M.Crosta. "Astrometry in the 21st century. From Hipparchus to Einstein" La Rivista del Nuovo Cimento 42 (2019)

M. Crosta et al. "General relativistic observable for gravitational astrometry in the context of the Gaia mission and beyond" PRD 96 (2017)

Light crossing a weak field "geometry"

$$g_{\alpha\beta} = \eta_{\alpha\beta} + h_{\alpha\beta} + O(h^2)$$

$$|h_{\alpha\beta}| \ll 1$$

according to the Virial Theorem

$$|h_{\alpha\beta}| \leq U/c^2 \sim v^2/c^2$$

$$k^\alpha k_\alpha = 0, \qquad \frac{dk^\alpha}{d\lambda} + \Gamma^\alpha_{\rho\sigma} k^\rho k^\sigma = 0$$

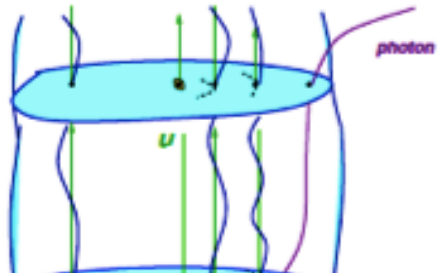

ε ~ v^2/c^2 ~ GM/rc^2 ~ mas accuracy

which requires determination of

g_{oo} even terms in ε, lowest order ε^2~mas

g_{oj} odd terms in ε, lowest order ε^3~μ-as

g_{ij} even terms in ε, lowest order ε^2~mas

Time variation of the order of $\epsilon|h_{\alpha\beta}|$

IAU metric for celestial reference system!

Body	$\delta\alpha_M$ (μas)	$\delta\alpha_Q$ (μas)
Sun	1.75×10^6	~1
Mercury	83	
Venus	493	
Earth	574	0.6
Moon	26	
Mars	116	0.2
Jupiter	16270	240
Saturn	5780	95
Uranus	2080	8
Neptune	2533	10

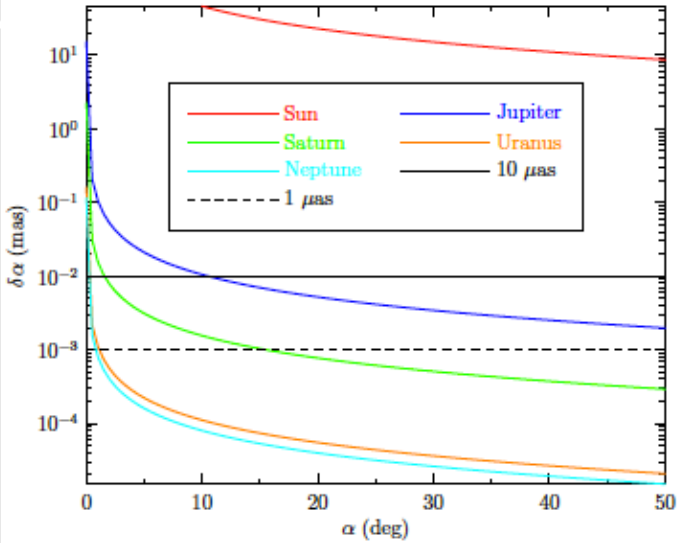

Angular separation from the perturbing body

In relativistic astronomy

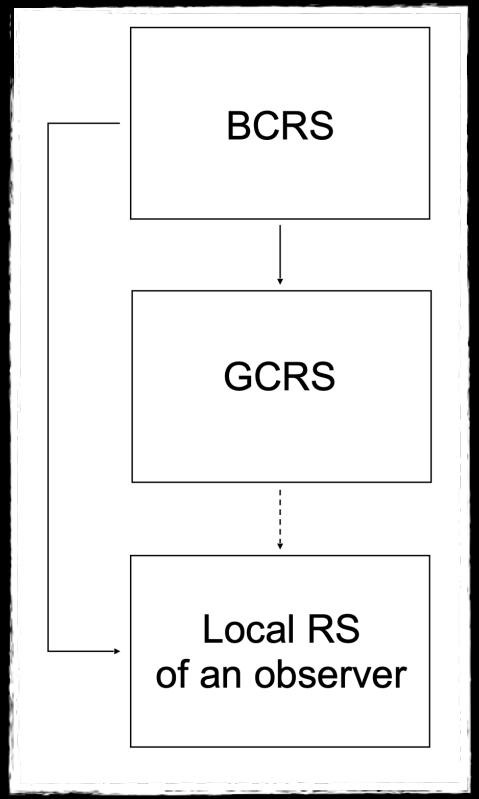

- BCRS (Barycentric Celestial Reference System)

  (x^i,t) global coordinates

- GCRS (Geocentric Celestial Reference System)

  (X^i,T) local coordinates

- Local Reference system of an observer

All these reference systems are defined by the form of corresponding metric tensor

Relationship between the global and local set of coordinates are given by the following mapping

$$x^{\mu}(cT_{(a)}, X^{i}_{(a)}) = z^{\mu}_{(a)}(cT_{(a)}) + e^{\mu}_{i}(cT_{(a)})X^{i}_{(a)} + O[(X^{i}_{(a)})^2],$$

triad of spacelike vectors (i = 1, 2, 3) undergoing some geometric transport along the body worldline

quadratic terms in the local space coordinate

Post-Newtonian & Minkowskian approximations

Post-Minkowskian approx. $h_{\mu\nu} = \sum G^n h^{(n)}_{\mu\nu}$ "absolute space-time"

Post-Newtonian approx. $h_{\mu\nu} = \sum \frac{1}{c^n} h^{(n)}_{\mu\nu}$ "absolute space and absolute time"

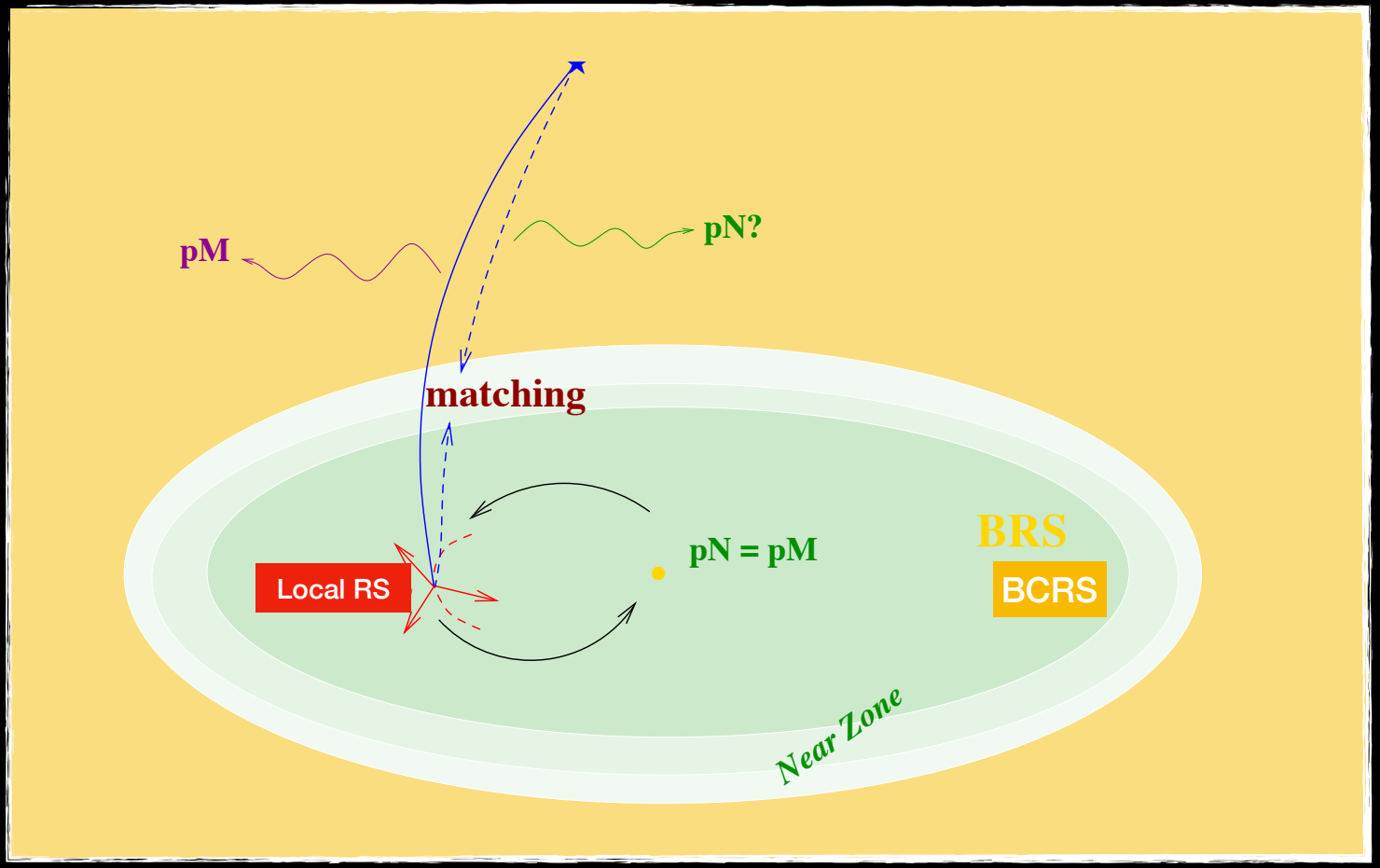

The (Celestial) Sphere Reduction/Reconstruction is Gaia's primary objective

first direct materialization of a dense absolute reference frame at visual bands

one of the most important fundamental physics task

quasi-inertial kinematically non-rotating global **optical** frame meeting the ICRS prescriptions/IAU recommendations

Credits:
ESA/Gaia/DPAC

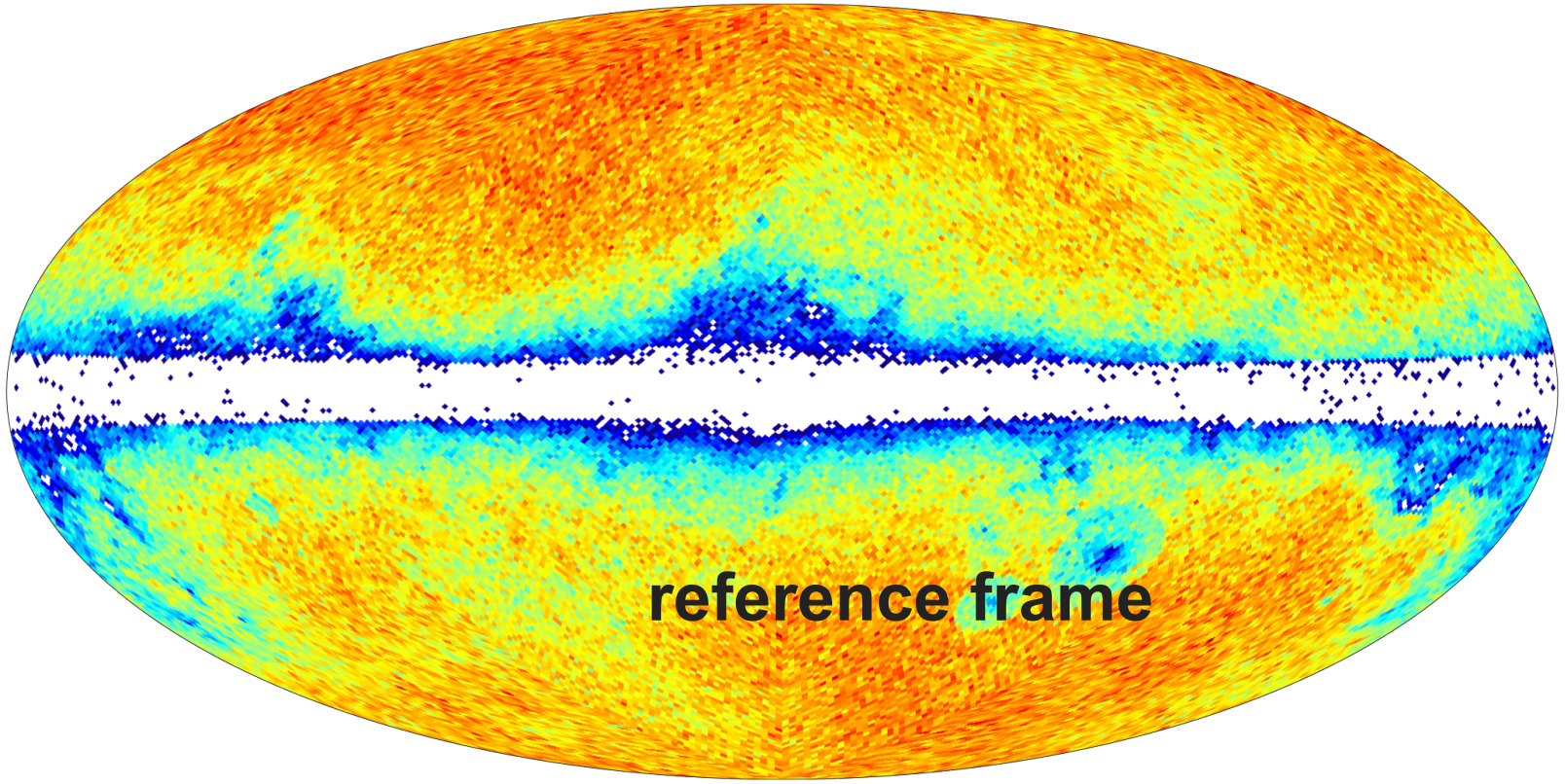

the Consortium constitued for the Gaia data reduction (DPAC) agreed to set up, respectively, two independent global sphere solutions: AGIS and **GSR**

TASK:

link of the optical to the radio reference frame

2 independent GR models:

GREM (**Gaia RElativistic Model**)

RAMOD (**Relativistic Astrometric MODel**)

Gaia, the ESA cornerstone mission, is a wide European effort involving almost 450 scientists

All Gaia operations activities (daily and cyclic) done in Italy are implemented at the DPCT, the Italian provided HW and SW operations system designed, built and run by ALTEC (To) and INAF-OATo for ASI.

This is the only Data Processing Center, among the six DPCs across Europe, which specializes in the treatment and validation of the satellite astrometric data -> **a big archive of raw data to exploit**!

Size at completion ~ 2 PB

The DPCT hosts the systems of the Astrometric Verification Unit (AVU), run by ALTEC (To) under the scientific supervision of the astrometric group INAF-OATo for ASI

AVU is in charge, for DPAC, of the verification, through the Global Sphere Reconstruction (GSR), of the absolute astrometry achieved through the baseline astrometric model

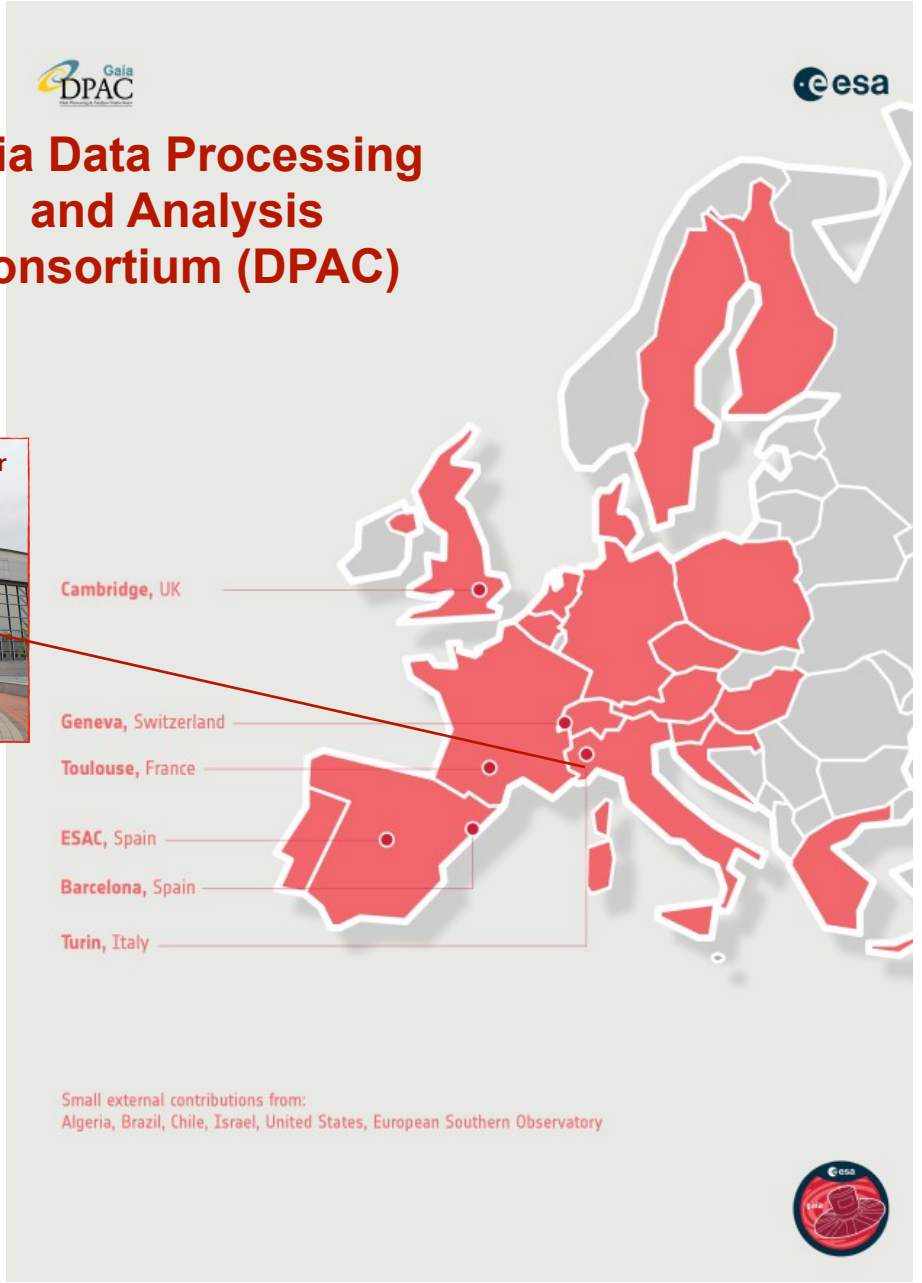

RAMOD vs. GREM: why?

they are based on a “GR framework”, but at first glance no evidence that

RAMOD = GREM (IAU based)?

-> **cross-checked theoretical models** are of capital importance to interpret the **same data**: need of a validation process!

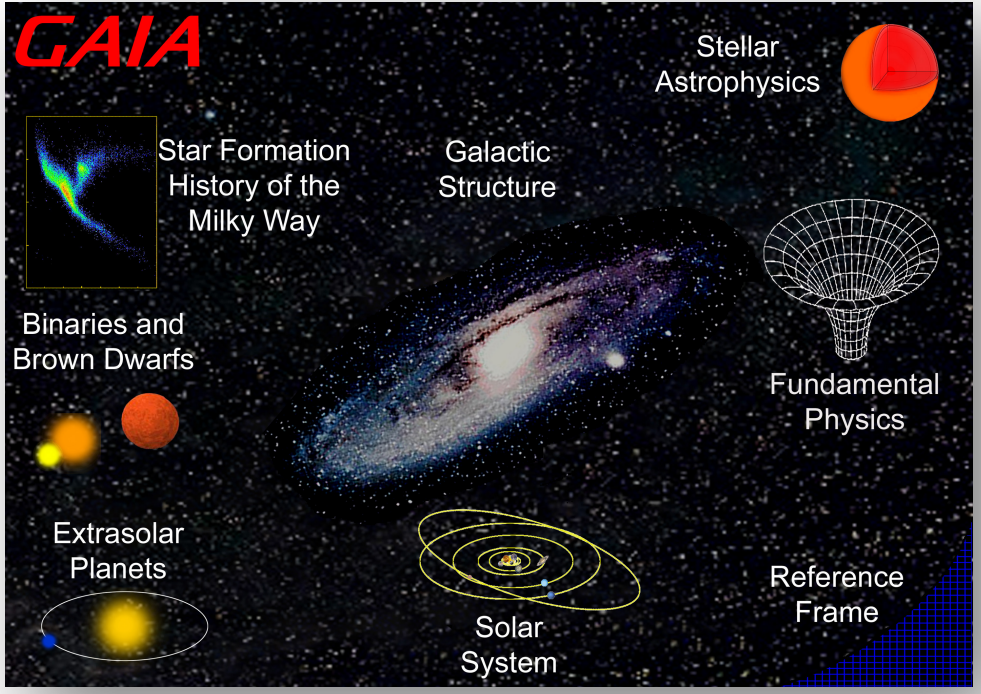

- **control on the error budget at the level of mu-as** for Gaia since the solar system generates **several varying perturbations** of the order of the measurement accuracy i**n different observation times and for different satellite positions**
- **rule out possible spurious contributions** (especially systematic errors)
- **consolidate the results via an independent mutual cross-checking**: independent relativistic astrometric model, independent relativistic attitude model
- **any discrepancy between the relativistic models**, if it can not be attributed to errors of different nature, **means either** a limit in the modeling/interpretation - that a correct application of GR should fix - and therefore **a validation of GR**, **or**, maybe, a clue that we **need to refine our approach to GR**

RAMOD is a framework of general relativistic astrometric models with increasing intrinsic accuracy, adapted to many different observer's settings, **interfacing numerical and analytical relativity**

fully based on alghorithms in General Relativity (GR) -> *no a priori approximations,* top-down approach

observations in a curved space-time -> RAMOD applies the measurement protocol in GR

direct comparison with TTF approach

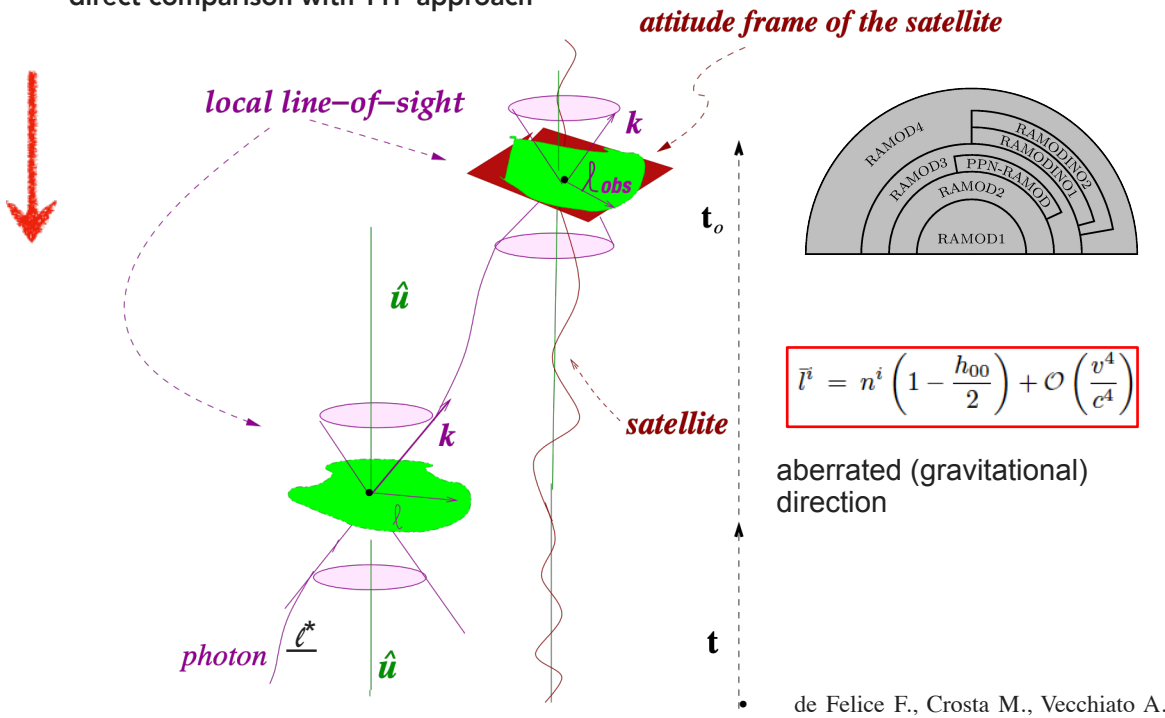

$$\vec{l}^{\,i} = n^i\left(1-\frac{h_{00}}{2}\right)+\mathcal{O}\left(\frac{v^4}{c^4}\right)$$

aberrated (gravitational) direction

$$x_* = F(x_{obs}, g_{\mu\nu}, \ell_{obs}, E_a, \ldots)$$

- de Felice F., Crosta M., Vecchiato A. and Lattanzi M. G., Astrophys. J., 607 (2004) 580
- Crosta M., Geralico A., Lattanzi M. G. and Vecchiato A., Phys. Rev. D, 96 (2107) 104030.
- S. Bertone et al. ,2014 Class. Quantum Grav. 31 015021

GREM,

baselined for the Astrometric Global Iterative Solution for Gaia (AGIS), based on post-Newtonian approximations

stellar direction in pN

$$x^i = x^i_o + k^i\Delta t + \Xi^i$$

$$\frac{d^2\Xi^i}{dt^2} = F^i$$

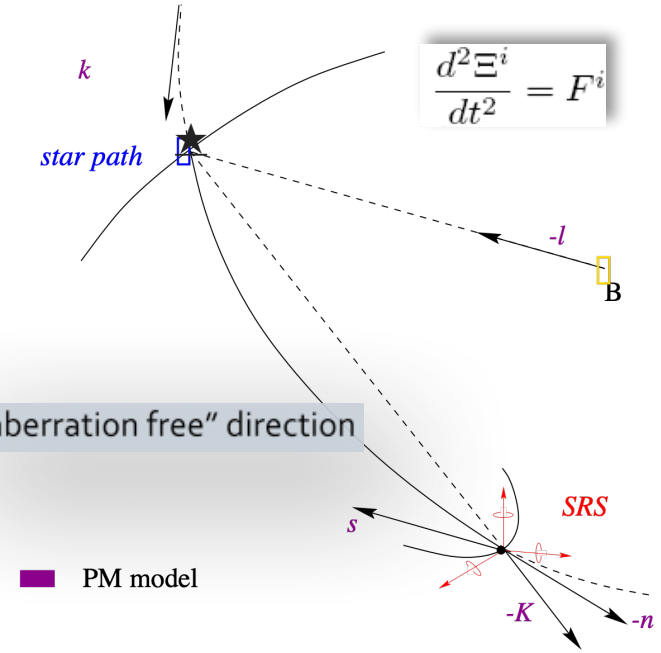

- Klioner S. A., Astron. Astrophys., 404 (2003) 783.

GREM observed direction converts into a coordinate one via several steps , which separate the effects of the aberration, the gravitational deflection, the parallax, and proper motion-> **bottom-up approach**

GR modulo distances via gravitational aberration

the adopted GR formalism for the GSR determines distances in a curved spacetime. i.e. from within local gravitational fields

"Geometric distance" depends on the local ephemerides and observer position

$$\vec{l}^{\,i} = n^i \left(1 - \frac{h_{00}}{2}\right) + \mathcal{O}\left(\frac{v^4}{c^4}\right)$$

Gravitationally aberrated direction

M. Crosta and A. Vecchiato, *Gaia relativistic astrometric models. Proper stellar direction and aberration, A&A 509, A37 (2010)*

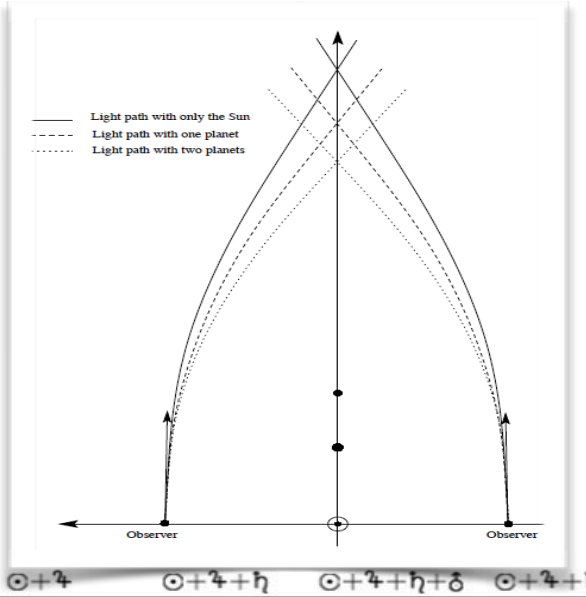

$h_{00}/2 \approx U/c^2$ (local potential)[IAU solution]

$$h_\odot \sim 100\mu as \quad @\ \text{L2}$$

$$m - M = 5\log r_{pc} - 5 \Rightarrow \sigma_{m\text{-}M} \approx 2\,\sigma_d/d \approx 0.2\ \text{mag}$$

relative error in mag with no planets (only the Sun) for d=10kpc

Parallaxes in the catalogue are the results of a processing procedure based on relativistic models.

	⊙	⊙+♃	⊙+♃+♄	⊙+♃+♄+♂	⊙+♃+♄+♂+♅
			distance ∼ 1 pc		
d (AU)	206261.338	206259.698	206259.216	206259.142	206259.054
p_i (″)	1.00001775	1.00002571	1.00002804	1.00002840	1.00002883
$p_\odot - p_i$ (μarcsec)		-7.95	-10.29	-10.65	-11.07
$\Delta\psi_i$ (μarcsec)		-8.00	-10.30	-10.60	-11.10
			distance ∼ 10 pc		
d (AU)	2062283.55	2062120.14	2062072.27	2062064.94	2062056.3
p_i (″)	0.10001777	0.10002569	0.10002802	0.10002837	0.10002879
$p_\odot - p_i$ (μarcsec)		-7.93	-10.25	-10.60	-11.02
$\Delta\psi_i$ (μarcsec)		-8.00	-10.30	-10.60	-11.00
			distance ∼ 100pc		
d (AU)	20589921.6	20573645.4	20568881.5	20568152.5	20567292.3
p_i (″)	0.01001777	0.01002569	0.01002801	0.01002837	0.01002879
$p_\odot - p_i$ (μarcsec)		-7.93	-10.25	-10.60	-11.02
$\Delta\psi_i$ (μarcsec)		-7.99	-10.30	-10.60	-11.00
			distance ∼ 1000 pc		
d (AU)	202664764	201098829	200644596	200575248	200493473
p_i (″)	0.00101776	0.00102569	0.00102801	0.00102837	0.00102879
$p_\odot - p_i$ (μarcsec)		-7.93	-10.25	-10.60	-11.02
$\Delta\psi_i$ (μarcsec)		-7.99	-10.30	-10.60	-11.00
			distance ∼ 10000 pc		
d (AU)	1751489760	1641052370	1611285280	1609051510	1603803810
p_i (″)	0.00011777	0.00012569	0.00012801	0.00012819	0.00012861
$p_\odot - p_i$ (μarcsec)		-7.93	-10.25	-10.42	-10.84
$\Delta\psi_i$ (μarcsec)		-7.99	-10.30	-10.60	-11.00

RAMOD framework

Coordinates are not "physical observers"

The **observer** is selected according to the chosen measurement, namely by its **specific kinematical status with respect to the background spacetime.**

To any time-like observer **u** we associate to tensorial operators, T and P, so that

$$ds^2 = g_{\alpha\beta}dx^\alpha dx^\beta = T_{\alpha\beta}dx^\alpha dx^\beta + P_{\alpha\beta}dx^\alpha dx^\beta$$

dT dL

1+3 decomposition = geometric measurement

an infinitesimal normal neighborhood of **u** the metric

Space time splitting

$$P(u)_{\alpha\beta} = g_{\alpha\beta} + u_\alpha u_\beta$$

$$T(u)_{\alpha\beta} = -u_\alpha u_\beta$$

$$g_{\alpha\beta} = P_{\alpha\beta} + T_{\alpha\beta}$$

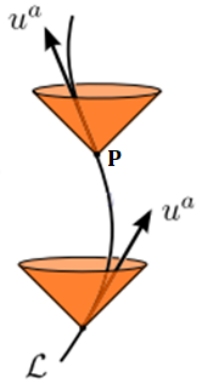

World line

The “splitting” with both tensor and tensorial differential operators **is a necessary tool to reproduce formal “1+3” or “ 3+1” expressions**, **keeping the geometric consistency and meaning**

The notions of time and space are complementary since a “time-like” means measuring the elapsing time at fixed point in space, while "constant time hypersurfaces" implies a synchronization of times at different points of space. For the former local time direction is fundamental, for the latter space is fundamental (non local correlation of local time, i.e. space at some moment of time)

[Quoting: R.T. Jantzen, P. Carini and D. Bini, Understanding Spacetime Splittings and Their Relationships or Gravitoelectromagnetism: the User Manual, https://homepage.villanova.edu/robert.jantzen/gem/gem.pdf]

Local barycentric observer

Given a metric, a family of time-like 4-vectors u constitutes a set of fiducial observes filling the space-time. A section orthogonal to the congruence describes the space-time evolution of the system as the time varies along the curves.

BCRS can be identified by a smooth family of space-like hypersurfaces with equation $t\left(x,y,z\right)=\text{constant}$

On each of these hypersurfaces one can choose a set of Cartesian-like coordinates centered at the barycenter of the system and running smoothly as parameters along space-like curves which point to distant cosmic sources.

At any space-time point, one can define a fiducial observer **u,** which is tangent to the world line of a physical observer at rest, locally and only locally, with respect to the spatial grid of the BCRS

The rest space of **u** can be locally identified by a spatial triad lying on a surface (green area) which differs from the t = constant one, but their spatial components point to the local coordinate directions as chosen by the BCRS

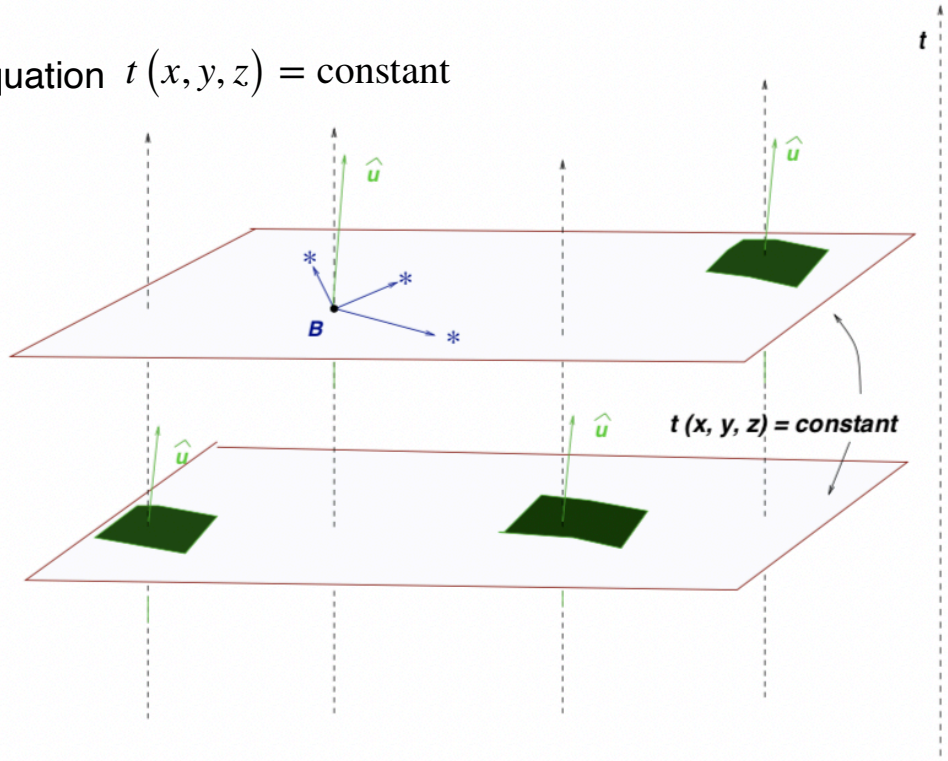

$$\hat{u}_B^\alpha=\frac{1}{\sqrt{-g_{00}}}\partial_0^\alpha\approx\left(1+\epsilon^2 w\right)\partial_0^\alpha \qquad \lambda_{\hat{a}}^\alpha=h_{0a}\delta_0^\alpha+\left(1-\frac{h_{00}}{2}\right)\delta_a^\alpha+\mathcal{O}\left(h^2\right)$$

asymptotically a Killing vector field

Null geodesic w.r.t the local barycentric observer

$$k^\alpha k_\alpha = 0, \qquad \frac{dk^\alpha}{d\lambda} + \Gamma^\alpha_{\rho\sigma} k^\rho k^\sigma = 0$$

$$\ell^\alpha = P^\alpha_\beta(u) k^\beta(\tau)$$

Projector operator w.r.t. the rest-space of $\mathbf{u_B}$

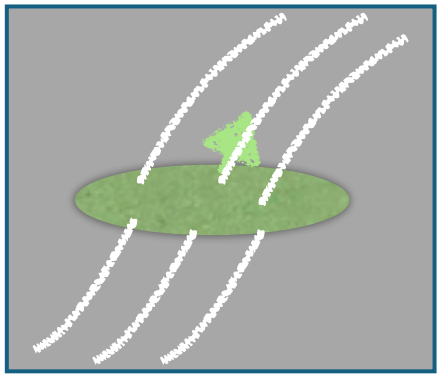

Crosta et al. Phys. Rev. D 96,104030, 2017 "*General relativistic observable for gravitational astrometry in the context of the Gaia mission and beyond*"

The covariant derivative generates the kinematics of a congruence

$$\nabla_\beta u^\alpha = -a^\alpha(u) u_\beta - k^\alpha_\beta(u),$$

acceleration 4-vector

$$a^\alpha(u) = P(u)^\alpha_\beta u^\gamma \nabla_\gamma u^\beta$$

kinematics tensor

$$k^\alpha_\beta(u) = \omega^\alpha_\beta(u) - \theta^\alpha_\beta(u),$$

RAMOD: general approach applicable to any metric

vorticity

$$\omega^{\alpha\beta} = P(u)^\mu_\alpha P(u)^\nu_\beta \nabla_{[\mu} u_{\nu]}$$

measures how a world-line of an observer rotates around a neighboring one

expansion

$$\theta^\alpha(u) = P(u)^\mu_\alpha P(u)^\nu_\beta \nabla_{(\mu} u_{\nu)}$$

measures the average expansion of the infinitesimally nearby surrounding geodesics

$$\frac{d\bar{\ell}(u)^\alpha}{d\sigma} + \Gamma^\alpha{}_{\mu\nu}\bar{\ell}(u)^\mu(\bar{\ell}(u)^\nu + u^\nu) + a(u)^\alpha - k(u)^\alpha{}_\sigma \bar{\ell}(u)^\sigma - \left[\bar{\ell}(u)^\mu \bar{\ell}(u)^\nu \theta(u)_{\mu\nu} + \bar{\ell}(u)^\mu a(u)_\mu\right](\bar{\ell}(u)^\alpha + u^\alpha) = 0$$

The concept of the Global Sphere reconstruction via general relativistic astrometric observable

Merging repeated observations of the same objects from different satellite orientations and on different times allows to estimate their angular positions, parallaxes, and proper motions, *i.e.* the actual materialization of an absolute Reference Frame.
This process is conventionally called Astrometric Sphere Reconstruction.

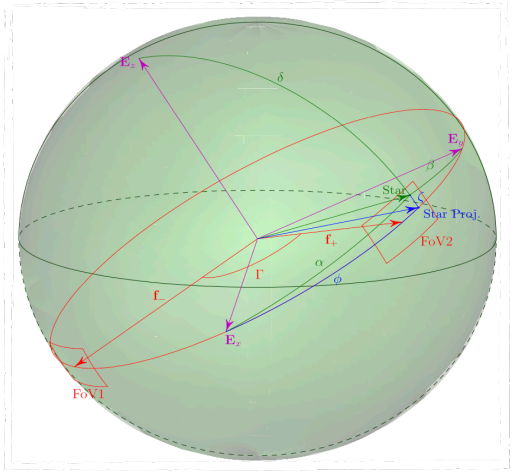

Projector operator onto the rest space of the satellite

Theoretical models

$$\cos\psi_{(E_{\hat{a}},\ell_{obs})} \equiv \mathbf{e}_{\hat{a}} = \frac{P(u')_{\alpha\beta}k^{\alpha}\boldsymbol{E}^{\beta}_{\hat{a}}}{(P(u')_{\alpha\beta}k^{\alpha}k^{\beta})^{1/2}}$$

$E_{\alpha}{}^{\beta}$ relativistic attitude tetrad" $E^{\alpha}_{\hat{a}} = \mathcal{R}(\alpha_i)_{\hat{a}}{}^{\hat{b}}\lambda^{\alpha}_{\hat{b}}$

-> essential to define the boundary condition

$$\lambda^{\alpha}_{(bs)\hat{a}} = P(u_s)^{\alpha}_{\beta}[\lambda^{\beta}_{\hat{a}} - \frac{\gamma(u_s,u)}{\gamma(u_s,u)+1}\nu(u,u_s)^{\alpha}(\nu(u,u_s)^{\rho}\lambda_{\hat{a}\rho})]$$

Bini , Crosta, and de Felice, Class.Quantum Grav. 20, 4695, 2003

Observation equation

$$\cos\phi \equiv F\left(\underbrace{\alpha_*,\delta_*,\varpi_*,\mu_{\alpha*},\mu_{\delta*}}_{\text{Astrometric parameters}},\underbrace{\sigma_1^{(1)},\sigma_2^{(1)},\sigma_3^{(1)},\sigma_1^{(3)},\sigma_2^{(3)},\sigma_3^{(3)}}_{\text{Attitude parameters}},\underbrace{c_1,c_2,\ldots}_{\text{Instrument}},\underbrace{\gamma,\ldots}_{\text{Global}}\right)$$

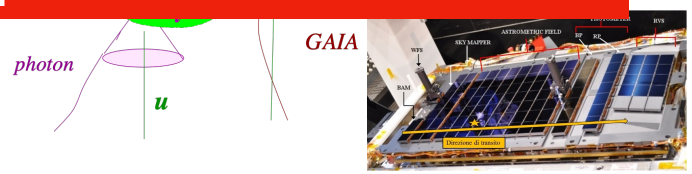

$$\mathbf{x}_* = \frac{1}{\varpi}(\cos\alpha\cos\delta, \sin\alpha\cos\delta, \sin\delta)$$

1 obs. ⇒ 1 condition eq. $\alpha(t) = \alpha(t_0) + \mu_\alpha(t-t_0) + O(\Delta t^2), \quad \delta(t) = \delta(t_0) + \mu_\delta(t-t_0) + O(\Delta t^2)$

(linearized) system of solution with dimensions ~$10^{10}\times10^{8}$

- de Felice F., Crosta M., Vecchiato A. , Lattanzi M. G. And B. Bucciarelli, Astrophys. J., 607 (2004) 580
- Crosta M., Geralico A., Lattanzi M. G. and Vecchiato A., Phys. Rev. D, 96 (2107) 104030.
- Vecchiato A. , B. Bucciarelli, M.G.Lattanzi et al., Astron. Astrophys., 620 (2018) A40

The concept of the Global Sphere Reconstruction

$$\cos\phi \equiv F\left(\underbrace{\alpha_*,\delta_*,\varpi_*,\mu_{\alpha*},\mu_{\delta*}}_{\text{Astrometric parameters}},\underbrace{\sigma_1^{(1)},\sigma_2^{(1)},\sigma_3^{(1)},\sigma_1^{(3)},\sigma_2^{(3)},\sigma_3^{(3)}}_{\text{Attitude parameters}},\underbrace{c_1,c_2,\ldots}_{\text{Instrument}},\underbrace{\gamma,\ldots}_{\text{Global}}\right)$$

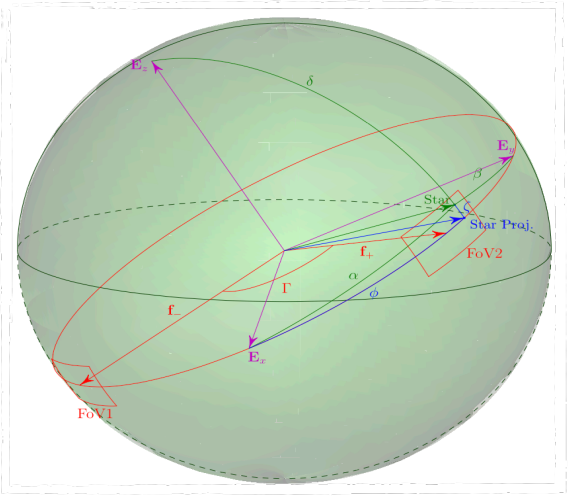

Solving the linearized GSR sphere in the Least-Squares sense

Known Unknown Unknown

$$\sin\psi_i^{(1)}\,\Delta\psi_i^{(1)} = \frac{\partial f}{\partial\alpha_i}\Delta\alpha_i + \frac{\partial f}{\partial\delta_i}\Delta\delta_i + \frac{\partial f}{\partial\pi_i}\Delta\pi_i + \boxed{?} + \frac{\partial f}{\partial\gamma}\Delta\gamma$$

$$\sin\psi_i^{(2)}\,\Delta\psi_i^{(2)} = \frac{\partial f}{\partial\alpha_i}\Delta\alpha_i + \frac{\partial f}{\partial\delta_i}\Delta\delta_i + \frac{\partial f}{\partial\pi_i}\Delta\pi_i + \boxed{?} + \frac{\partial f}{\partial\gamma}\Delta\gamma$$

$$\sin\psi_i^{(n)}\,\Delta\psi_i^{(n)} = \frac{\partial f}{\partial\alpha_i}\Delta\alpha_i + \frac{\partial f}{\partial\delta_i}\Delta\delta_i + \frac{\partial f}{\partial\pi_i}\Delta\pi_i + \boxed{?} + \frac{\partial f}{\partial\gamma}\Delta\gamma$$

1 obs. ⇒ 1 condition eq.

(linearized) system of solution with dimensions ~$10^{10}\times10^{8}$

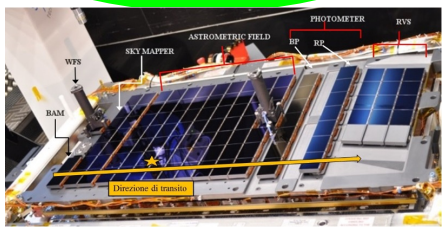

Solution method (Vecchiato, Bucciarelli, Lattanzi et al. 2018)

Talk outline

Background

- Motivation: Astrometry from Hipparcus to Einstein, Gaia
- Relativistic/Gravitational Astrometry

Challenging the Galactic Models with Milky Way stars

- Local cosmology as ΛDCM laboratory
- Testing General Relativity/Gravity @MilkyWay scale
- The impact for Dark Matter interpretation
- ΛCDM model predictions @MilkyWay scale

Gravitational astrometry @ Milky Way scale: investigating the effects of gravity on photons <u>at all scales within the Milky Way</u>, and then compare them to the predictions of current Gravity theories and Cosmological formation scenarios including stellar and planetary formation.

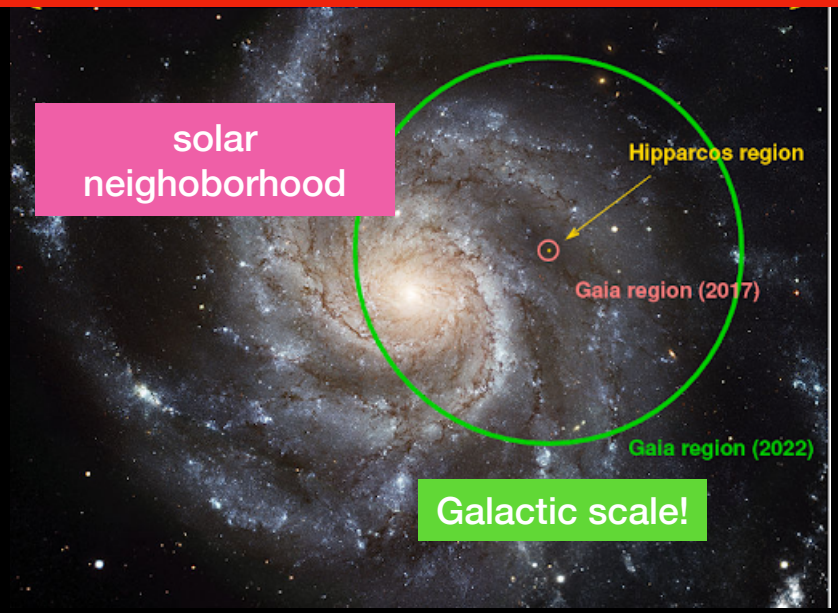

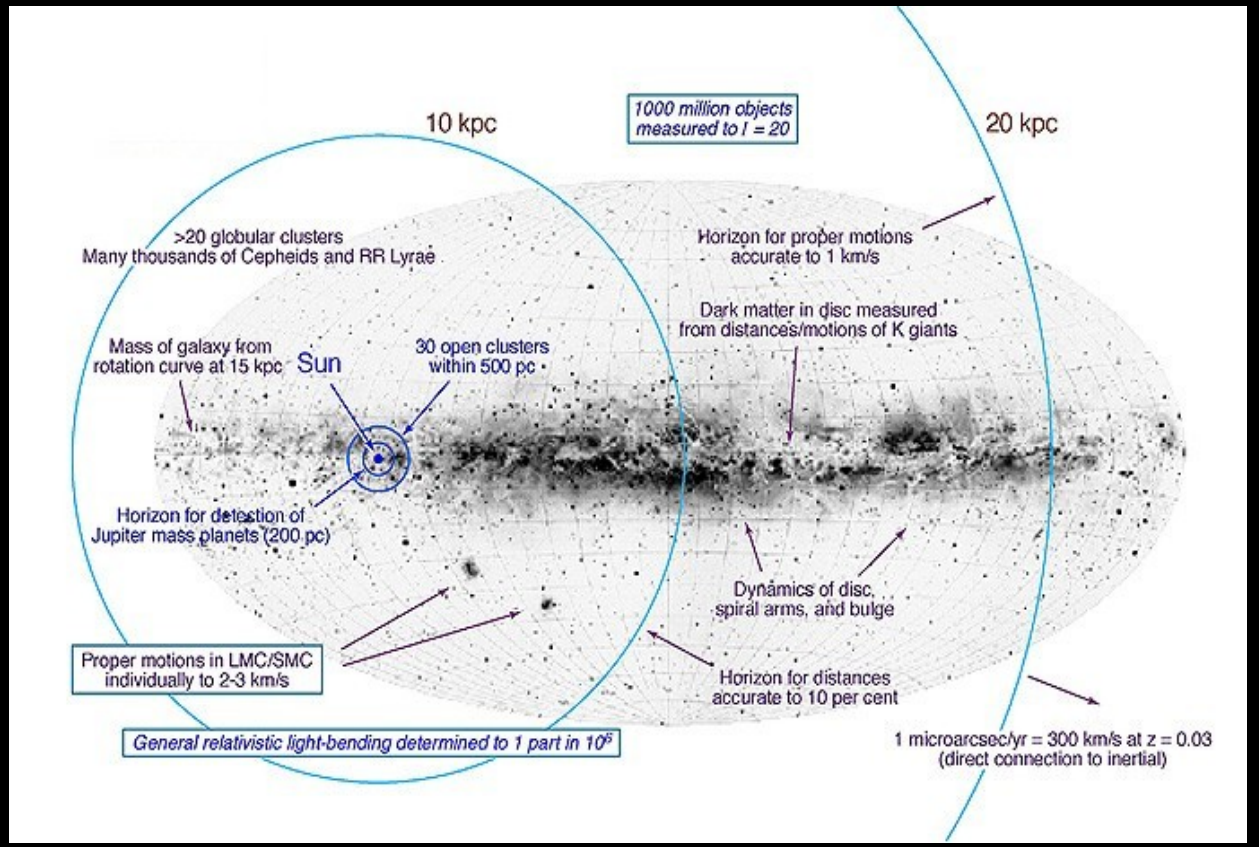

Chart the 6-dimensional phase space (positions & velocities) throughout our Galaxy to kiloparsec scale (at least to 10 kpc all around the Sun)

Probing MW gravitational potential and searching for signatures of Cosmic evolution

MW as the laboratory of «local» Cosmology
(much like what the Sun is to stellar Astrophysics)

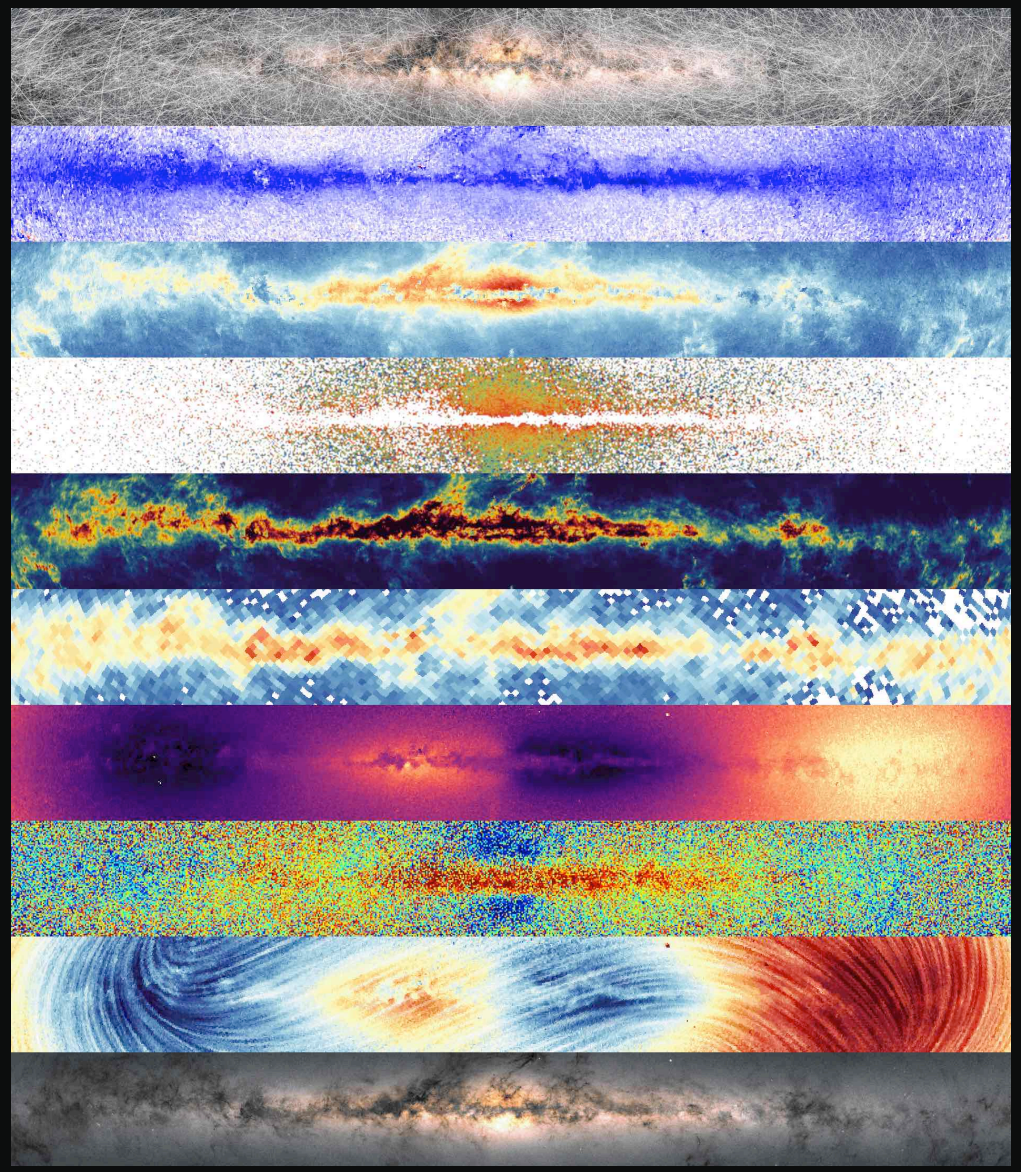

To guarantee Gaia's scientific outputs, we must rely on General Relativity.

Given that the data analysis and processing follow a GR approach, any subsequent exploitation of the results must remain consistent with the theoretical framework underlying the astrometric model.

A fully relativistic model for the Milky Way (MW) should be pursued!

➢ **Local Cosmology:** Lambda-CDM model predictions at the scale of the Milky Way

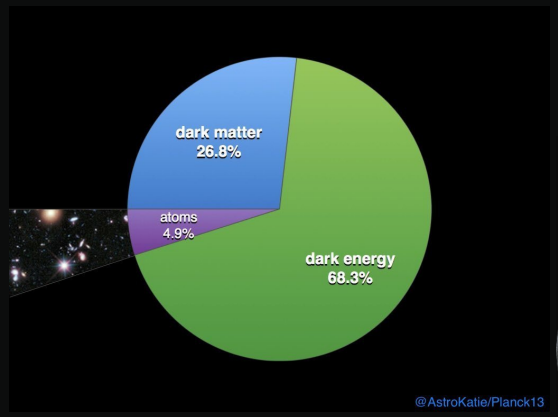

Gaia can provide values (true observables) to estimate model parameters

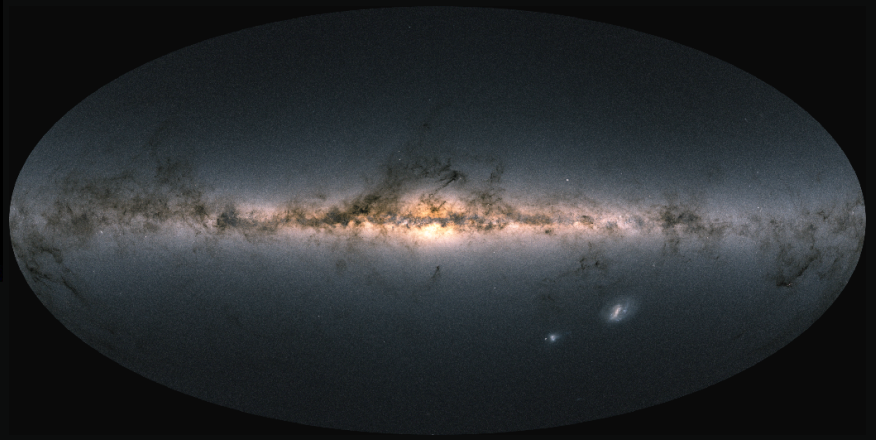

ΛCDM: Cosmological Concordance model

Absence of “evidences” of extra matter (Concordance Cosmological Model):

- galaxy cluster
- large structure at Mpc scale
- CMB
- gravitational lensing
- **rotation curve at galactic scale**

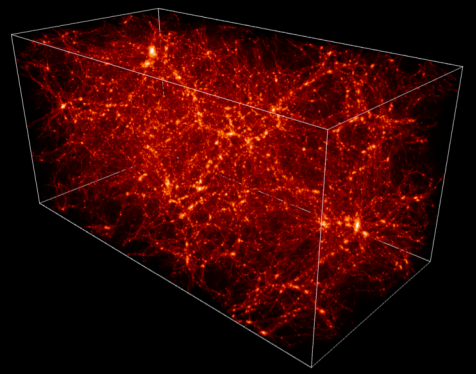

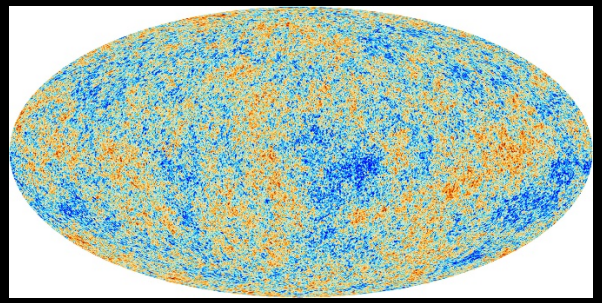

  - Candidates
  - white/brown dwarfs
  - no baryonic particle (axions, WIMP)/SUSY
  - self-interaction
  - neutrinos (sterile, massive, etc..)
  - scalar fields/modified gravity via MOND etc..

In the most advanced simulations standards Λ-CDM cosmology assumes an average FLRW evolution while growth in structure is treated by Newtonian N-body simulations:
“ Friedman tells space how to curve
and Newton tells mass how to move”

arXiv:1612.09309v2 *Coley, Wiltshire*

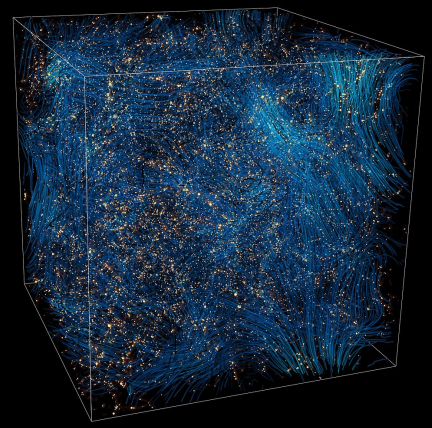

General Relativity (GR) is only partially considered

-> G-evolution: GR code for simulated large structures and expansion in Λ-CDM (Adameck et al. 2016)
-> GRAMSES (Barrera-Hinojosa & Li 2020)

ΛCDM - Hierarchical scenario

The growth of cosmic structures:

- primordial density fluctuations produced during inflation
- dominant mass component is cold dark-matter (CDM)
- fluctuations grow under the action of gravity
- ΛCDM power spectrum: small objects collapse first
- Gas cooling and star formation
- Galaxy evolution and merging

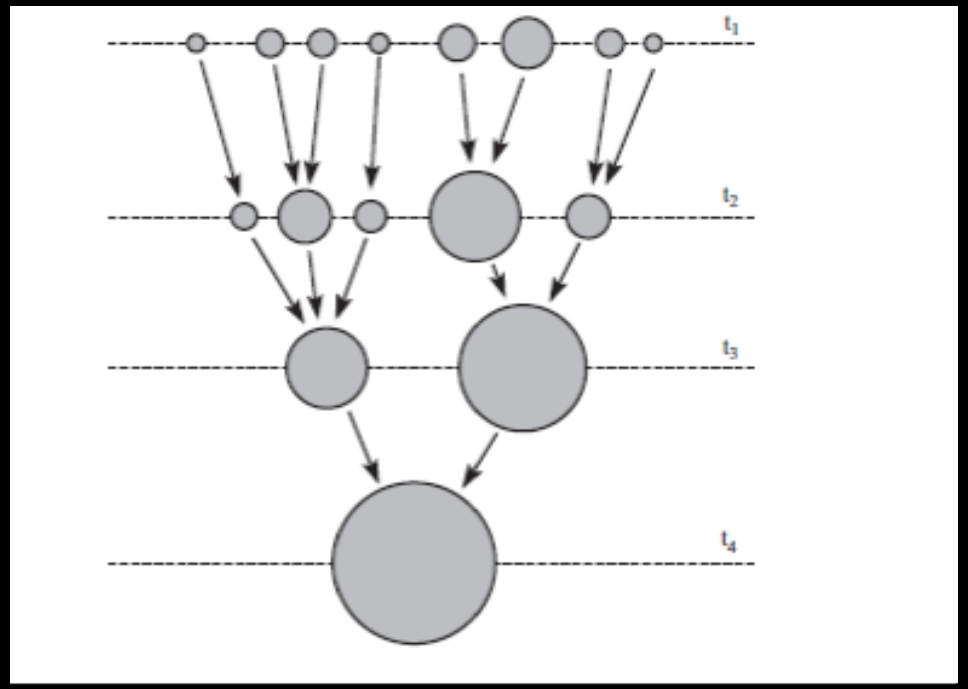

Examples of galactic building blocks in protogalaxies observed by JWST

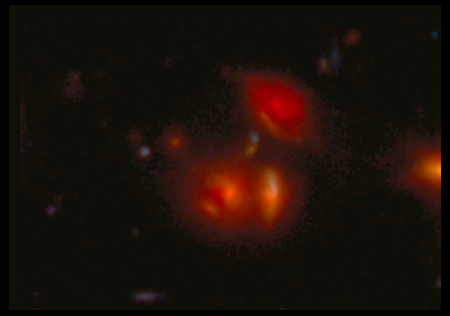

”The cosmic rose” (0.1 Gyr)

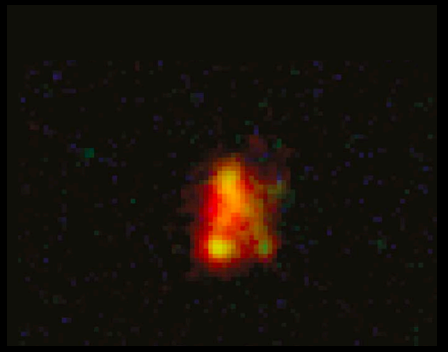

"The big clumpy” (0.3 Gyr)

Galactic components

Satellites

Halo streams

Thin/thick disc

Stellar halo
(in situ, accreted satellites,
heated disc stars)

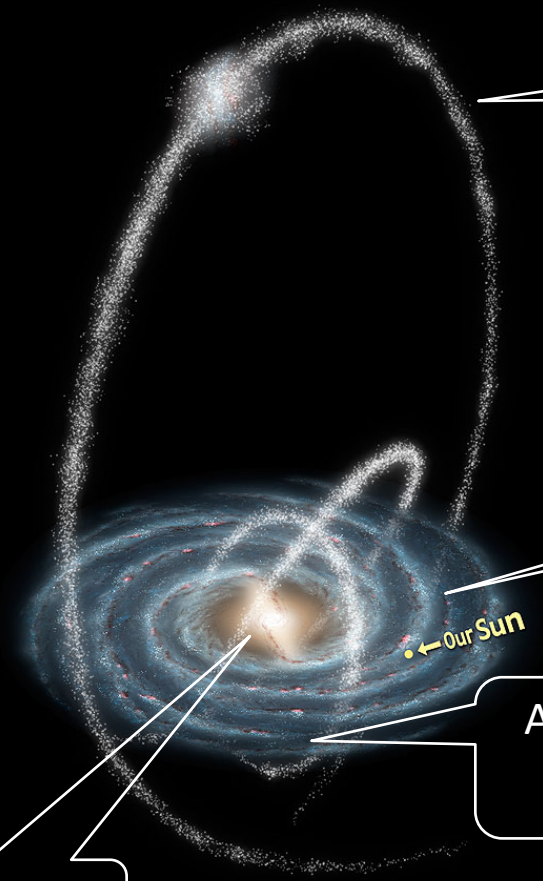

Accreted/unevolved
disc star

Bulge

Open questions

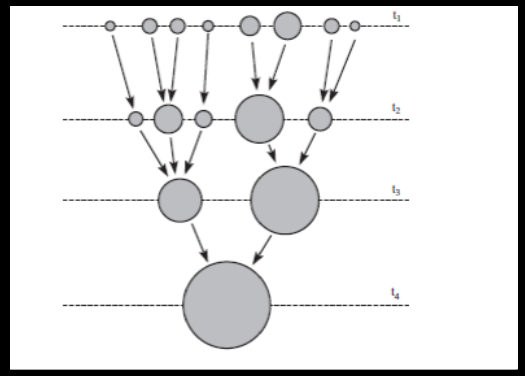

- How many mergers in the history of the Milky Way?
- How large were they?
- When did the mergers take place?
- How the mergers have affected the Milky Way?

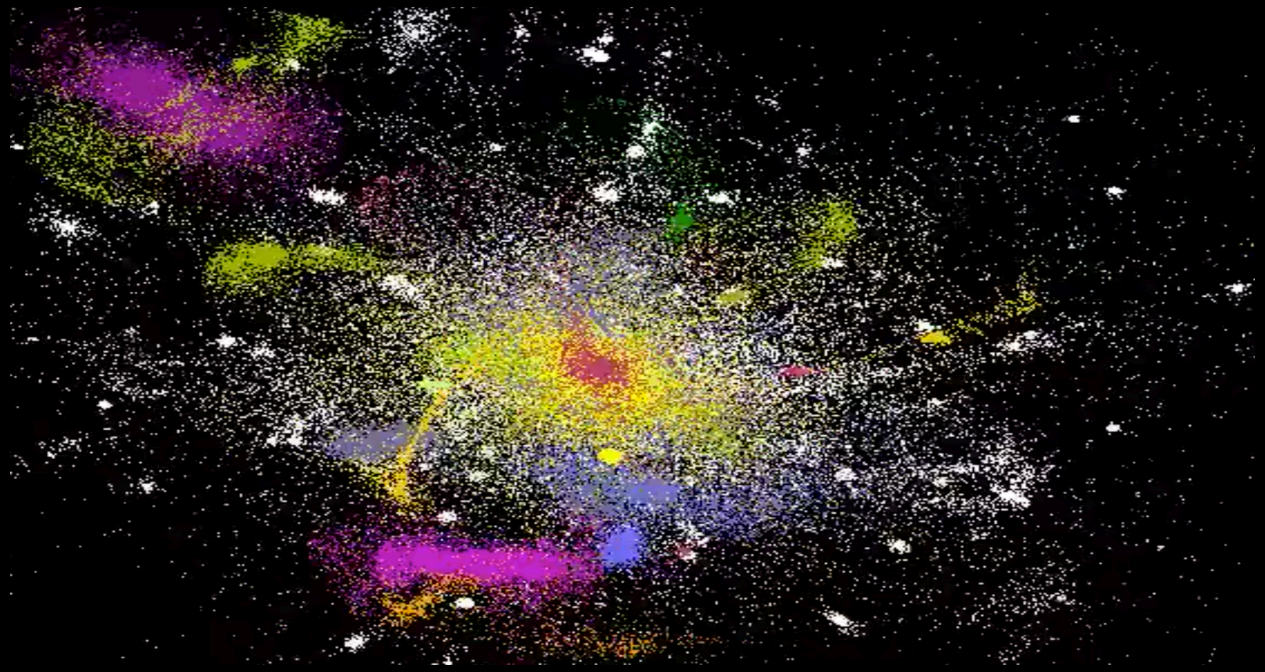

Galactic halo formation -merging contributions

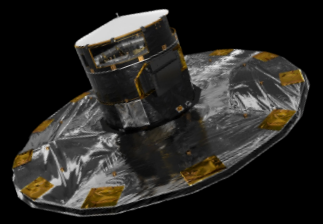

Major merger: *Gaia – Sausage – Enceladus (GSE)*

Amina Helmi et al. 2018, "*The merger that led to the formation of the Milky Way's inner stellar halo and thick disk",* Nature, 563, 85

Abstract. … We demonstrate that the inner halo is dominated by debris from an object which at infall was slightly more massive than the Small Magellanic Cloud.

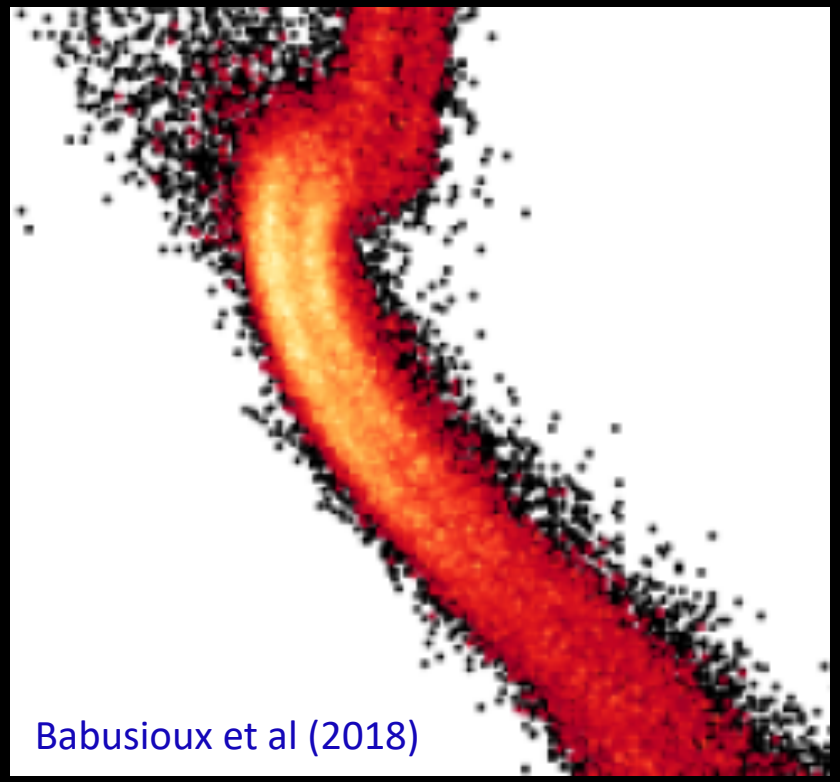

Babusioux et al (2018)

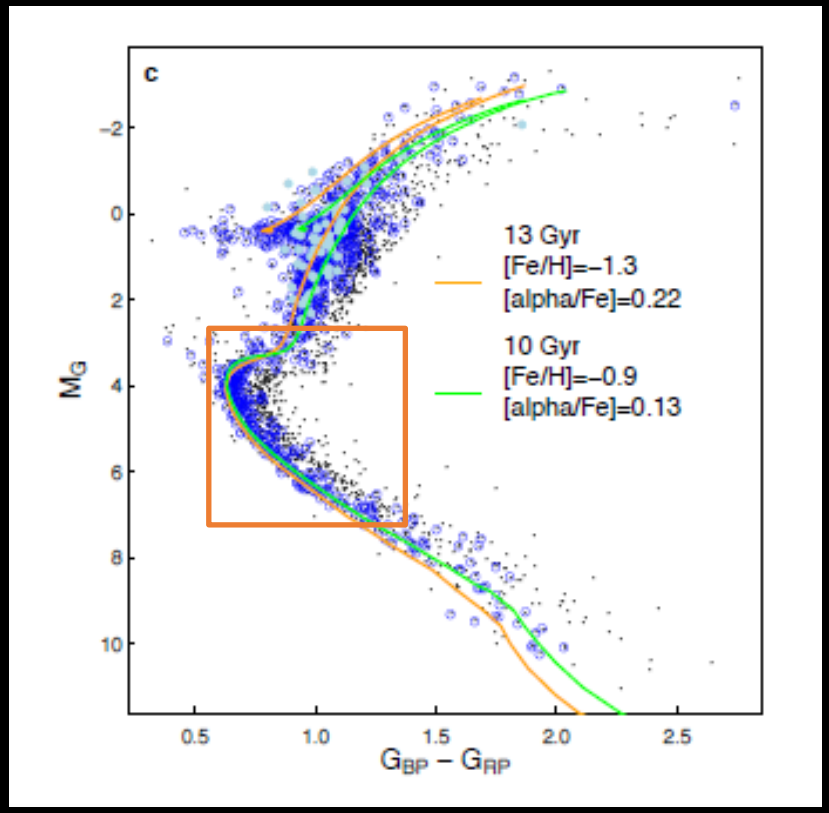

Sagittarius dwarf galaxy interaction with the MW

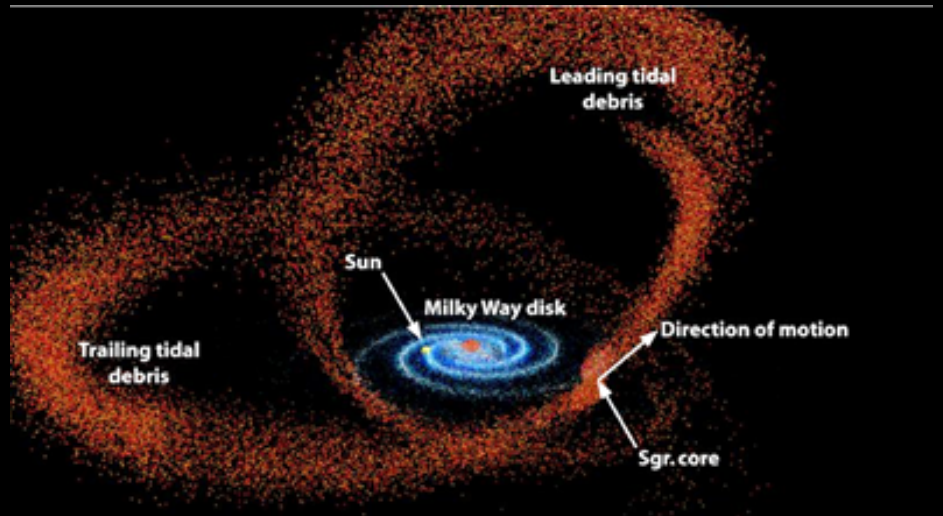

D ≈ 26 kpc

L ≈ 10^8 $L_\odot$

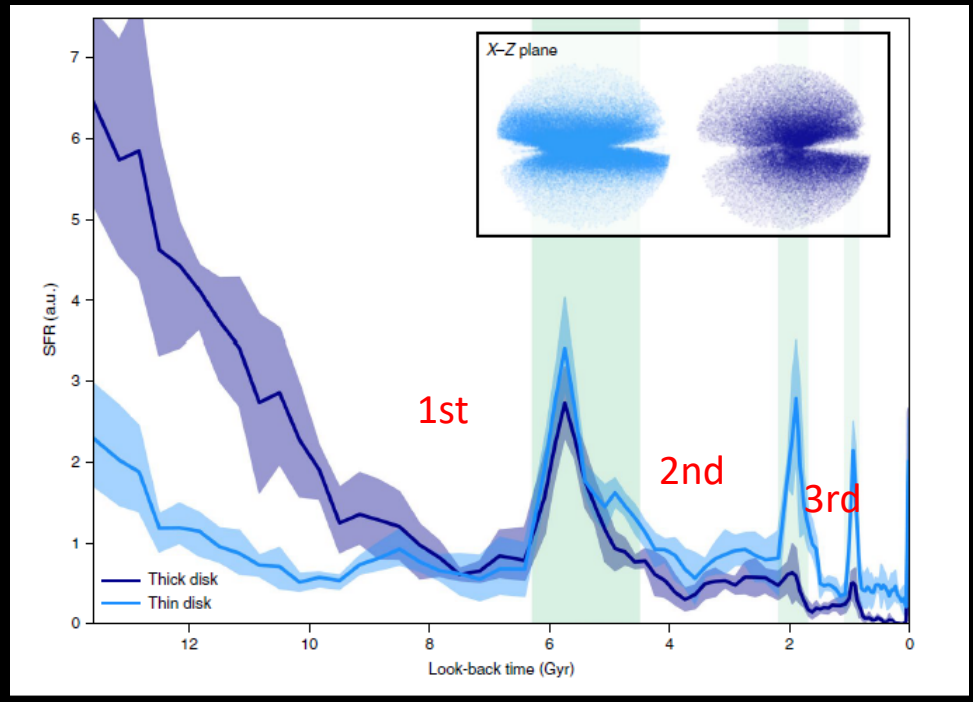

Star Formation History in the ~2-kpc-radius bubble around the Sun distinguishing between the thin and thick disks (selected on the basis of tangential velocity).
Green-shaded areas highlight the location of the detected star-forming bursts.
Three conspicuous and narrow episodes of enhanced star formation that we can precisely date as having occurred 5.7, 1.9 and 1.0 Gyr ago, which coincide with proposed pericentre passages of the Sagittarius dwarf galaxy.

Ruiz Lara et al 2020

Galactic halo formation - substructures

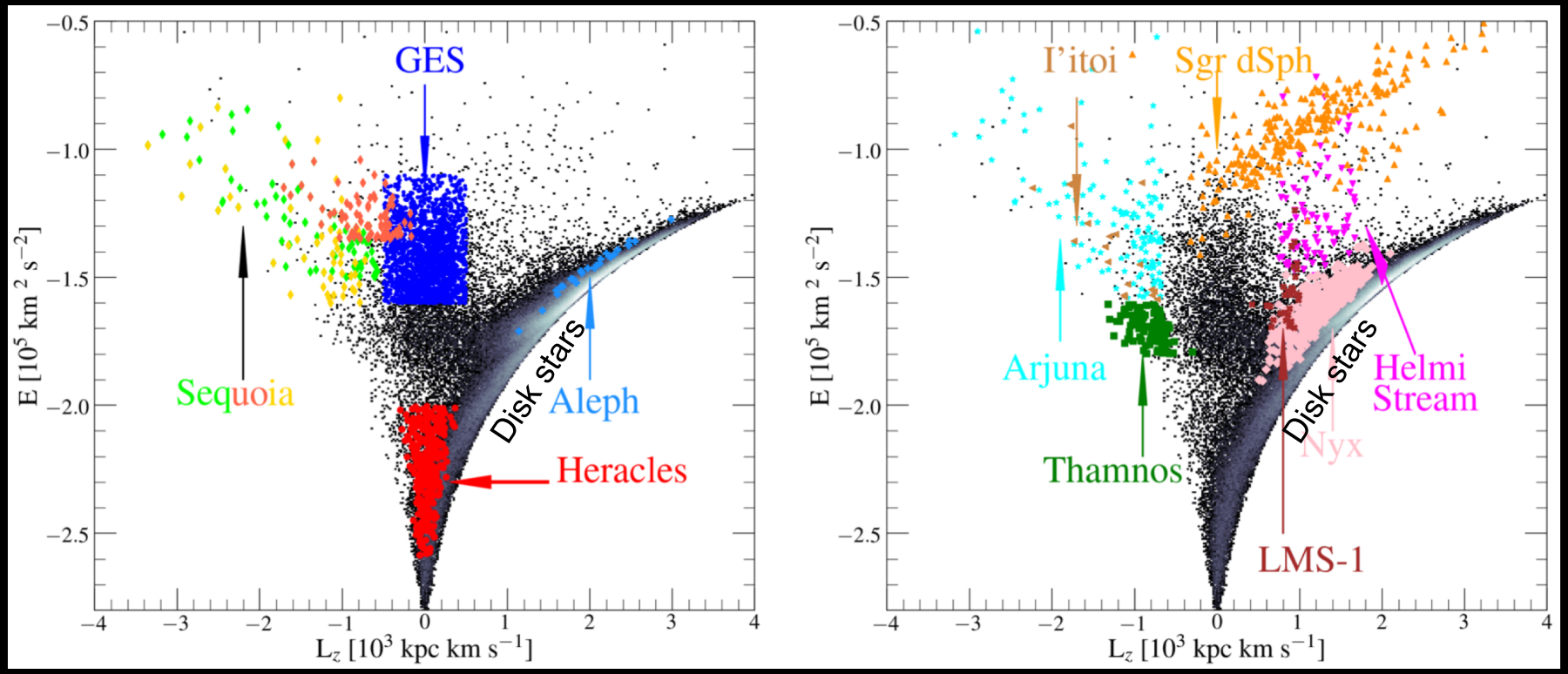

Halo substructures in the orbital energy vs. angular momentum w.r.t. the Galactic disc plane, among the MW sample from Gaia-APOGEE (white/black are high/low density regions). The coloured markers illustrate different halo structures.

(e.g. Ibata+1994; Helmi+1999, 2018; Belokurov+2018; Myeong+2019; Koppelman+2019; Necib+2020; Naidu+2020; Horta+2021,2022)

Galactic disc - Icarus: accreted/unevolved stars

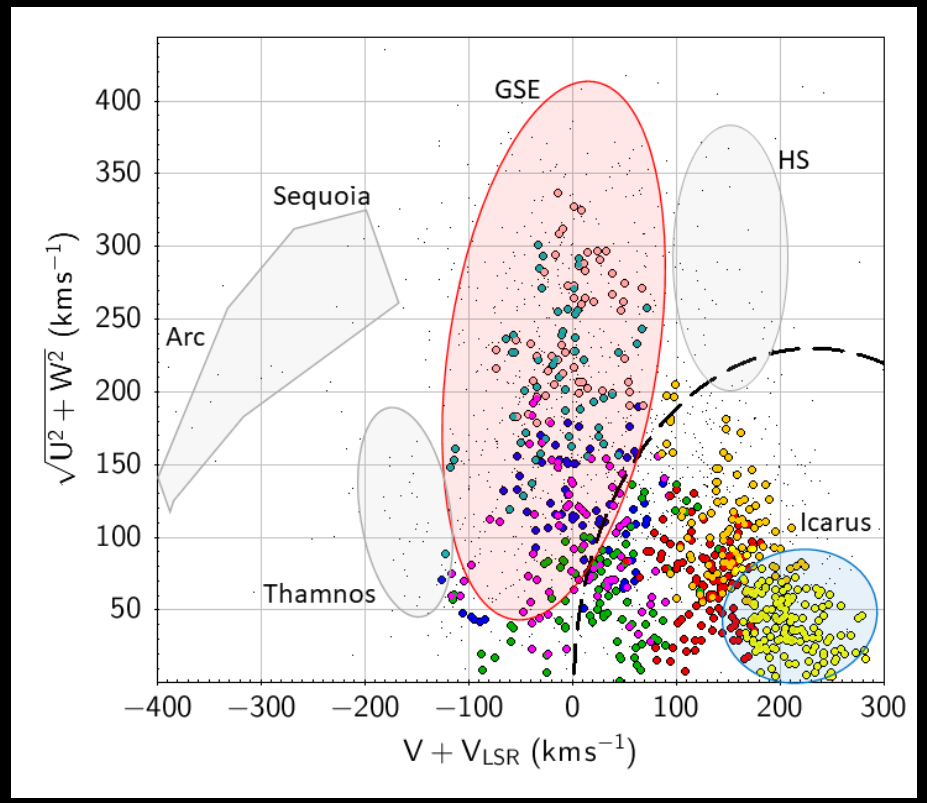

Toomre diagram.

The traditional kinematic selection for halo stars, $|\mathbf{v} - \mathbf{v}_{LSR}| > 230$ km/s, represented by the dashed line.

Re Fiorentin et al (2021, 2024)

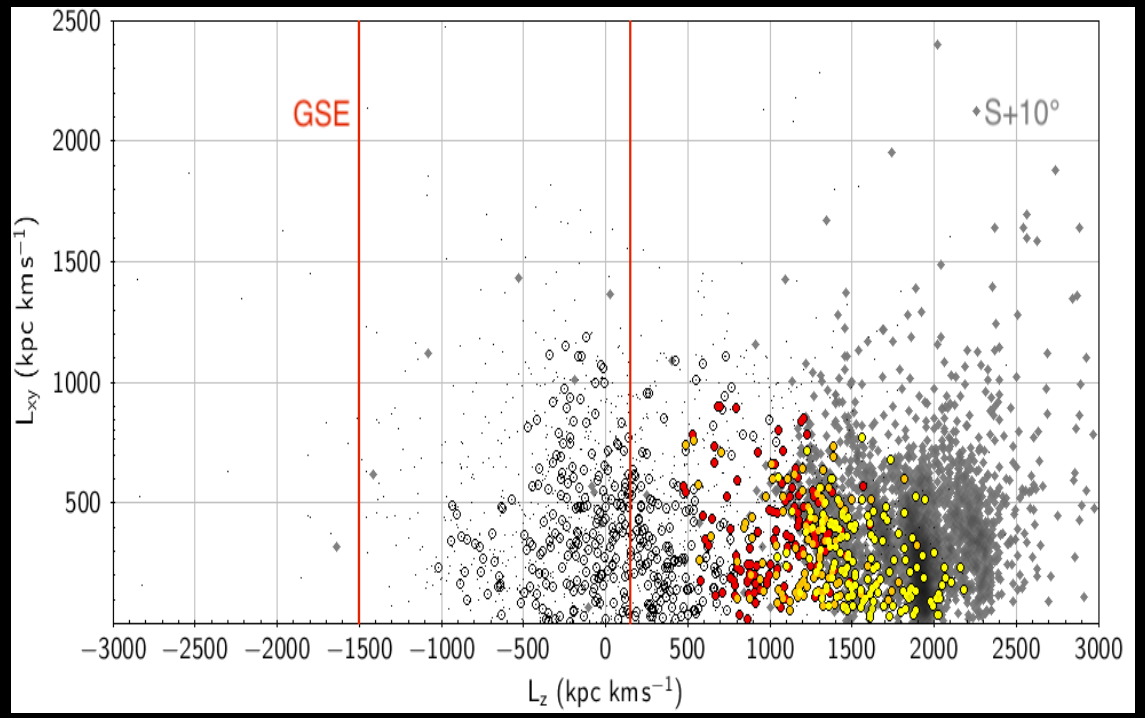

L_{XY} vs. L_Z distribution of Icarus stars (yellow and red dots)

The red solid lines indicate the GSE locus (Helmi+2018).
The debris of the simulated 10°-inclination prograde satellite with a stellar mass of **~$10^9 M_{Sun}$** analysed in Re Fiorentin+2015 are overplotted for comparison (grey diamonds).

Gaia BH1, Gaia BH2, Gaia BH3, and Gaia NS1

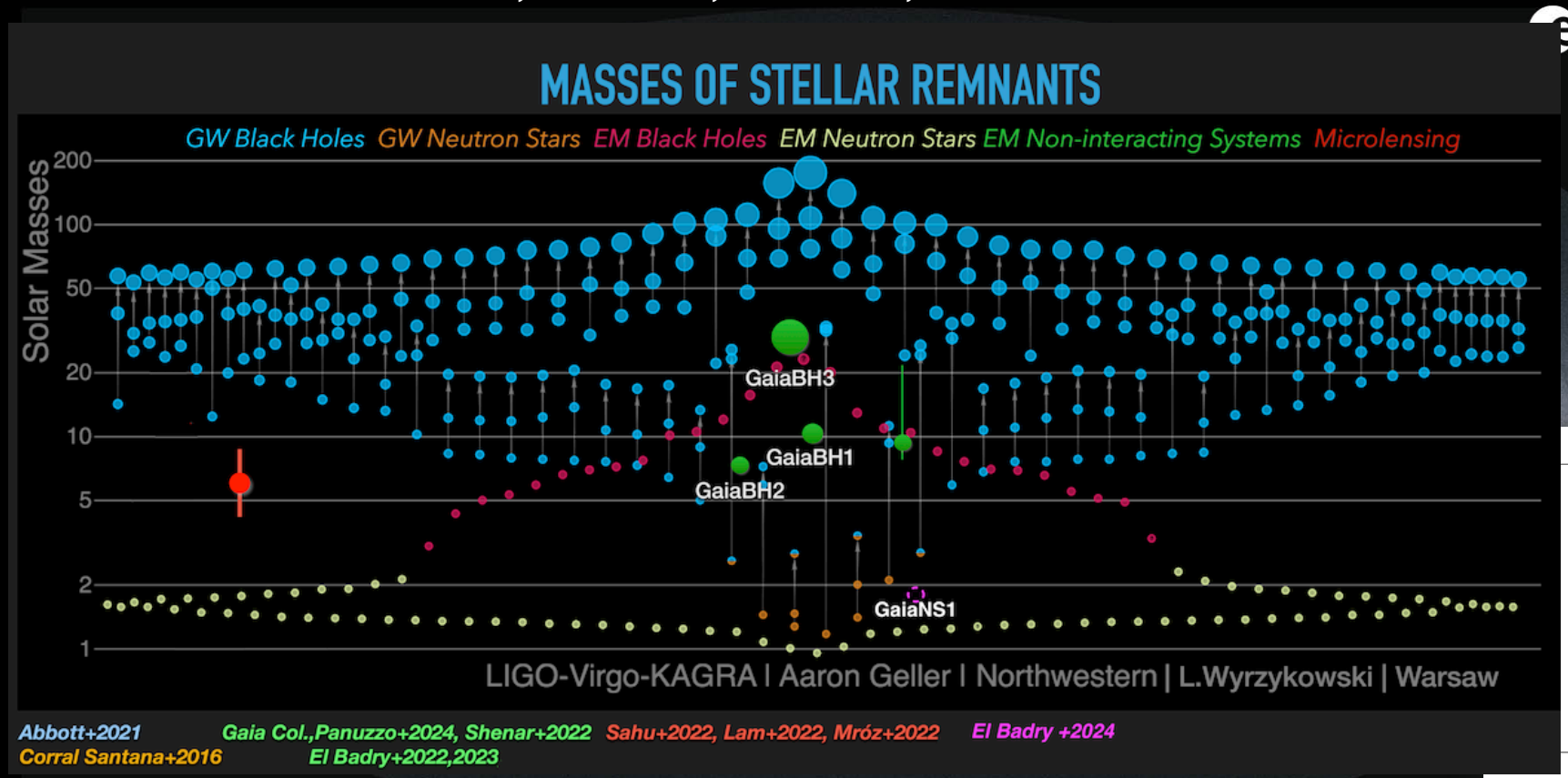

Credits: Adapted from LIGO-VIRGO-KAGRA, Aaron Geller, Northwestern / L. Wyrzykowski, Warsaw by ESA/Gaia/DPAC.

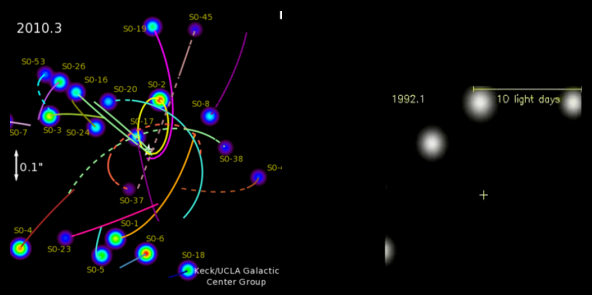

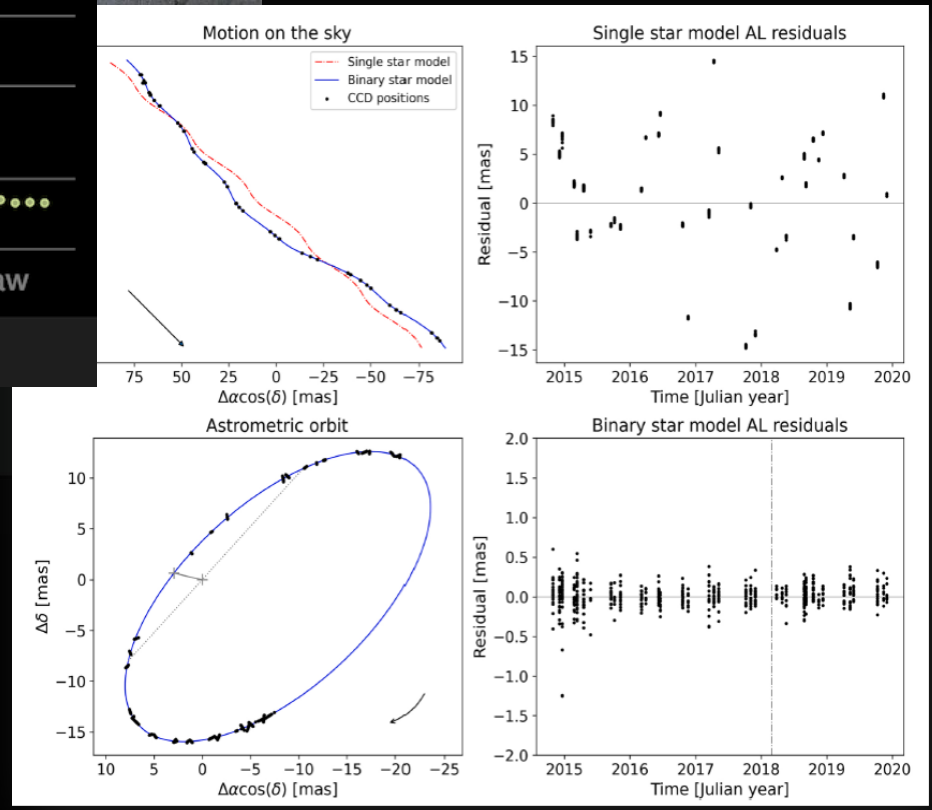

Gaia RV's discover BH3 (25-30 solar mass at 500 pc from the Sun!) and Gaia astrometry (shown in Figure) confirms it as the most massive stellar Black Hole ever discovered in our Galaxy (from Gaia Collaboration: Panuzzo et al., 2024, A&A, 686, L2)

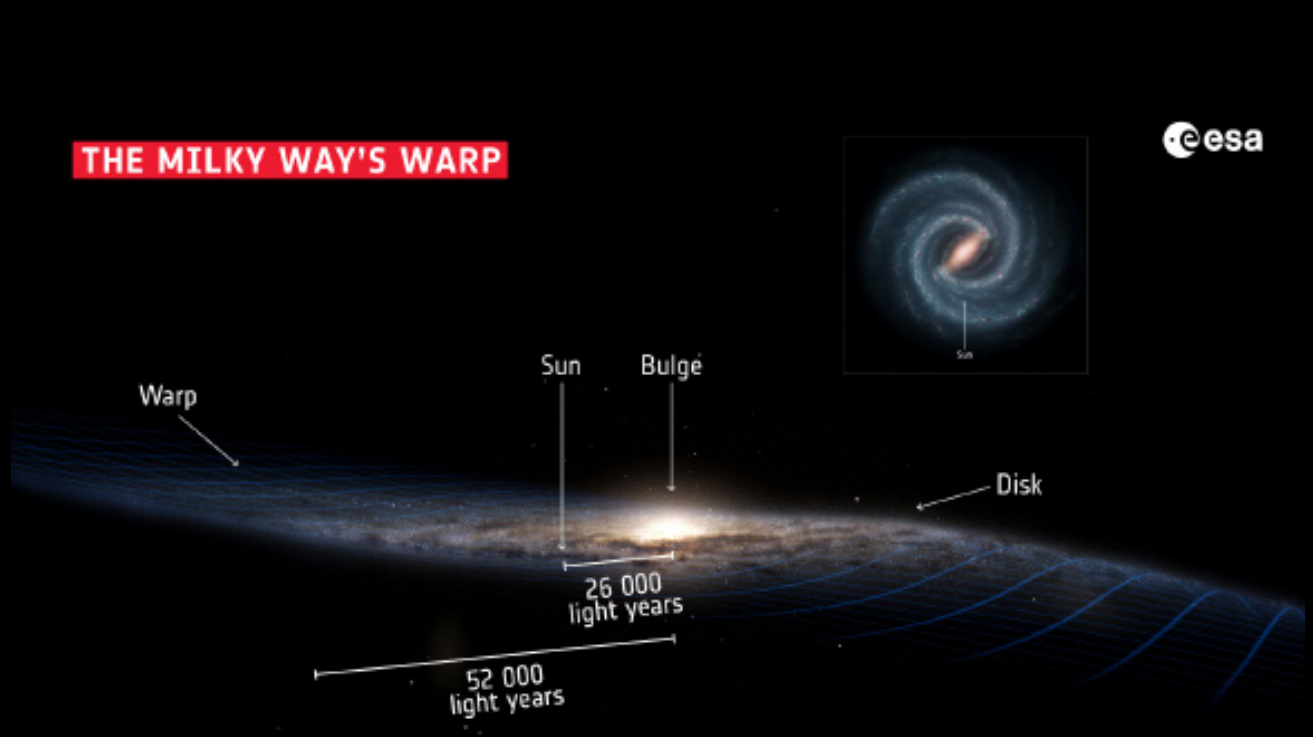

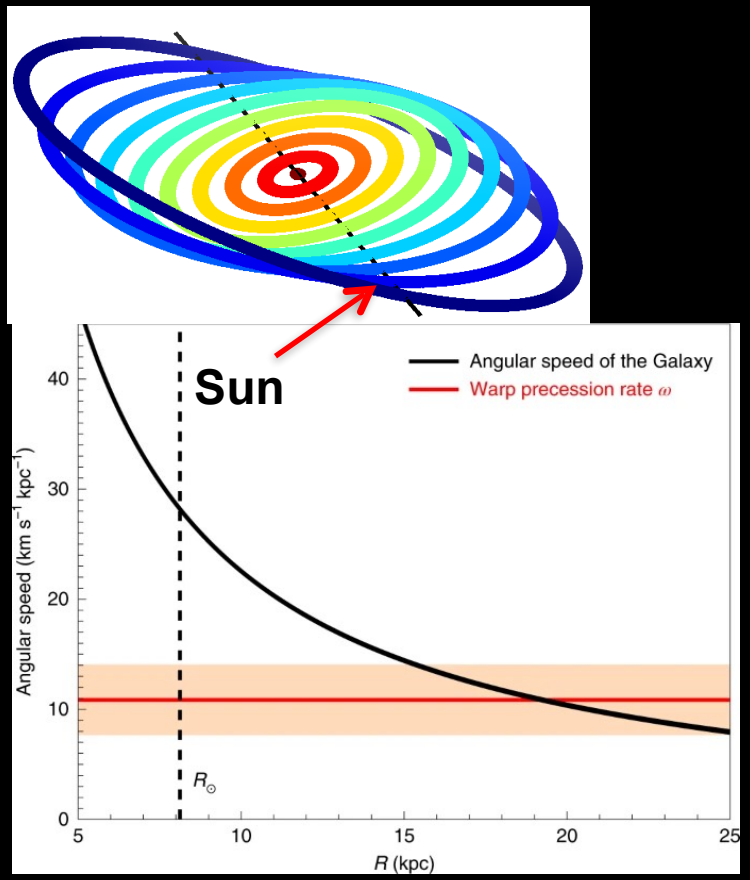

Warp is precessing at 10.86 ± 0.03 (statistical) ± 3.20 (systematic) km/s*kpc in the direction of Galactic rotation.

The warp would complete one rotation around the center of the Milky Way in 600 to 700 million years

Much faster than expected based on predictions from other models, such as those looking at the effects of the non-spherical halo

The direction and magnitude of the warp's precession rate favor the scenario that the warp is the result of a recent or ongoing encounter with a satellite galaxy, rather than the relic of the ancient assembly history of the Galaxy

Galactic disc: rotation curves

Flat rotation curves in disk galaxies - a longest outstanding problem in astronomy - provide the main observational support to the **hypothesis of surrounding dark matter.**
Adding a “dark matter” halo **allows a good fit to data**

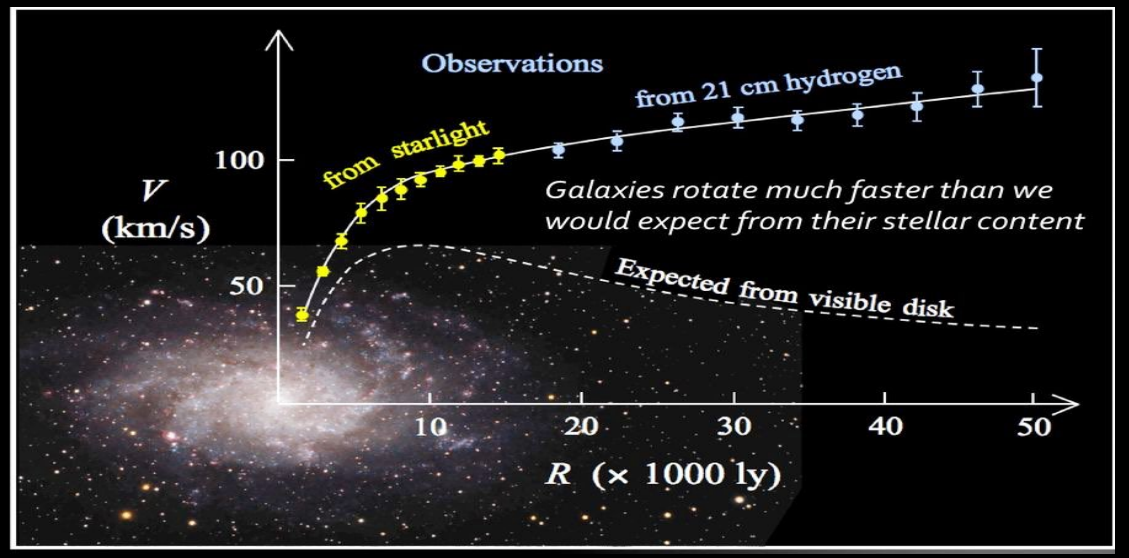

Rotation curves are distinctive features of spiral galaxies like our Milky Way, a sort of a kinematical/dynamical signature, like the HR diagram for the astrophysical content

Stellar kinematics, as tracer of gravitational potential, is the most reliable observable for gauging different matter components

-> the rotation curve of the MW used as a first test for a GR Galaxy

weak field regime @Milky Way scale

In general one assumes that:
gravitational potential or "relativistic effects" at the MW scale are usually "small", then

✓negligible..

✓locally Newton approximation is retained valid at each point..

but $(v_{Gal}/c)^2 \sim 0{,}69 \times 10^{-6}$ (rad) ~100 mas

$(v_{Gal}/c)^3 \sim 0{,}57 \times 10^{-9}$ (rad) ~ $120\mu as$

the individual astrometric error is $\leq 100\mu as$ throughout most of its magnitude range

"weakly" relativistic effect could be relevant?

For the Gaia-like observer the weak gravitational regime turns out to be "strong" when one has to perform high accurate measurements

$\varepsilon \sim v^2/c^2 \sim GM/rc^2 \sim$ mas accuracy

which requires determination of

g_{oo} even terms in ε, lowest order ε^2~mas

g_{oj} odd terms in ε, lowest order ε^3~μ-as

g_{ij} even terms in ε, lowest order ε^2~mas

The small curvature limit in General Relativity may not coincide with the Newtonian regime

need to compare the GR model and the classical one

Lesson from the past

- Neptune as “dark” planet in the orbit of Uranus….a new “Newtonian” planet!

1846 observed by Johann Galle within a degree from the position predicted by Le Verrier

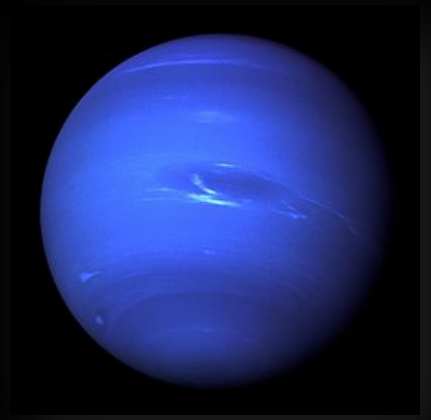

- advancement of Mercury’s perihelion: instead of correcting the dynamics by adding a "dark planet" (Vulcano) following the case of Neptune, GR cured the anomalous precession by accounting for the weak non-linear gravitational fields overlapping nearby the Sun.

It amounts to only 43"/century, because of the small curvature, however the effect was ”strong” enough to justify a modification of the Newtonian theory

excess of the perihelion shift of Mercury 43”/100yr

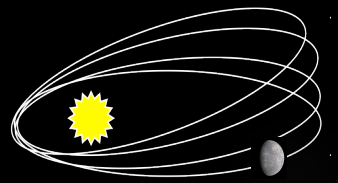

Lense-Thirring effect, the distortion of space-time due to rotating masses: new (weak) relativistic effect!

Lense-Thirring effect

”Classic” Milky Way (MWC) model with NFW dark matter halo

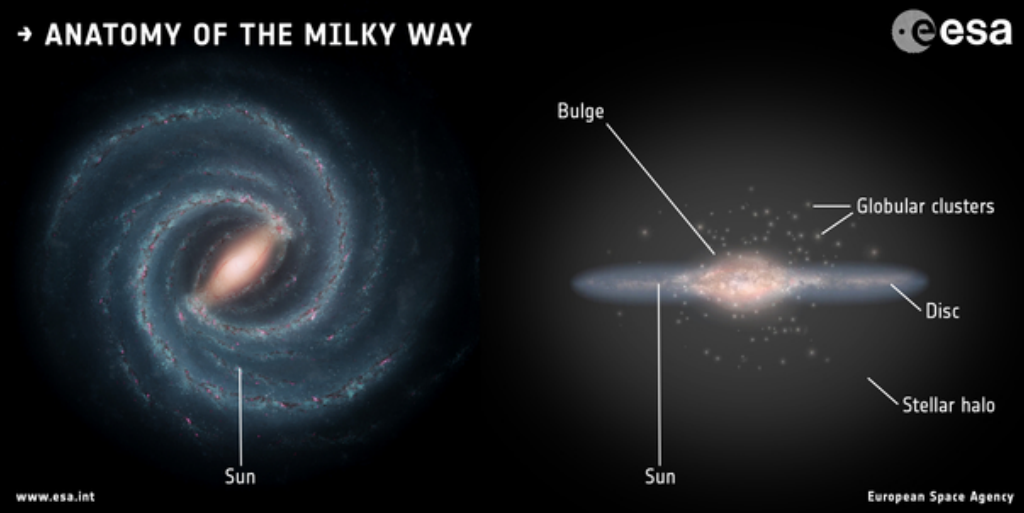

- Newtonian limit applied for Galactic dynamics -> Poisson’s equation

$$\nabla^2\Phi_{tot} = 4\pi G(\rho_b + \rho_{td} + \rho_{Td} + \rho_h)$$

1. Plummer **bulge**

$$\rho_b = \frac{3b_b^2 M_b}{4\pi(r^2 + b_b^2)^{5/2}}$$

Pouliasis, E., Di Matteo, P.

Haywood, M. 2017, A&A, 598, A66

2. Miyamoto-Nagai **thin and thick discs**

$$\rho_d(R,z) = \frac{M_d b_d^2}{4\pi} \frac{\left[a_d R^2 + (a_d + 3\sqrt{z^2 + b_d^2})(a_d + \sqrt{z^2 + b_d^2})^2\right]}{\left[R^2 + (a_d + \sqrt{z^2 + b_d^2})^2\right]^{5/2} (z^2 + b_d^2)^{3/2}}$$

Bovy, J. 2015, ApJs, 216, 29
Korol, Rossi & Barausse (2019)

3. **Navarro-Frank-White DM halo**

$$\rho_h(r) = \rho_0^{halo} \frac{1}{(r/A_h)(1 + r/A_h)^2}$$

McMillan, P. J. 2017, MNRAS, 465, 76-94

Navarro, J. F., Frenk, C. S. and White, S. D. M. 1996, ApJ, 462, 563

M_b, M_{td}, M_{Td}, a_{td}, a_{Td} , b_b, bd, ρ_0^{halo} and **A_h** correspond to the bulge mass, the masses and the scale lengths/heights of the thin and thick discs, the halo scale density, and the halo radial scale

$$\nabla^2\Phi_{tot} = 4\pi G(\rho_b + \rho_{td} + \rho_{Td} + \rho_h) \quad \Rightarrow \quad V_c^2 = R\left(d\Phi_{tot}/dR\right)$$

MWC velocity profile

MOND

Same baryonic distribution of MWC

EINASTO DENSITY PROFILE

$$\mathbf{g}_{MOND} = \eta\left(\frac{g_N}{g_0}\right)\mathbf{g}_0$$

gravitational acceleration

g_N conventional Newtonian acceleration, baryonic matter alone

$$\eta\left(\frac{g_N}{g_0}\right) = (1 - e^{-\sqrt{g_N/g_0}})^{-1}$$

interpolation function

setting the transition between the Newtonian and the deep MOND regimes through the acceleration scale g_0

$$\mathbf{g_0} = (\mathbf{1.20 \pm 0.02})\mathbf{10^{-10}ms^{-2}}$$

acceleration scale

constrained by the observed Radial Acceleration Relation of external galaxies (Lelli et al. 2017)

gravitational acceleration g_{MOND} = centripetal acceleration

$$V_{MOND}(R, V_{bar}) = \frac{V_{bar}}{\sqrt{1 - e^{-V_{bar}/\sqrt{Rg_0}}}}$$

$$\rho_{\mathrm{Einasto}}(r) = \rho_s \exp\left\{-\frac{2}{\alpha}\left[\left(\frac{r}{r_s}\right)^{\alpha} - 1\right]\right\}$$

Cold dark matter distribution

parameters of the Einasto profile

$C_{200} \equiv r_{200}/r_s$. **halo concentration** Li et al. (2019)

virial radius r_{200}: the enclosed average density is 200 times the critical density of the Universe (Planck Collaboration et al. 2014; Dutton & Maccio` 2014)

$$V_{200} = 10 C_{200} r_s H_0$$ **rotation velocity**

$$M_{200} = \frac{V_{200}^3}{10 G^2 H_0^2}$$ **enclosed halo mass at the virial radius**

GR model for the Milky Way

Einstein equation are very difficult to solve analytically and Galaxy is a multi-structured object making it even the more difficult to detail a metric for the whole Galaxy

in a stationary and axisymmetric space-time there exist two commuting Killing vector fields, **k** (time-like) and **m** (always zero on the axis of symmetry), and a coordinate system adapted to the symmetries whose line element takes the form (Stephani et al.2009, de Felice & Clarke 1990)

Lewis-Weyl-Papapetrou class

$$ds^2 = -e^{2U}(dt + Nd\phi)^2 + e^{-2U}\left[e^{\nu}\left(dr^2 + udz^2\right) + r^2 d\phi^2\right]$$

$$m^{\alpha} = \partial^{\alpha}_{\phi},\ k^{\alpha} = \partial^{\alpha}_{t},\ \partial_t g_{ij} = \partial_{\phi} g_{ij} = 0,\ g_{\phi a} = g_{ta} = 0,$$

$$-e^{2U} = (k|k),\ -Ae^{2U} = (k|m),\ e^{-2U}W^2 - A^2 e^{2U} = (m|m).$$

Regularity condition, if violated singularities on the axis

$$\lim_{r\to 0}\ \left[r^{-1}e^{U-\gamma}(e^{-2U}W^2 - e^{2U}A^2)^{1/2}\right] = 1$$

Galactic metric-disc

Stationarity and axisymmetry spacetime

Reflection symmetry (around the galactic plane)

$|z| < r_{in}$

Masses inside a large portion of the Galaxy interact only gravitationally and reside far from the central bulge region

GR model for the Milky Way disc

$$2r\gamma_z + e^{4U} A_r A_z - 2r^2 U_r U_z = 0$$

$$4r\gamma_r + e^{4U}\left(A_r^2 - A_z^2\right) - r^2\left(U_r^2 - U_z^2\right) = 0$$

$$4r^2\left(\gamma_{rr} + \gamma_{zz}\right) + e^{4U}\left(A_r^2 + A_z^2\right) + 4r^2\left(U_r^2 + U_z^2\right) = 0$$

$$A_{rr} + A_{zz} - \frac{A_r}{r} + 4\left(A_r U_r + A_z U_z\right) = 0$$

$$2U_{rr} + 2U_{zz} + \frac{2U_r}{r} + \frac{e^{4U}}{r^2}\left(A_r^2 + A_z^2\right) = 8\pi G\rho e^{2\gamma}$$

$$T^{\mu\nu} = \rho u^\mu u^\nu$$

$$\nabla_\mu(\rho u^\mu) = 0 \qquad u^\mu \nabla_\mu u^\nu = 0$$

The Bianchi identities imply stationarity of the mass distribution and that dust particles follow geodesics

Galactic metric-disc

Stationarity and axisymmetry spacetime

Reflection symmetry (around the galactic plane)

Disc is an equilibrium configuration of a pressure-less rotating perfect fluid (a GR dust)

Masses inside a large portion of the Galaxy interact only gravitationally and reside far from the central bulge region

Stellar encounters become effective below the parsec scale, on the other hand the Galaxy could be considered globally isolated around 25 kpc.

Observer in circular motion

$$u^\alpha = \Gamma\left(k^\alpha + \beta m^\alpha\right)$$

β coordinate angular velocity, Γ normalization factor

or

$$u^\alpha = \gamma\left(e^\alpha_{\hat{0}} + \zeta^{\hat{\phi}} e^\alpha_{\hat{\phi}}\right)$$

orthonormal frame adapted to the ZAMO

ZAMO frames = locally non-rotating observers, move on worldlines orthogonal to the hypersurfaces t=constant

(de Felice and Bini, "Classical measurements in curved space-time")

$$\gamma = M\Gamma$$

γ Lorentz factor

$$Z^\alpha = (1/M)(\partial_t - M^\phi \partial_\phi)$$

a suitable foliation of the space time manifold that reflects the assumed symmetries

spatial velocity w.r.t the local non-rotating observer

non local correlation of local time, namely synchronisation of times in different points of space

$$\zeta^{\hat{\phi}} = \frac{\sqrt{g_{\phi\phi}}}{M}(\beta + M^\phi) = \zeta^{\hat{\phi}}_k + \zeta^{\hat{\phi}}_d$$

$$ds^2 = -M^2 dt^2 + (r^2 - N^2)\left(d\phi + M^\phi dt\right)^2 + e^\nu(dr^2 + dz^2)$$

Crosta M., Giammaria M., Lattanzi M. G., Poggio E., (2020)

Geometric terms

β coordinate angular velocity

$$\zeta^{\hat{\phi}}_k = \frac{\sqrt{g_{\phi\phi}}}{M}\beta \qquad \zeta^{\hat{\phi}}_d = \frac{\sqrt{g_{\phi\phi}}}{M}M^\phi$$

Relativistic kinematics, valid regardless the adopted exact solution

GR model for the Milky Way disc

Denoting A= -*N*(*r*,*z*), $e^{2U}=1$, $e^{2\gamma}=e^{\nu}$ -> rigidly rotation dust

$$ds^2 = -(dt - Nd\phi)^2 + r^2 d\phi^2 + e^{\nu}(dr^2 + dz^2)$$

the function *N*(*r*,*z*) was solved by Balasin & Grumiller (BG)

$$N(r,z) = V_0(R_{out} - r_{in}) + \frac{V_0}{2}\sum_{\pm}\left(\sqrt{(z \pm r_{in})^2 + r^2} - \sqrt{(z \pm R_{out})^2 + r^2}\right)$$

(Balasin and Grummiler, Int.J. Mod. Phys., 2008)

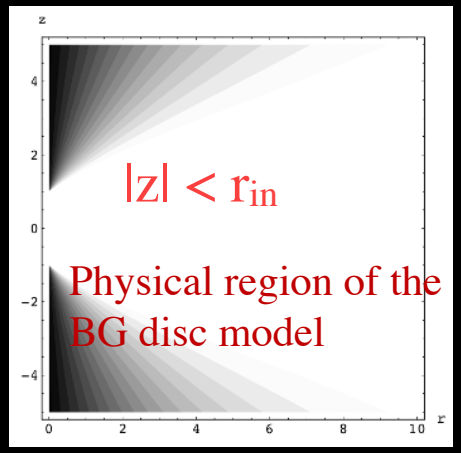

✓Einstein equation allows to treat separately velocities and density

$$r\partial_z\nu + \partial_r N\partial_z N = 0$$

$$2r\partial_r\nu + (\partial_r N)^2 - (\partial_z N)^2 = 0$$

$$2r^2(\partial_r\partial_r\nu + \partial_z\partial_z\nu) + (\partial_r N)^2 + (\partial_z N)^2 = 0$$

$$r(\partial_r\partial_r N + \partial_z\partial_z N) - \partial_r N = 0$$

$$(\partial_r N)^2 + (\partial_z N)^2 = kr^2\rho e^{\nu}$$

Einstein field Eq.

$$\rho(R,z) = e^{-\nu(R,z)}\frac{1}{8\pi R^2}\left[\left(\partial_R N(R,z)\right)^2 + \left(\partial_z N(R,z)\right)^2\right]$$

- physical boundaries: for r >> N, far from r = 0, and |z| < r_{in}
  - **r_{in} = bulge size**
  - **R_{out} = extension of the MW disk-> Galaxy size**
  - **V_0 = velocity in the flat regime**
  - **+ $e^{\nu(r,z)}$ conformal factor (new parameter)**

Stationarity and axisymmetry spacetime may include Kerr solution for the bulge as well as different disc solutions

Regions around the bulge and the bar need relativistic hydrodynamics, where equilibrium conditions are not possible

$$\zeta^{\hat{\phi}} = \frac{\sqrt{g_{\phi\phi}}}{M}(\beta + M^{\phi})$$

If β is negligible or zero

$$\zeta_d^{\hat{\phi}}(r,z) = N(r,z)/r \propto g_{0\phi}$$

Different from the IAU metric!

Gravitational dragging working at disc scale?

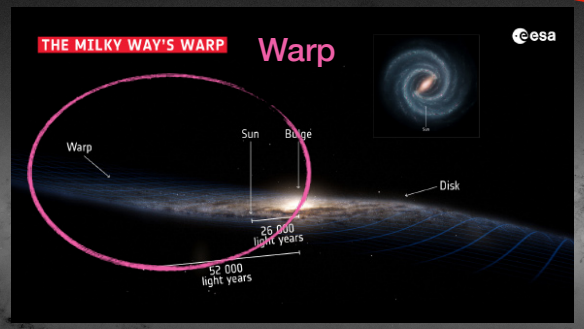

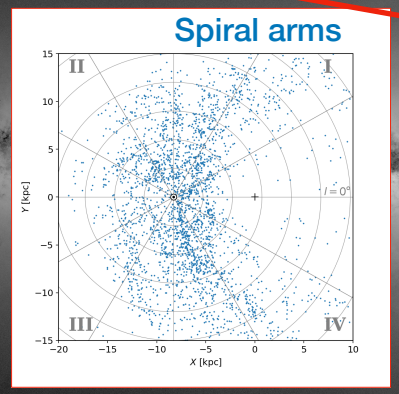

MW core
Relativistic hydrodynamics for the bulge/bar?

Disc

Flaring?

Streams?

On testing CDM and geometry-driven Milky Way rotation curve models with *Gaia* DR2- Crosta M., Giammaria M., Lattanzi M. G., Poggio E.,MNRAS, Volume 496, Issue 2, August 2020, Pages 2107–2122

The Galaxy is a multistructured object, global solutions are unrealistic

Peering into hidden parts is utmost fundamental to establish boundary matching conditions between internal/external Einstein's solutions

Our ansatz: the flatness of MW rotation curve is geometry driven?

-> the rotation curve of the MW used as a first test for a GR Galaxy

Further considerations

- **3 congruences of observers within our framework**:

i) the local barycentric observer tied to the BCRS metric (based on the post-Newtonian approximation to GR) and RAMOD modelling for Gaia (based on the measurement protocol in GR involving splitting formalism)

ii) the co-rotating static observer associated with the BG metric in the stationary axisymmetric spacetime

iii) the ZAMO observers, which locally do not rotate with respect to the local geometry

- It is expected that the static observer and the locally barycentric observer at infinity coincide. However, the BCRS is connected to a quasi-inertial rather than inertial system. Therefore, **our ansatz could turn into verifying whether asymptotically these observers can indeed coincide.**

- Quoting Jantzen et al. (1992): stationary axisymmetric spacetimes possess both a preferred threading by a time-like Killing vector field (i.e., the static observers), and a preferred slicing by a family of space-like hypersurfaces orthogonal to the ZAMOs. For the former local time direction is fundamental, for the latter space is fundamental (**non local correlation of local time, namely synchronisation of times in different points of space**).

- In this context, the **ZAMOs are employed as gauges of a potential dragging**. The local barycentric observer aligns at infinity with the congruence of curves that are orthonormal, vorticity-free and expansion-free -> the threading and slicing point of views coincide

- With static dust, this relative spatial velocity inherently reflects the angular velocity attributed solely to the gravitational dragging effects within the BG spacetime -> **our assumption is to compare this rotational velocity with the observed rotation curve measured by Gaia, i.e. with respect to an observer at rest w.r.t. distant quasars**

Data sample: full reconstruction of disc kinematics based on Gaia data only

i. **Complete Gaia astrometric dataset** ($\alpha, \delta, \mu_\alpha, \mu_\delta$, parallax) and corresponding covariance matrix
ii. **Three Gaia photometric bands (G, BP, RP**) all available and RUWE < 1.4 [to discard sources with problematic astrometric solutions, astrometric binaries, and other anomalous cases]
iii. **Parallaxes good to 20%** (i.e. parallax_over_error ≥ 5) [parallaxes to better than 20% allow to deal with similar (quasi–gaussian) statistics when transforming to distances]
iv. **Gaia-measured** velocity along the line of sight, i.e. **radial velocity, with better than 20% uncertainties**

i.+ii.+iii.+iv—> proper 6D reconstruction of the phase-space location occupied by each individual star as derived by the same observer

1. Full transformation (including complete error propagation) from the ICRS equatorial to heliocentric galactic coordinates
2. translation to the galactic center

-> independency from the local standard of rest.

angular-momentum sustained stellar population of the Milky Way that better traces its observed RC

DR2: **very homogenous sample of 5277 early type stars and 325 classical type I Cepheids.**

DR3: **a much larger sample of high-quality astrometric and spectro-photometric data of unprecedented homogeneity of**
719143 young disc stars within |z| < 1 kpc and up to R = 19 kpc
241'918 OBA stars, 475'520 RGB giants, and 1'705 Cepheides
radial cut at 4.5 kpc to avoid the bar influence

v. Cross-matched entry in the 2MASS catalogue for the actual characterization of the sample in case of DR2 and EDR3

Ref: On testing CDM and geometry-driven Milky Way rotation curve models with *Gaia* DR2- Crosta M., Giammaria M., Lattanzi M. G., Poggio E.,MNRAS, Volume 496, Issue 2, August 2020, Pages 2107–2122

Gaia DR3 disc tracers

From ~33 million stars with high-precision astrometry and spectroscopic LOS velocities, we focus on three disc populations, namely:

O-,B-,A-type stars	Red Giants	Classical Cepheids
6D phase space: 5 astrometric parameters + spectroscopic radial velocities		
Trigonometric distances (parallax error < 20%)		Photometric distances
Kinematic selection: thin disk stars with low velocity dispersion, to minimize possible halo contaminants $\sqrt{V_R^2 + (V_\phi - V_\phi^{LSR})^2 + V_z^2} < 180 \ \mathrm{km\,s^{-1}}$	Disc-like kinematics and nearly-circular orbits (eccentricity < 0.1) $\lvert V_R \rvert < 50\,\mathrm{km\,s^{-1}}$ $\lvert V_z \rvert < 30\,\mathrm{km\,s^{-1}}$ and $100 < V_\phi < 350\,\mathrm{km\,s^{-1}}$	
Close to the galactic plane and far from the bar: $\lvert z \rvert < 1\ kpc$ and $R > 4.5\ kpc$		

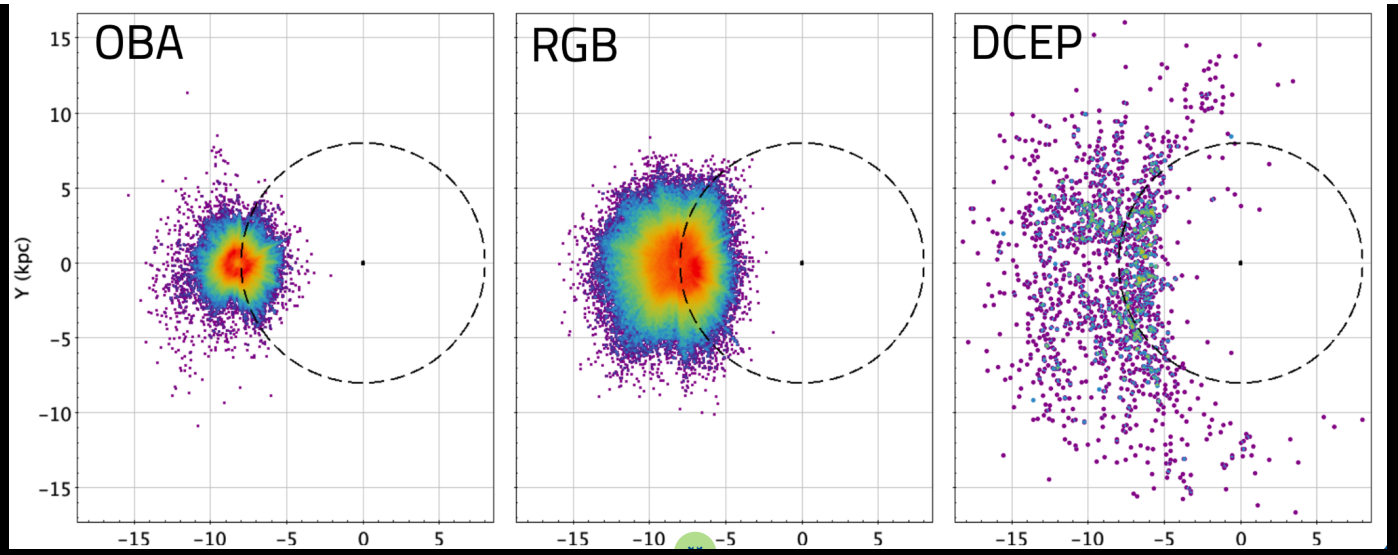

Spatial distribution for the three samples of tracers. OBA stars, RGB giants with (quasi) circular orbits, DCEP in the Galactic plane. The position of the Galactic centre is shown by the black dot on the right; the dashed line represents a Galactocentric circle passing through the Sun's position at (x,y)=(-8.249 kpc, 0 kpc).

To avoid the influence of the MW bar a radial cut at 4.5 kpc is set, while halo stars are further discarded requiring |z|<1 kpc. The final sample comprises 719'143 stars including 241'918 OBA, 475'520 RGB and 1'705 DCEP.

MCMC fit with DR2 data

Best fit estimates as the median of the posteriors and their 1σ level credible interval

BG model	θ	σ_θ^-	σ_θ^+
r_{in} [kpc]	0.39	-0.25	+0.36
R_{out} [kpc]	47.87	-14.80	+23.96
V_0 [km/s]	263.10	-16.44	+25.93
$e^{-\nu}$ [$\cdot 10^{-7}$]	3.59	-0.47	+0.65

MWC model	θ	σ_θ^-	σ_θ^+
$M_b[10^{10}\mathrm{M}_\odot]$	1.0	-0.4	+0.4
$M_{td}[10^{10}\mathrm{M}_\odot]$	3.9	-0.4	+0.4
$M_{Td}[10^{10}\mathrm{M}_\odot]$	4.0	-0.5	+0.5
a_{td}[kpc]	5.2	-0.5	+0.5
a_{Td}[kpc]	2.7	-0.4	+0.4
$\rho_0^{halo}[\mathrm{M}_\odot \mathrm{pc}^{-3}]$	0.009	-0.003	+0.004
A_h [kpc]	17	-3	+4

Stars = dust grains in axysimmetric and stationary spacetime (circular motion)

5277 **early-type stars** e **325 classical type I Cepheides**

parallax/sigma_parallax > 5

RV/sigma_RV > 5 dalla Gaia DR2

Velocity profiles - Classical (MWC) and GR (BG) RC

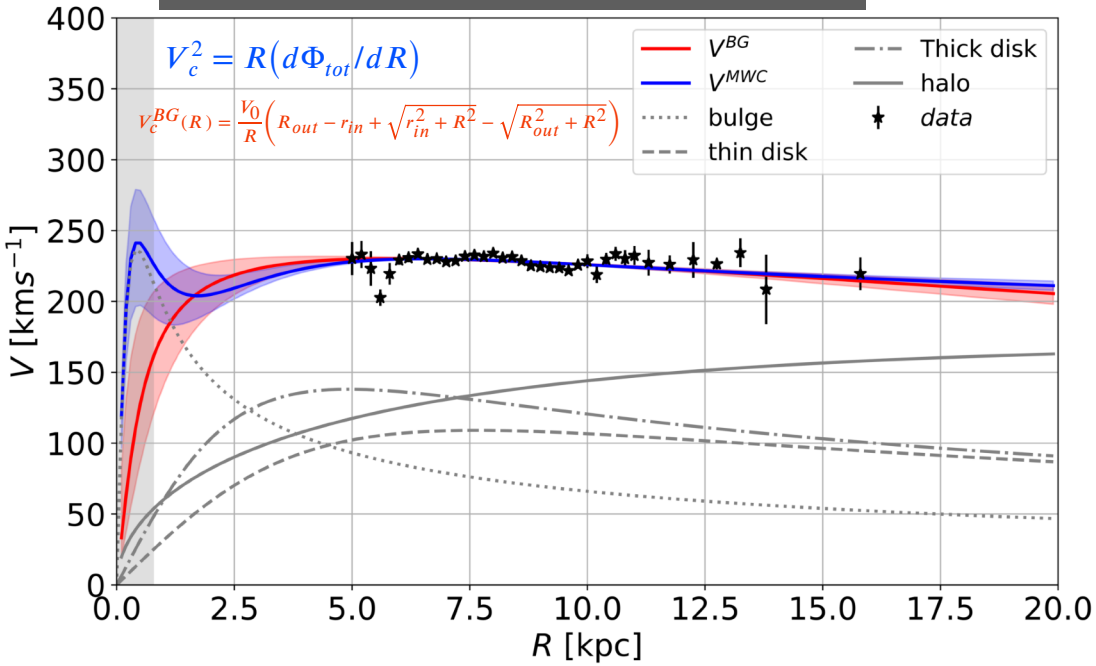

barionic density profiles: relativistic (red)/classic (blu)

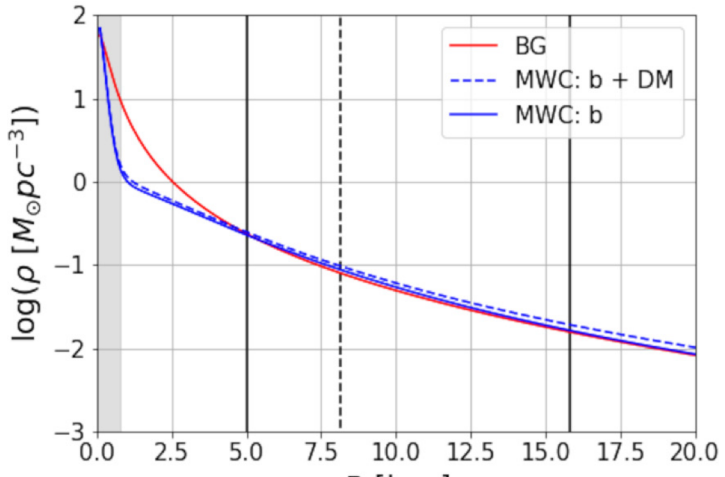

Dragging effect vs. halo effect

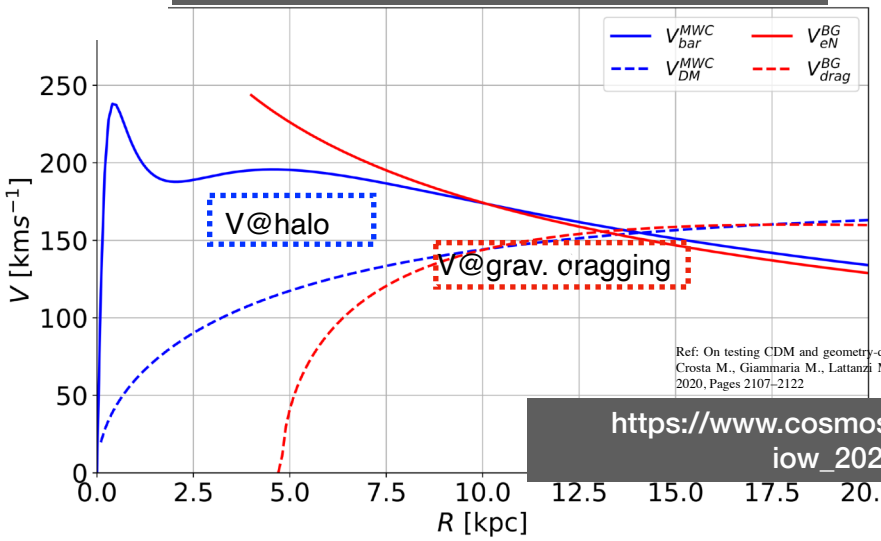

Ref: On testing CDM and geometry-driven Milky Way rotation curve models with *Gaia* DR2-Crosta M., Giammaria M., Lattanzi M. G., Poggio E.,MNRAS, Volume 496, Issue 2, August 2020, Pages 2107–2122

https://www.cosmos.esa.int/web/gaia/iow_20200716)

MCMC fit to the Gaia DR3 data - Classical (MWC) MOND, **EINASTO** GR
I.Results: azimuthal velocity profile of the MW

The red, blue, green, and yellow curves show the best-fitting to the BG, MWC, MOND, and ΛCDM models, respectively

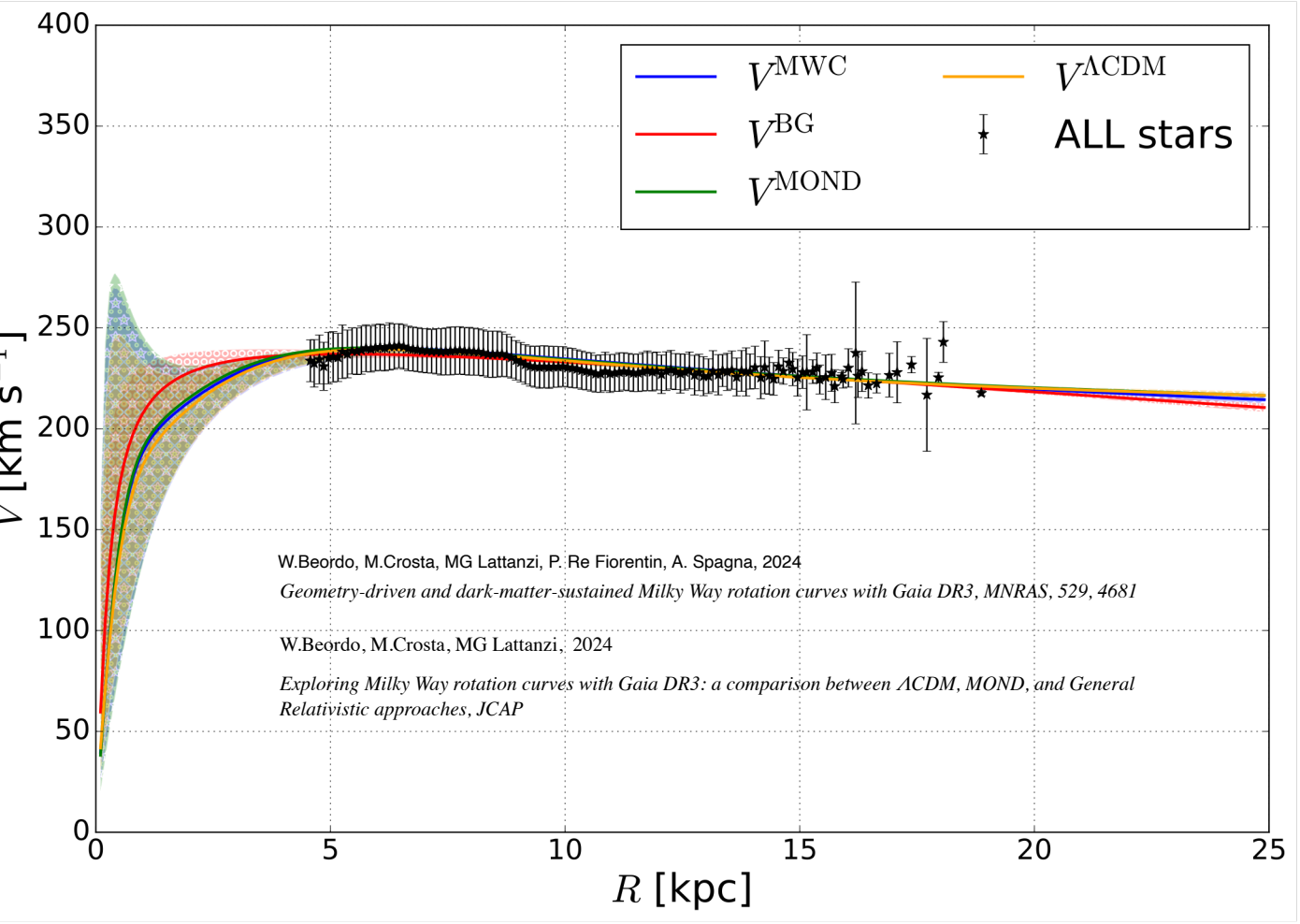

The four velocity profiles are all good representations of the observed (binned) data. **The four models are found to be statistically equivalent**

comparisons with the WAIC and LOO tests show almost identical values

- Black starred symbols represent the median azimuthal velocity at the median distance from the galactic centre of the stellar population within each of the radial bins
- Robust Scatter Estimate (RSE) adopted as a robust measure of the azimuthal velocity dispersion of the population in each radial bin
- The filled areas represent the 68 per cent reliability intervals of each rotation curve
- For R ≲ 4.5 kpc both the classical and the relativistic curves are very uncertain because of the lack of data in that region

MCMC fit to the Gaia DR3 data - Classical (MWC) and GR (BG) RC- velocity profile for each sample

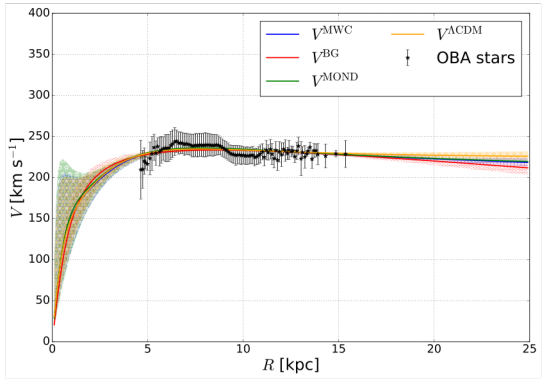

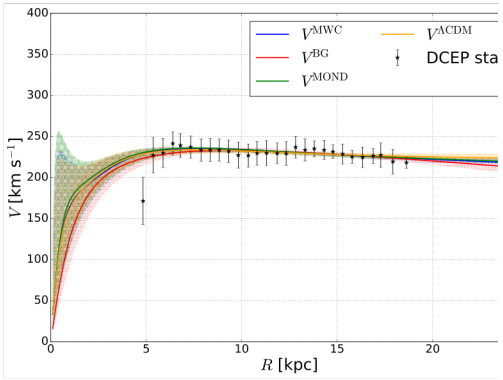

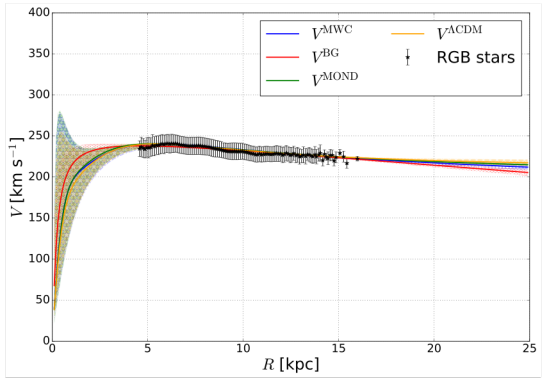

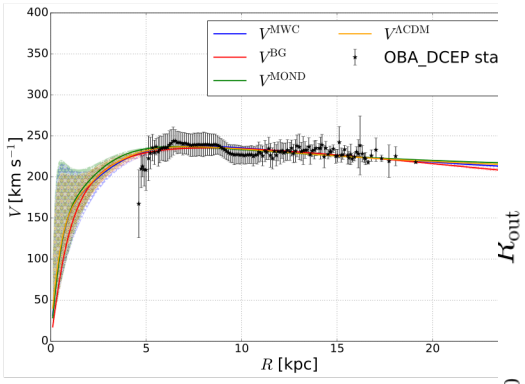

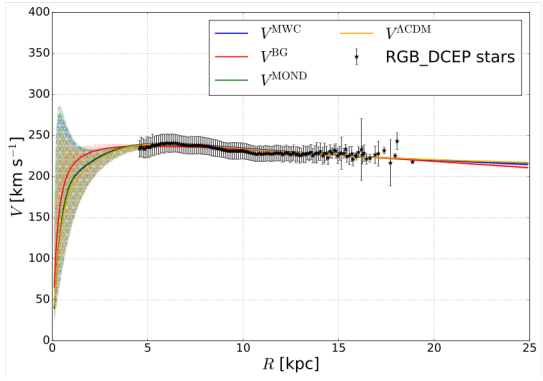

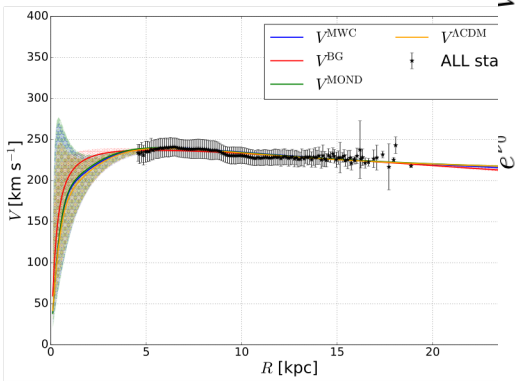

BG model	
r_0 [kpc]	$0.20^{+0.18}_{-0.13}$
R [kpc]	71^{+13}_{-11}
V_0 [km/s]	256^{+10}_{-7}

best-fit estimates
the medians of the posteriors
and their 1σ credible intervals

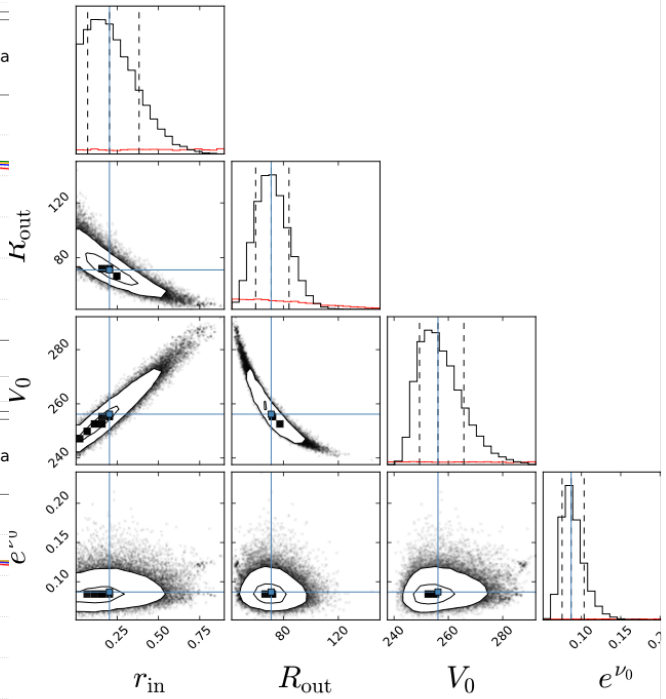

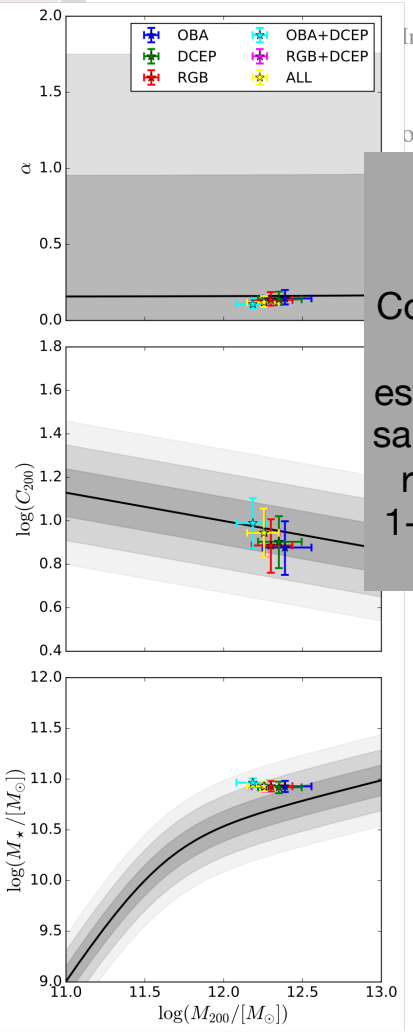

Black lines ΛCDM cosmological priors.

Coloured data points are the best parameter estimates for each stellar sample. The shaded grey regions represent the 1-,2-,3-σ ranges around the mean relations.

MCMC fit to the Gaia DR3 data - II. Results: radial density profile of the MW at z=0

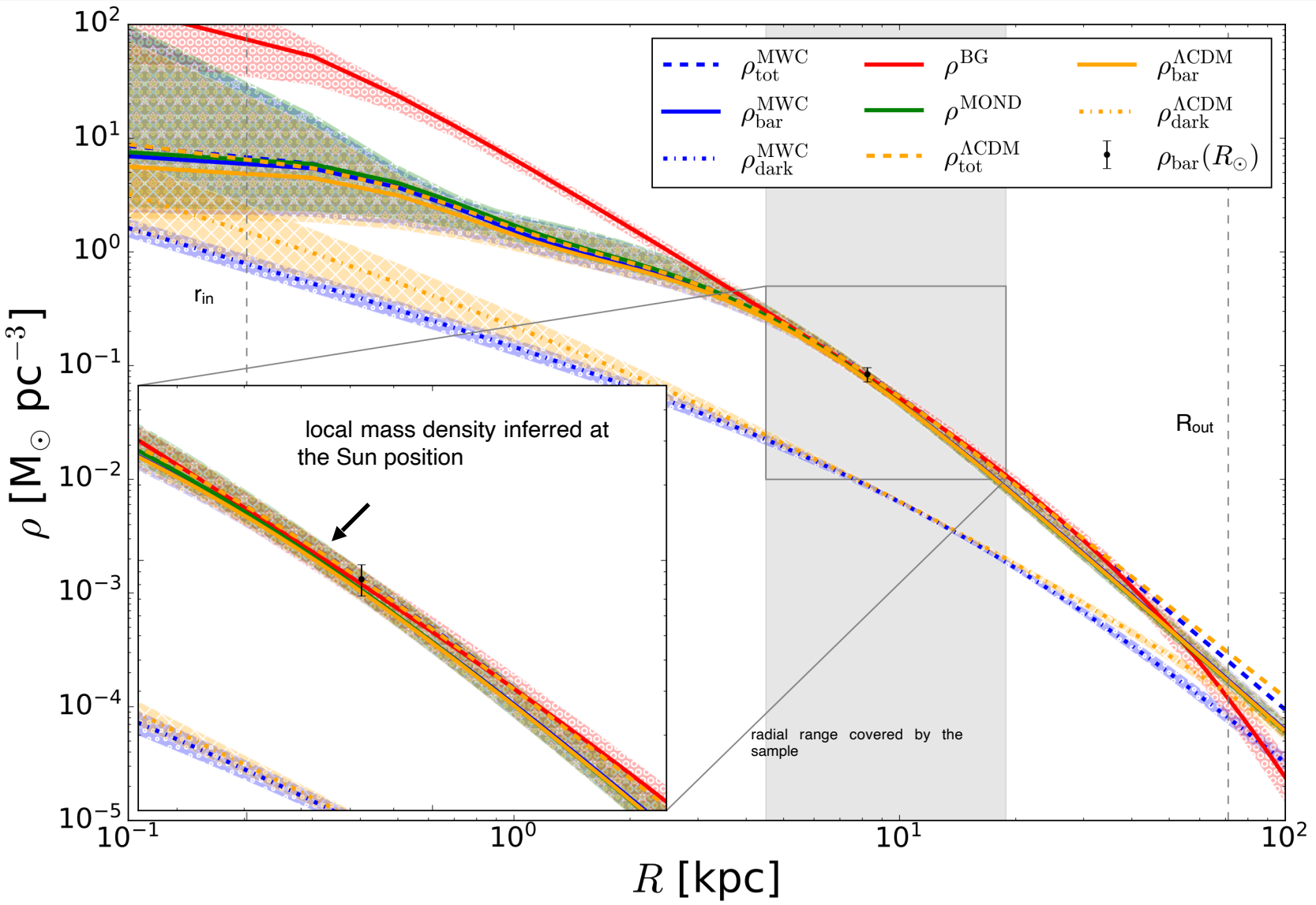

solid lines baryonic matter contributions

MWC and ΛCDM total matter density profiles (dashed lines) are almost coincident while departing from each other only at very large radii

Einasto profile of the ΛCDM model results larger than the NFW one both in the inner and outer parts of the Galaxy (dash-dotted lines)- > **more dark matter in the ΛCDM scenario compared to the case of an NFW halo** without cosmological constraints

BG and MOND density profiles are **consistent with** both the baryonic and total density profiles of **MWC**

baryonic matter density observed at the Sun

$\varrho_{\rm bar}(R_\odot) = 0.084 \pm 0.012\ M_\odot pc^{-3}$

estimates of the local baryonic density $\varrho^{\Lambda\rm CDM}$ and $\varrho^{\rm MOND}$ around $0.080 M_\odot pc^{-3}$

Crosta et. al, 2020, Beordo et al. 2024, Garbari et al. 2012; Bienaymé et al. 2014; McKee et al. 2015

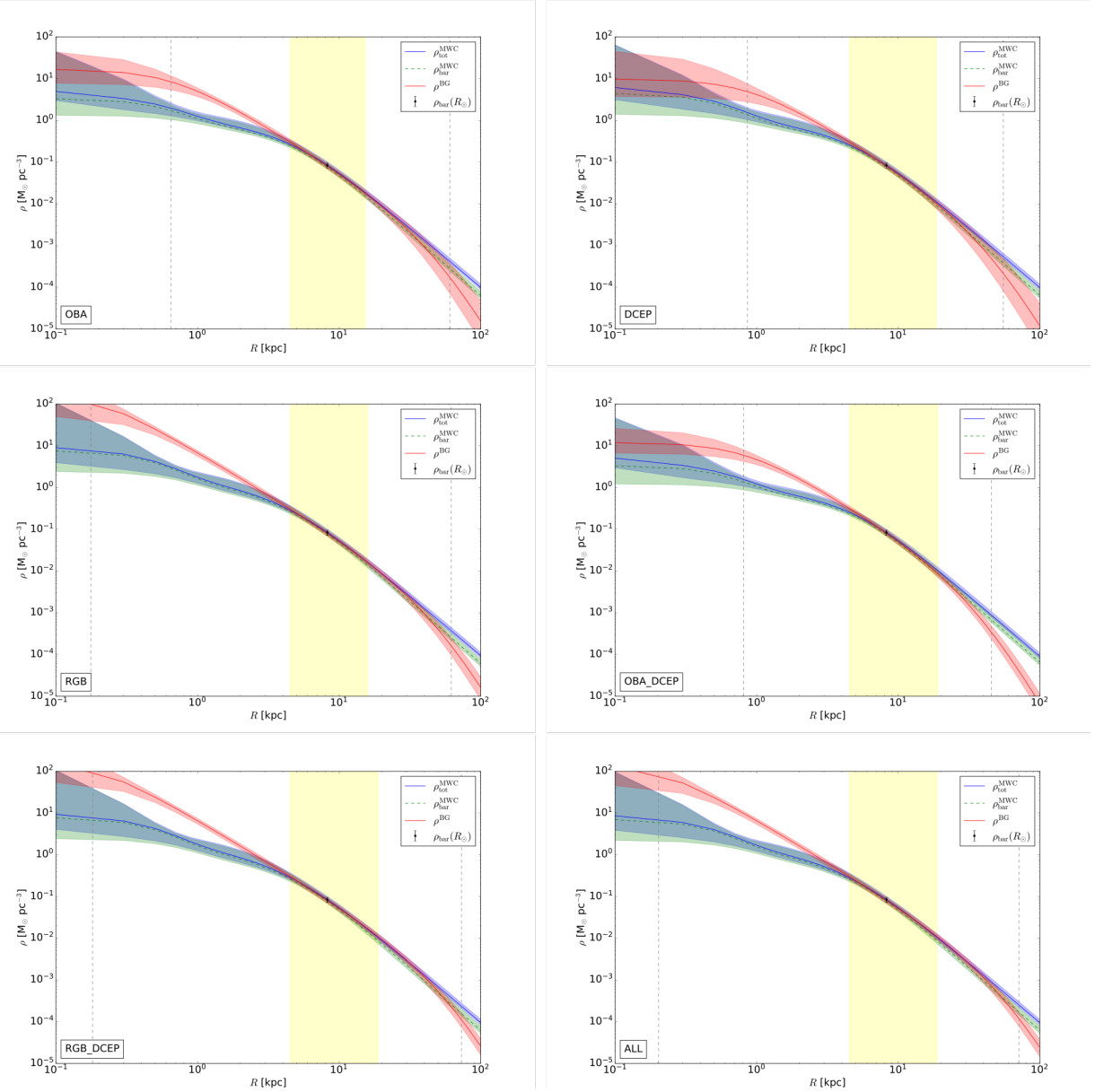

barionic density profiles: relativistic (red)/classic (blu)

In the radial range probed by DR3, the relativistic mass density profile is consistent within 1σ of the total mass density profile and that of the baryonic-only contribution (derived by fitting to the classical model)

In agreement, with current independent estimates

$0.077 \pm 0.007\ M_{sun}\, pc^{-3}$
(Bienayme et al. 2014, A&A, 571)

$0.084 \pm 0.012\ M_{sun}\, pc^{-3}$
(McKee et al. 2015, ApJ, 814, 13)

$0.098^{+0.006}\ M_{sun}\, pc^{-3}$
(Garbari et al. 2012MNRAS, 425, 1445)

Eilers et al. 2019; Wang et al. 2022; Cautun et al. 2020; Widmark et al. 2021

$$\log \mathcal{L} = -\frac{1}{2}\sum_i \left(\frac{\left[V_\phi(R_i) - V_\phi^{\exp}(R_i|\theta)\right]^2}{\sigma^2_{V_\phi}} + \log\left(\sigma^2_{V_\phi}\right) \right) - \frac{1}{2}\left(\frac{\left[\rho(R_\odot) - \rho^{\exp}(R_\odot|\theta)\right]^2}{\sigma^2_{\rho_\odot}} + \log\left(\sigma^2_{\rho_\odot}\right) \right),$$

$$\rho(R,z) = e^{-\nu(R,z)} \frac{1}{8\pi R^2}\left[\left(\partial_R N(R,z)\right)^2 + \left(\partial_z N(R,z)\right)^2\right]$$

Only one reliable estimate for the baryonic matter density

$$\frac{1}{r^2}\left(N_r^2 + N_z^2\right) = k\rho e^{\nu}$$

BG model	
e^{ν_0}	0.09 ± 0.01

→ We can constrain $e^{\nu(r,z)}$ only at the Sun (e^{ν_0})

Komar integral: $$M = -2\int (T_0^0 - \frac{1}{2}T)\sqrt{-g}\ d^3x,$$

$M_{\rm bar}^{\rm MWC}\ [10^{10}\,M_\odot] \sim 1.48$

$M^{\rm BG}\ [10^{10}\,M_\odot] \sim 1.54$

- Relativistic mass in agreement with the baryonic mass within the region of validity of the model

MCMC fit to the Gaia DR3 data - III. Results: Total mass estimates

Density profile in agreement between all four models within the region of validity of BG

The **total** baryonic mass predicted by the ΛCDM scenario is slightly smaller than the values expected for the MWC and MOND models

The dynamical mass is supplied by more dark matter in the ΛCDM scenario compared to a NWF halo without cosmological constraints

Quantity	OBA	DCEP	RGB	OBA + DCEP	RGB + DCEP	ALL
$\rho^{\rm MWC}_{\rm bar,\odot}$ [$M_\odot\,pc^{-3}$]	$0.080^{+0.012}_{-0.012}$	$0.080^{+0.012}_{-0.012}$	$0.080^{+0.012}_{-0.012}$	$0.080^{+0.012}_{-0.012}$	$0.080^{+0.012}_{-0.012}$	$0.080^{+0.012}_{-0.012}$
$\rho^{\rm MWC}_{\rm h,\odot}$ [$M_\odot\,pc^{-3}$]	$0.0092^{+0.0009}_{-0.0009}$	$0.0092^{+0.0009}_{-0.0009}$	$0.0084^{+0.0007}_{-0.0007}$	$0.0083^{+0.0007}_{-0.0007}$	$0.0088^{+0.0006}_{-0.0007}$	$0.0088^{+0.0006}_{-0.0007}$
$\rho^{\rm BG}_{\odot}$ [$M_\odot\,pc^{-3}$]	$0.080^{+0.012}_{-0.012}$	$0.080^{+0.013}_{-0.012}$	$0.080^{+0.013}_{-0.012}$	$0.081^{+0.012}_{-0.012}$	$0.080^{+0.012}_{-0.012}$	$0.080^{+0.012}_{-0.012}$
$M^{\rm MWC}_{\rm bar}$ [$10^{10}\,M_\odot$]	∼1.62	∼1.83	∼1.25	∼1.96	∼1.36	∼1.48
$M^{\rm BG}$ [$10^{10}\,M_\odot$]	∼1.81	∼2.39	∼1.11	∼2.37	∼1.39	∼1.54
$M^{\rm MWC}_{\star}$ [$10^{10}\,M_\odot$]	$9.24^{+1.07}_{-1.01}$	$9.30^{+1.12}_{-1.10}$	$9.35^{+0.95}_{-0.93}$	$10.15^{+0.99}_{-0.95}$	$9.22^{+0.94}_{-0.91}$	$9.27^{+0.90}_{-0.95}$
$M^{\rm MWC}_{\rm vir}$ [$10^{10}\,M_\odot$]	∼114	∼109	∼103	∼85	∼105	∼103
$R^{\rm MWC}_{\rm vir}$ [kpc]	∼222	∼218	∼214	∼201	∼216	∼215

(0.34 ± 0.02) GeV cm^{-3}

Quantity	OBA	DCEP	RGB	OBA + DCEP	RGB + DCEP	ALL
$\rho^{\Lambda\rm CDM}_{\rm bar,\odot}$ [$M_\odot pc^{-3}$]	$0.080^{+0.012}_{-0.012}$	$0.080^{+0.012}_{-0.012}$	$0.080^{+0.012}_{-0.012}$	$0.080^{+0.012}_{-0.012}$	$0.080^{+0.012}_{-0.012}$	$0.080^{+0.012}_{-0.012}$
$\rho^{\Lambda\rm CDM}_{\rm h,\odot}$ [$M_\odot pc^{-3}$]	$0.0099^{+0.0008}_{-0.0008}$	$0.0098^{+0.0008}_{-0.0008}$	$0.0088^{+0.0078}_{-0.0007}$	$0.0085^{+0.0006}_{-0.0006}$	$0.0091^{+0.0006}_{-0.0006}$	$0.0090^{+0.0006}_{-0.0006}$
$\rho^{\rm MOND}_{\odot}$ [$M_\odot pc^{-3}$]	$0.080^{+0.012}_{-0.012}$	$0.080^{+0.012}_{-0.012}$	$0.081^{+0.012}_{-0.012}$	$0.081^{+0.012}_{-0.012}$	$0.081^{+0.012}_{-0.012}$	$0.081^{+0.012}_{-0.012}$
$M^{\Lambda\rm CDM}_{\rm bar}$ [$10^{10}\,M_\odot$]	$8.49^{+1.10}_{-1.03}$	$8.31^{+1.11}_{-1.04}$	$8.51^{+1.06}_{-0.95}$	$9.23^{+0.95}_{-0.93}$	$8.43^{+0.96}_{-0.91}$	$8.49^{+0.96}_{-0.89}$
$M^{\rm MOND}$ [$10^{10}\,M_\odot$]	$10.12^{+0.33}_{-0.30}$	$10.05^{+0.48}_{-0.45}$	$9.32^{+0.27}_{-0.24}$	$9.59^{+0.19}_{-0.18}$	$9.59^{+0.21}_{-0.19}$	$9.56^{+0.21}_{-0.19}$
$M^{\Lambda\rm CDM}_{200}$ [$10^{12}\,M_\odot$]	$2.45^{+1.16}_{-0.68}$	$2.24^{+0.88}_{-0.59}$	$1.99^{+0.74}_{-0.49}$	$1.53^{+0.35}_{-0.33}$	$1.82^{+0.44}_{-0.40}$	$1.80^{+0.43}_{-0.39}$

Within the overlapping range of 10–18 kpc, our rotation curves exhibit slightly declining profiles, aligning with recent findings that indicate a pronounced decline only beyond 18–19 kpc

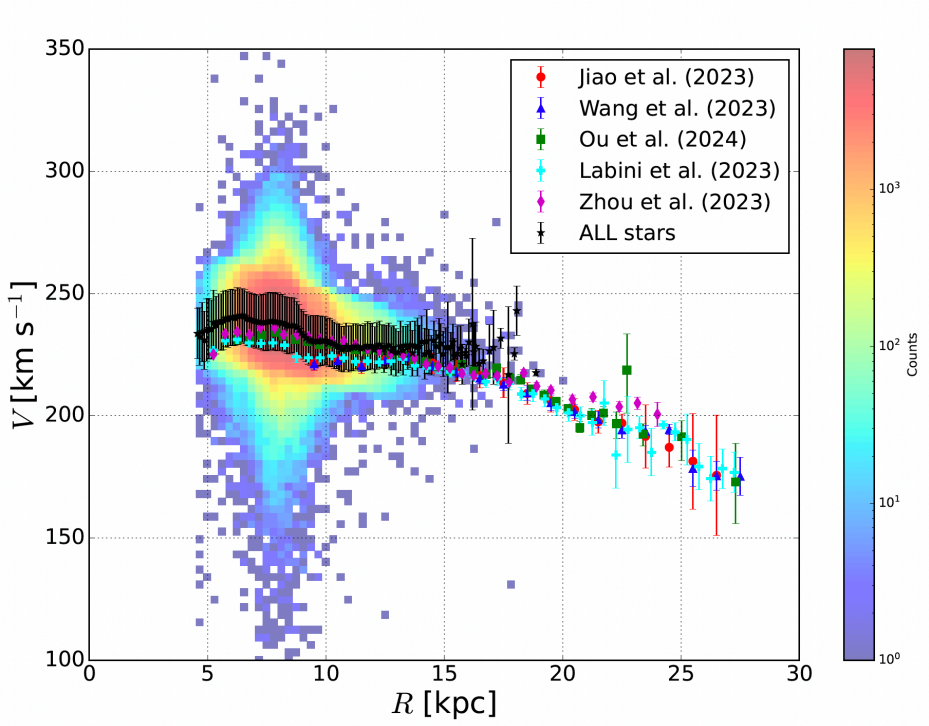

Instead of employing various techniques to extend the measured rotation curve to 30 kpc, we imposed a stringent requirement of errors on parallaxes smaller than 20%.

The Jeans analysis on our selected sample shows a further slight increase within error bars suggesting that the lack of the Jeans analysis in our procedure is unlikely to be the cause of the discrepancy observed at around 15 kpc.

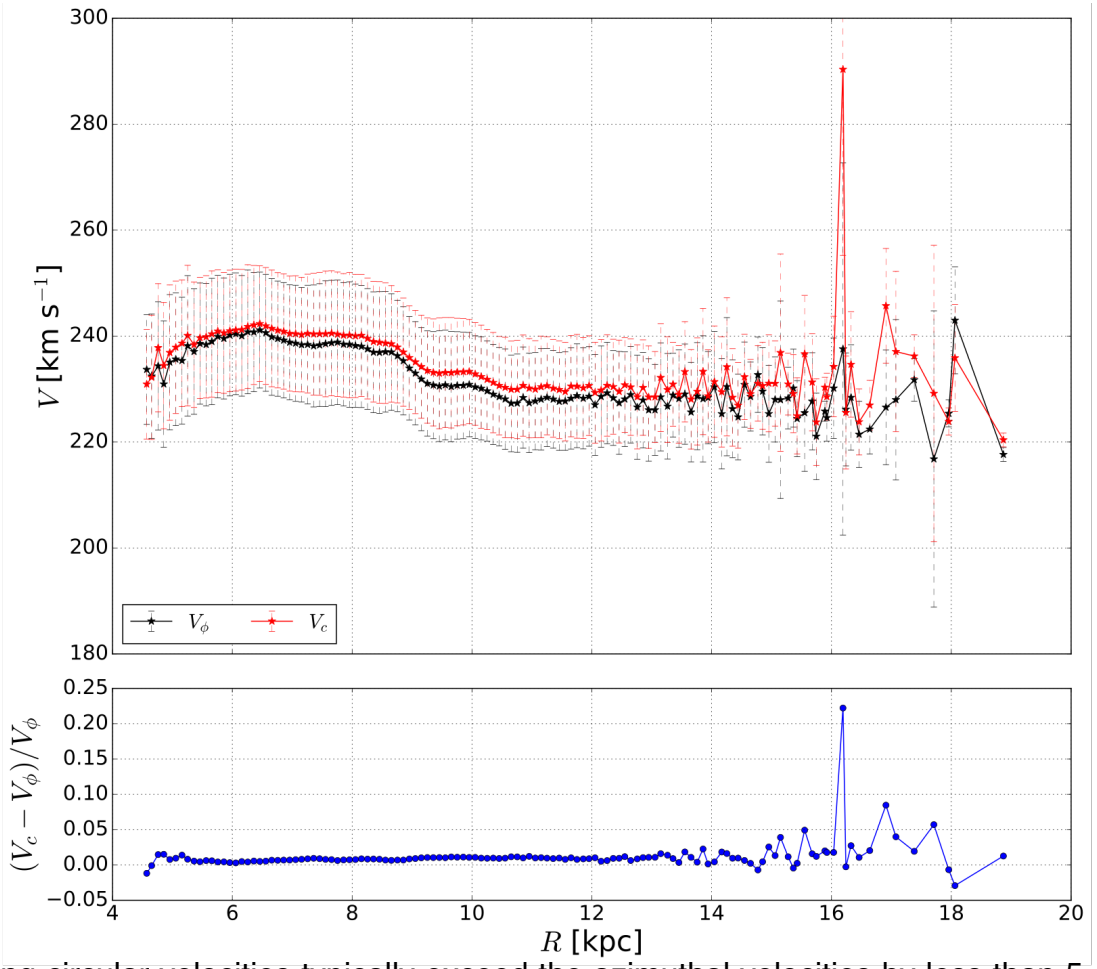

The resulting circular velocities typically exceed the azimuthal velocities by less than 5 per cent and fall well within the error bars- The eccentricity selection for the orbits of RGB stars removes the effects of the asymmetric drift to match the OBA and DCEP rotation curves

MCMC fit to the Gaia DR3 data - IV.Results: Non-Newtonian contributions vs dark matter halo

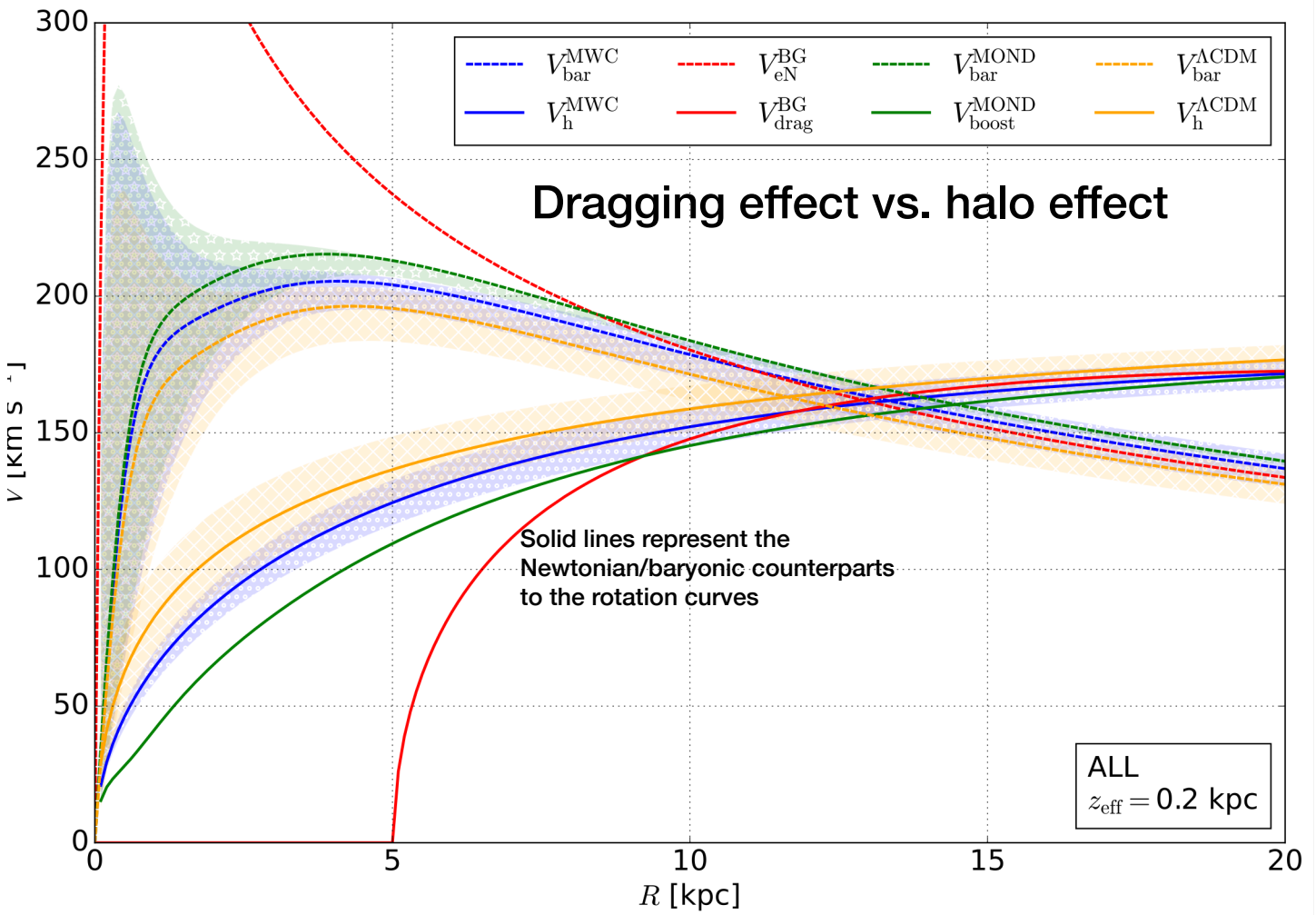

Non-Newtonian contributions to the rotation curve are consistent with that of the dark matter halo: they become predominant over the classical baryonic counterpart from 10-15 kpc outwards and, at the Sun distance, they are responsible for the 30-37% of the velocity profile.

The relativistic dragging effect has no newtonian counterpart, thus we compared:

(i) the MWC baryonic-only contribution with the effective Newtonian profile (Binney & Tremaine 1988) calculated by using the BG density: $\nabla^2\Phi_{eN} = 4\pi G\rho_{BG}$

(ii) the MWC dark matter-only contribution (halo) with the "dragging curve" traced by subtracting *effective Newtonian profile* to V_{BG} .

$$\sum_{i=1}^{N} \frac{[V_{bar}^{MWC}(r_i) - V_{eN}^{BG}(r_i; z_k)]^2}{N} \quad |z_k| < r_0$$

$$\longrightarrow \quad |z_{eff}| = 0.20\ kpc = r_{in}$$

$$(V_{drag}^{BG}(R_i; |z|_{eff}|) = \sqrt{(V^{BG}(R))^2 - (V_{eN}^{BG}(R; |z|_{eff}))^2}$$

$$V_{\rm drag}^{\rm BG} = \sqrt{V_{\rm BG}^2 - V_{\rm eN}^2}$$

amount of rotational velocity across the MW plane due to gravitational dragging

$$V_{\rm boost}^{\rm MOND} = \sqrt{V_{\rm MOND}^2 - V_{\rm bar}^2} = V_{\rm bar}\sqrt{\eta(R, V_{\rm bar}) - 1}$$

pure Mondian boost

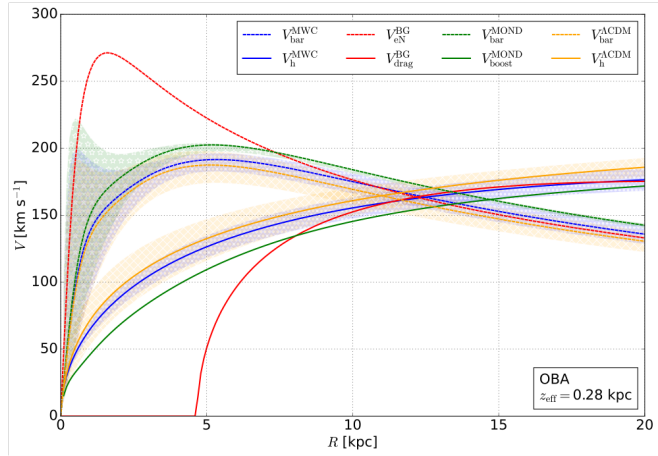
$V_{\rm bar}^{\rm MWC}$ $V_{\rm eN}^{\rm BG}$ $V_{\rm bar}^{\rm MOND}$ $V_{\rm bar}^{\rm ACDM}$
$V_{\rm h}^{\rm MWC}$ $V_{\rm drag}^{\rm BG}$ $V_{\rm boost}^{\rm MOND}$ $V_{\rm h}^{\rm ACDM}$
OBA
$z_{\rm eff} = 0.28$ kpc
V [km s^{-1}]
R [kpc]

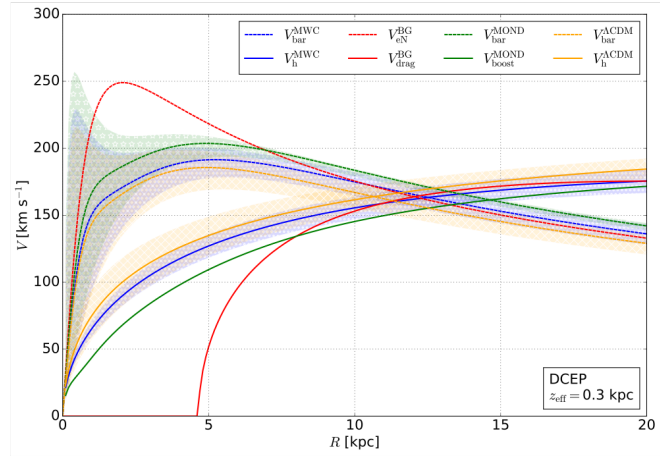
$V_{\rm bar}^{\rm MWC}$ $V_{\rm eN}^{\rm BG}$ $V_{\rm bar}^{\rm MOND}$ $V_{\rm bar}^{\rm ACDM}$
$V_{\rm h}^{\rm MWC}$ $V_{\rm drag}^{\rm BG}$ $V_{\rm boost}^{\rm MOND}$ $V_{\rm h}^{\rm ACDM}$
DCEP
$z_{\rm eff} = 0.3$ kpc
V [km s^{-1}]
R [kpc]

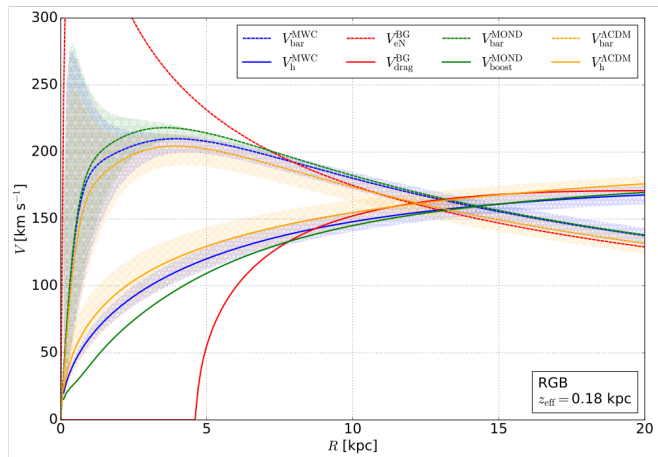
$V_{\rm bar}^{\rm MWC}$ $V_{\rm eN}^{\rm BG}$ $V_{\rm bar}^{\rm MOND}$ $V_{\rm bar}^{\rm ACDM}$
$V_{\rm h}^{\rm MWC}$ $V_{\rm drag}^{\rm BG}$ $V_{\rm boost}^{\rm MOND}$ $V_{\rm h}^{\rm ACDM}$
RGB
$z_{\rm eff} = 0.18$ kpc
V [km s^{-1}]
R [kpc]

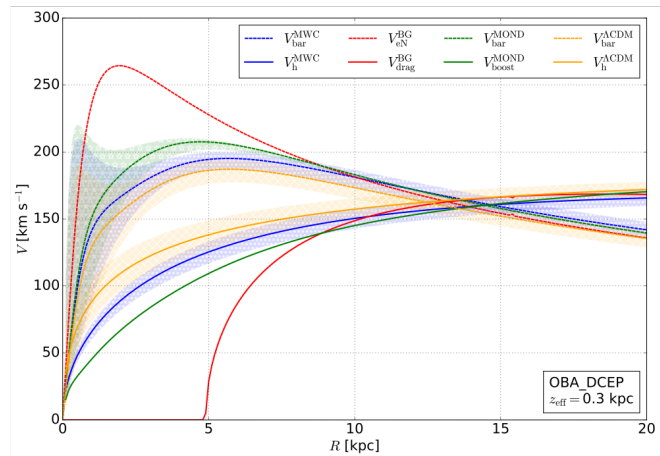
$V_{\rm bar}^{\rm MWC}$ $V_{\rm eN}^{\rm BG}$ $V_{\rm bar}^{\rm MOND}$ $V_{\rm bar}^{\rm ACDM}$
$V_{\rm h}^{\rm MWC}$ $V_{\rm drag}^{\rm BG}$ $V_{\rm boost}^{\rm MOND}$ $V_{\rm h}^{\rm ACDM}$
OBA_DCEP
$z_{\rm eff} = 0.3$ kpc
V [km s^{-1}]
R [kpc]

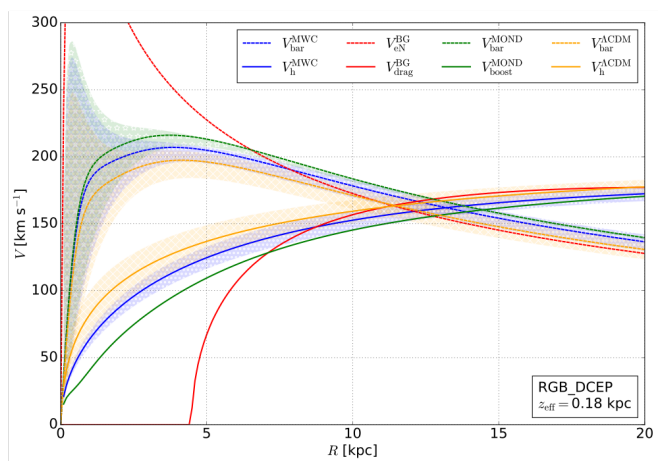
$V_{\rm bar}^{\rm MWC}$ $V_{\rm eN}^{\rm BG}$ $V_{\rm bar}^{\rm MOND}$ $V_{\rm bar}^{\rm ACDM}$
$V_{\rm h}^{\rm MWC}$ $V_{\rm drag}^{\rm BG}$ $V_{\rm boost}^{\rm MOND}$ $V_{\rm h}^{\rm ACDM}$
RGB_DCEP
$z_{\rm eff} = 0.18$ kpc
V [km s^{-1}]
R [kpc]

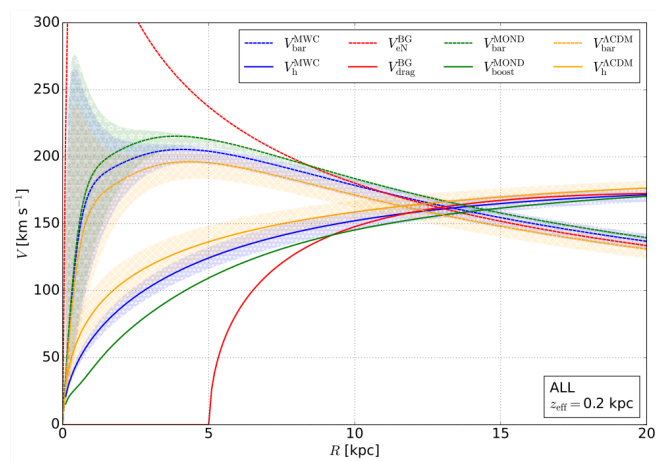
$V_{\rm bar}^{\rm MWC}$ $V_{\rm eN}^{\rm BG}$ $V_{\rm bar}^{\rm MOND}$ $V_{\rm bar}^{\rm ACDM}$
$V_{\rm h}^{\rm MWC}$ $V_{\rm drag}^{\rm BG}$ $V_{\rm boost}^{\rm MOND}$ $V_{\rm h}^{\rm ACDM}$
ALL
$z_{\rm eff} = 0.2$ kpc
V [km s^{-1}]
R [kpc]

MCMC fit to the Gaia DR3 data - Classical (MWC) MOND EINASTO GR

Best fit estimates as the median of the posteriors and their 1σ level credible interval

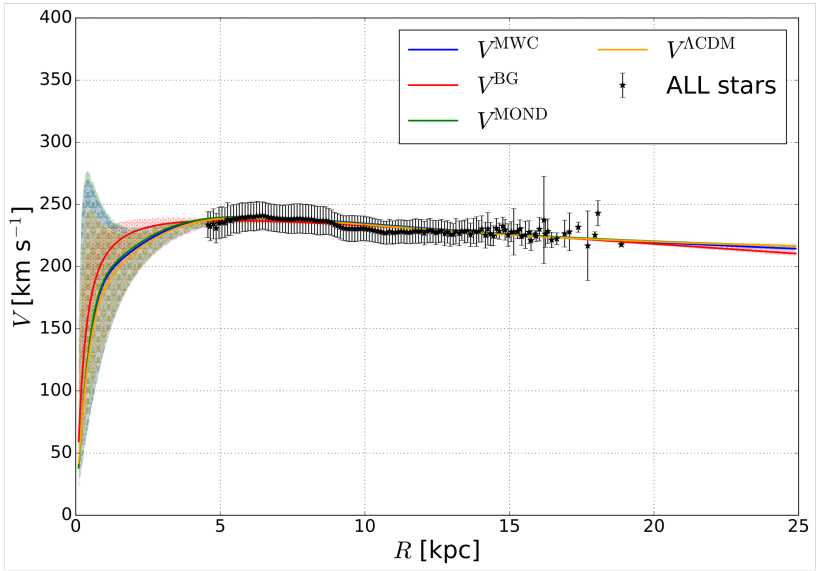

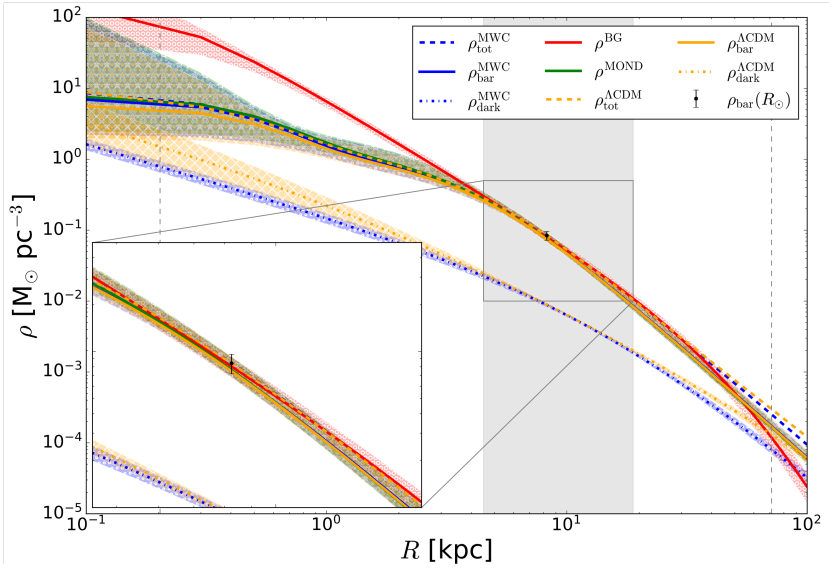

The four models are found to be statistically equivalent

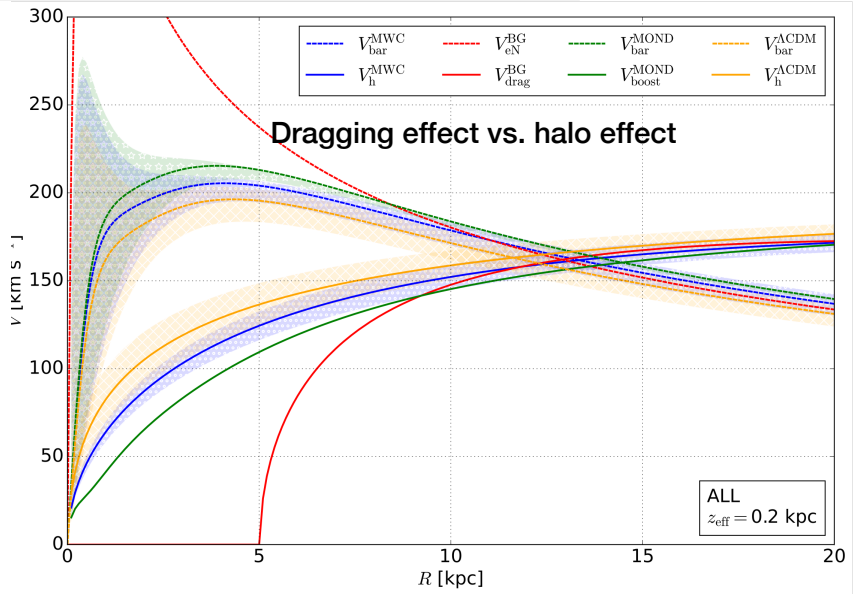

This again favourably points to the fact that a gravitational dragging-like effect could sustain a flat rotation curve

Crosta M., Giammaria M., Lattanzi M. G., Poggio E.,
On testing CDM and geometry-driven Milky Way rotation curve models with Gaia DR2, MNRAS, Volume 496, Issue 2, 2020

W.Beordo, M.Crosta, MG Lattanzi, P. Re Fiorentin, A. Spagna, 2024
Geometry-driven and dark-matter-sustained Milky Way rotation curves with Gaia DR3, MNRAS, 529, 4681

Exploring Milky Way rotation curves with Gaia DR3: a comparison between ΛCDM, MOND, and General Relativistic approaches, JCAP 2024

Talk outline

Background

- Motivation: Astrometry from Hipparcus to Einstein, Gaia
- Relativistic/Gravitational Astrometry

Challenging the Galactic Models with Milky Way stars

- Local cosmology as ΛDCM laboratory
- Testing General Relativity/Gravity @MilkyWay scale
- The Dark Matter interpretation in GR
- ΛCDM model predictions @MilkyWay scale

Wrap-up

Data are independent from the theoretical models that we use for the predictions and that is exactly why they constitute the testing ground.

For our likelihood analysis the three models appear almost identically consistent with the data

- GR model has only 4 parameters, the classical model needs at least 10 parameters +1 for MOND , +3 for Lambda CDM

DM: does not absorb or emit light but it exerts and responds only to the gravity force; it enters the calculation as extra mass (halo) required to justify the flat galactic rotational curves.

MOND requires an adjustment in the low acceleration regime

Einasto ΛCDM model results larger than the NFW one, dynamical mass supplied by more dark matter in the ΛCDM scenario compared to the case of an NFW halo without cosmological constraints

GR could imply a gravitational dragging "DM-like" effect driving the Galaxy velocity rotation curve, i.e. the geometry - unseen but perceived as manifestation of gravity according to Einstein's equation - is responsible of the flatness at large Galactic radii.

"space tells mass how to move"

Our interpretation with Gaia DR2/DR3 **depends only on the background geometry**

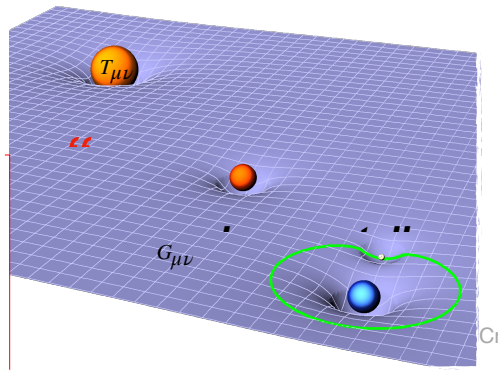

GR is the standard theory of gravity over 60 order of magnitudes

Hypotehsis non fingo&Occam's razor

By setting a coherent GR framework, we are pursuing to:

- ✓**Treat separately velocities and density with Einstein's equations [**contrary to what is done in classical models**]**
- ✓**Any modification of GR should be done with GR as background theory**
- ✓ **Any modification should recover what is already confirmed, cross-checked comparisons**
- ✓**Establish to what extent the MW structure is dictated by the standard theory of gravity [**avoiding replica of the common assumption that invalidate GR, i.e the GR effects are small in the linear approximation**] or, viceversa, why it should fail and requires Newtonian/alternative dynamics**
- ✓ **At Galactic scale MW dynamics can be dominated, e.g., by Weyl, Lewis-Papapetrou spacetimes, whereas the Newtonian approximation is valid locally (e.g in the Solar System, binaries, …)**

✓Extend the MW “geometries” to other galaxies:, the “geometries" of the Galaxy can play a reference role for other galaxies, just like the Sun for stellar models

MCMC fit to external Galaxies

Velocity profiles (SPARC data)

Classical (MWC) GR (BG)

Best fit estimates as the median of the posteriors and their 1σ level credible interval

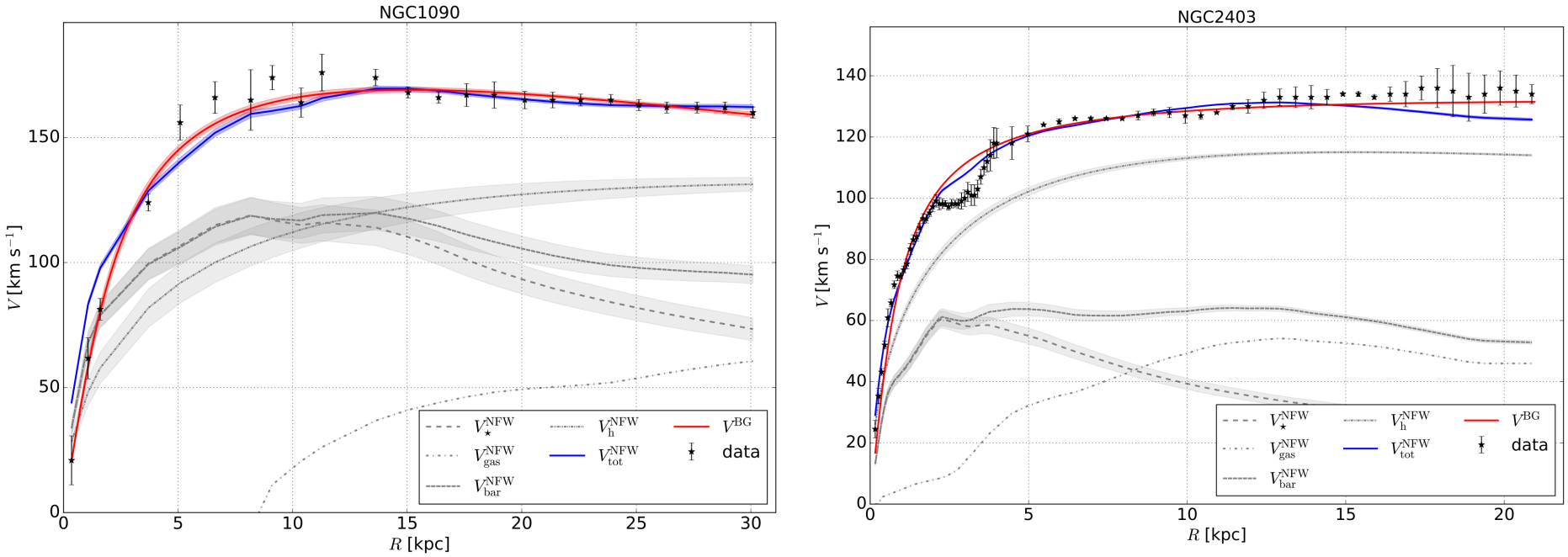

Crosta et al. in submission

Next developments

GR models offer the unique possibility of establishing a multi-laboratory for extensively testing gravity theories from Solar System to Milky Way and cosmological scales.

In view of the next Gaia data release (inside-out approach):

- Improve the GR models by including more realistic solutions, e.g. metric solutions to describe the structure and evolution of a multi-structured Galaxy and its local Universe
- Fix boundary matching conditions between internal/external Einstein's solutions [e.g. Mars and Senovilla "On the construction of global models describing rotating bodies; uniqueness of the exterior gravitational field" (gr-qc/9806094v1)]
- Using hydrodynamical simulation for the inner part, exploring semi-analytical solutions or Einstein-Vlasov system
- Adopt suitable gluing procedures [see J. Corvino 2025, S. Czimek and I. Rodnianski, 2022, P. T Chruściel and Wan Cong 2023, Aretakis S, Czimek S and Rodnianski I 2021]
- Explore more "geometrical" observables enabling to prove the Milky Way formation and evolution
- Export the fine-tuned template of our Galaxy to other galaxies, check other effects (e.g. weak lensing) and set the limits
- Set comparisons at the scale of the Milky Way disc with the Lambda-CDM model predictions (outside-inside approach)

Talk outline

Background

- Motivation: Astrometry from Hipparcus to Einstein, Gaia
- Relativistic/Gravitational Astrometry

Challenging the Galactic Models with Milky Way stars

- Local cosmology as ΛDCM laboratory
- Testing General Relativity/Gravity @MilkyWay scale
- Dark Matter interpretation in GR
- Simulations of CDM model predictions @MilkyWay scale

Formation History of the Milky Way disc

Giammaria, Spagna, Lattanzi, Murante, Re Fiorentin, and Valentini (2021) MNRAS, 502, 2, 2251–2265

(Cosmological) Initial conditions AqC4 (Spergel et al. 2008) and MUPPI (MUlti Phase Particle Integrator, sub-resolution model of star formation and feedback) implementation as in Giammaria et al (2021), following Murante et al. (2015).

Select a cube of the cosmological volume of side 200-300 Mpc. MUPPI is then applied to a $(10\ \mathrm{Mpc})^3$ where stellar production and evolution is followed.

At z=0, our AqC4 corresponds in (virial mass), ~1.6 x 10^{12} $M_\odot$, and size (virial radius), ~237 Kpc, to current estimates of the size of the MW. In particular, virial mass values ~ 1-1.3 x 10^{12} $M_\odot$ were reported in Posti & Helmi (2019) and Watkins et al. 2019) using dynamics of globular clusters, and in Eilers et al. (2019) and Crosta et al. (2020) utilizing observed galactic rotation curves.

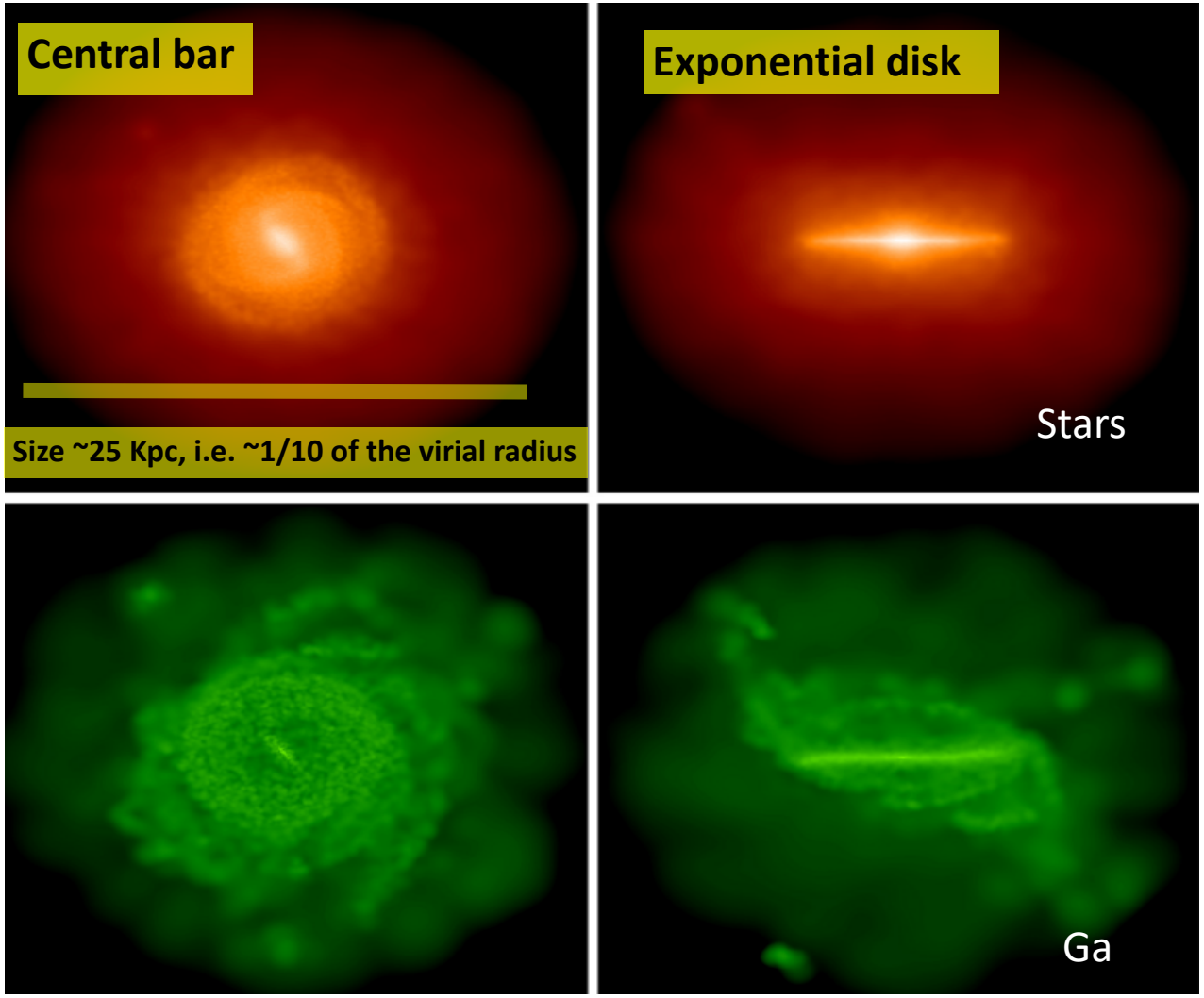

Figure 1. Stellar (upper panels) and gas (lower panels) projected density for the AqC4 simulation (face-on and edge-on view on left- and right-hand panels, respectively). The Z-axis of the coordinate system is aligned with the angular momentum vector of multiphase gas and stars enclosed within 8 kpc from the position of the minimum of the gravitational potential. The total box size is 50 kpc.

(Giammaria et 2021)

Table 1. Cosmological hydrodynamical simulations of MW-like disc galaxies. Main properties of recent high resolution zoom-in simulations.

Project	Mass particle ($M_\odot$)	Softening (pc)	Reference
Eris	$M_{\rm DM} \sim 1 \times 10^5$	$\epsilon_* \sim 120$	Guedes et al. (2011)
	$M_{\rm gas} \sim 2 \times 10^4$	$\epsilon_{\rm gas} \sim 120$	–
Auriga	$M_{\rm DM} \sim 3 \times 10^5$	$\epsilon_* \sim 369$	Grand et al. (2017)
	$M_{\rm gas} \sim 5 \times 10^4$	–	–
GIZMO	$M_{\rm DM} \sim 3 \times 10^5$	$\epsilon_* \sim 50$	Ma et al. (2017)
	$M_{\rm gas} \sim 6 \times 10^4$	$\epsilon_{\rm gas} \sim 14$	–
Illustris	$M_{\rm DM} \sim 7 \times 10^6$	$\epsilon_* \sim 740$	Nelson et al. (2018)
(TNG100)	$M_{\rm gas} \sim 1 \times 10^6$	$\epsilon_{\rm gas} \gtrsim 185$	–
EAGLE	$M_{\rm DM} \sim 1 \times 10^6$	–	Mackereth et al. (2019)
	$M_{\rm gas} \sim 2 \times 10^5$	$\epsilon_{\rm gas} \lesssim 350$	–
NIHAO-UHD	$M_{\rm DM} \sim 1 \times 10^5$	$\epsilon_* \sim 273$	Buck et al. (2020)
(g7.08e11)	$M_{\rm gas} \sim 2 \times 10^4$	$\epsilon_{\rm gas} \sim 273$	–
AqC4	$M_{\rm DM} \sim 4 \times 10^5$	$\epsilon_* \sim 223$	Giammaria et al (2021)
	$M_{\rm gas} \sim 7 \times 10^4$	$\epsilon_{\rm gas} \sim 223$	–

Gravitomagnetism on galaxy scales

Beordo, Bruni, Barrera-Hinojosa, Crosta in submission
W. Beordo, PhD thesis

On large scales, the universe is typically described using the Friedmann-Lemaître-Robertson-Walker metric, with small perturbations treated within the framework of cosmological perturbation theory. On smaller, highly non-linear scales, the standard approach involves Newtonian N-body simulations, which provide a robust description of gravitational clustering and accurately capture many aspects of non-linear structure formation

- Post-Friedmann approach: expansion of the FLRW metric in terms of c^{-1} in Poisson gauge.

$$g_{00} = -\left[1 - \frac{2U_{\mathrm{N}}}{c^2} + \frac{1}{c^4}\left(2U_{\mathrm{N}}^2 - 4U_{\mathrm{P}}\right)\right] + O\left(\frac{1}{c^6}\right) ,$$

$$g_{0i} = -\frac{a}{c^3}B_i^{\mathrm{N}} - \frac{a}{c^5}B_i^{P} + O\left(\frac{1}{c^7}\right) ,$$

$$g_{ij} = a^2\left[\left(1 + \frac{2V_{\mathrm{N}}}{c^2} + \frac{1}{c^4}\left(2V_{\mathrm{N}}^2 + 4V_{\mathrm{P}}\right)\right)\delta_{ij} + \frac{1}{c^4}h_{ij}\right] + O\left(\frac{1}{c^6}\right)$$

- At leading order, Newtonian dynamics is recovered, but an additional equation arises for the **gravitomagnetic vector potential** (or frame-dragging potential).

$$\nabla \times \nabla^2 \mathbf{B}^N = -(16\pi G\bar{\rho}a^2)\nabla \times [(1+\delta)\mathbf{v}].$$

- If set to zero, it would correspond to an extra constraint on the Newtonian dynamics.
- It is the cosmological manifestation of the ubiquitous relativistic effect of frame dragging.
- It doesn't influence matter dynamics at leading order: density and velocity fields can be extracted from Newtonian simulations.

→ Cosmological scales: Bruni et al. 2014; Thomas et al. 2015.

→ **Galaxy scales: Illustris-TNG suites**
In collaboration with ***Marco Bruni***, Institute of Cosmology and Gravitation, Portsmouth (UK) and ***Cristian Barrera-Hinojosa***.

- **Delaunay Tessellation Field Estimator** to accurately reconstruct density and velocity fields (and their gradients) on a grid from particle data.

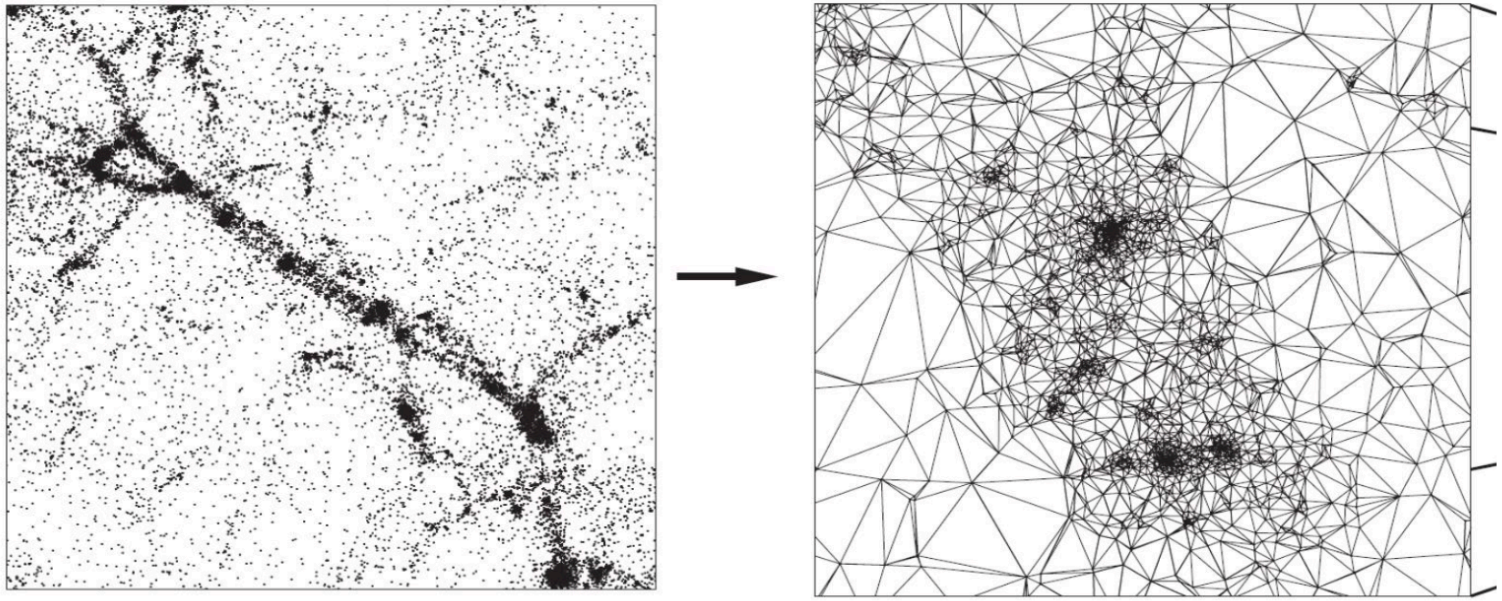

© Cautun et al. 2011

Partitions of the simulation domain into a unique tessellation of tetrahedra, whose vertices are defined by the particle positions

The field is linearly interpolated in n points inside the tetrahedron in which the grid point is located and the value in this point is computed as the volume-weighted average of the field inside the tetrahedron

$$\nabla \times \nabla^2 \mathbf{B}^N = -(16\pi G\bar{\rho}a^2)\nabla \times [(1+\delta)\mathbf{v}]. \qquad \nabla \cdot \mathbf{B} = 0$$

- Power spectra:

$$P_{\mathbf{B}^N}(k) = \left(\frac{16\pi G a^2 \bar{\rho}}{k^3}\right)^2 P_{\nabla\times[(1+\delta)\mathbf{v}]}(k) \quad \text{with} \quad \langle \tilde{\mathbf{v}}(\mathbf{k}) \cdot \tilde{\mathbf{v}}^*(\mathbf{k}')\rangle = (2\pi)^3 \delta^3(\mathbf{k}-\mathbf{k}') P_{\mathbf{v}}(k).$$

- Global solution via Fast-Fourier-Transforms:

$$\widetilde{B_x}(\mathbf{k}) = \frac{16\pi G a^2 \bar{\rho}}{k^4}\left[k_y^2 \widetilde{p_x} - k_x k_y \widetilde{p_y} + k_z(k_z \widetilde{p_x} - k_x \widetilde{p_z})\right],$$

$$\widetilde{B_y}(\mathbf{k}) = \frac{16\pi G a^2 \bar{\rho}}{k^4}\left[k_x^2 \widetilde{p_y} - k_x k_y \widetilde{p_x} + k_z(k_z \widetilde{p_y} - k_y \widetilde{p_z})\right],$$

$$\widetilde{B_z}(\mathbf{k}) = \frac{16\pi G a^2 \bar{\rho}}{k^4}\left[(k_x^2 + k_y^2)\widetilde{p_z} + k_z(k_x \widetilde{p_x} + k_y \widetilde{p_y})\right].$$

Beordo et al. in submission
W. Beordo, PhD thesis

Matter density

Scalar potential

Vector potential

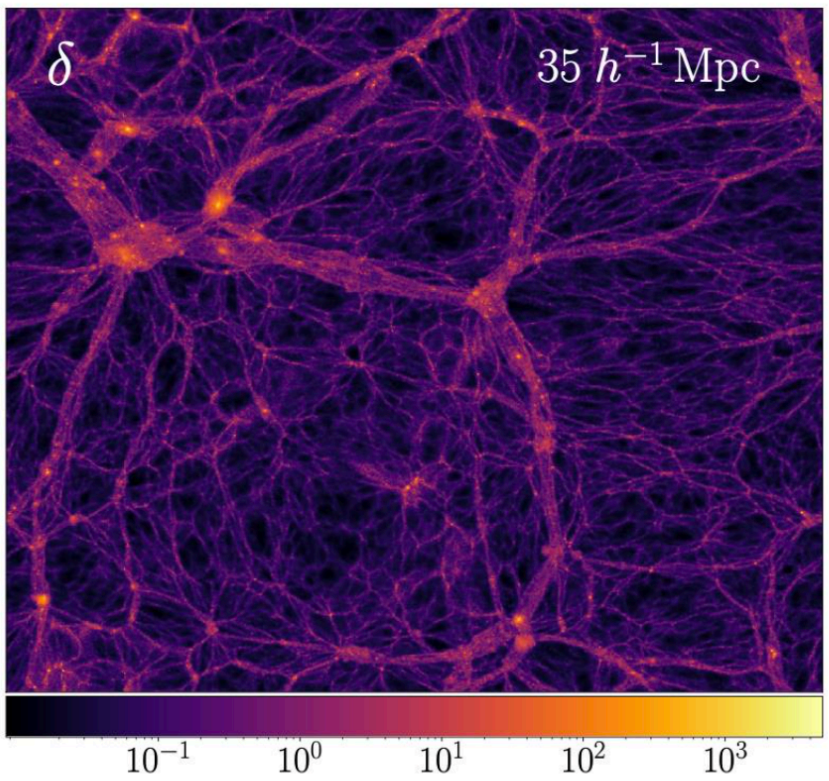

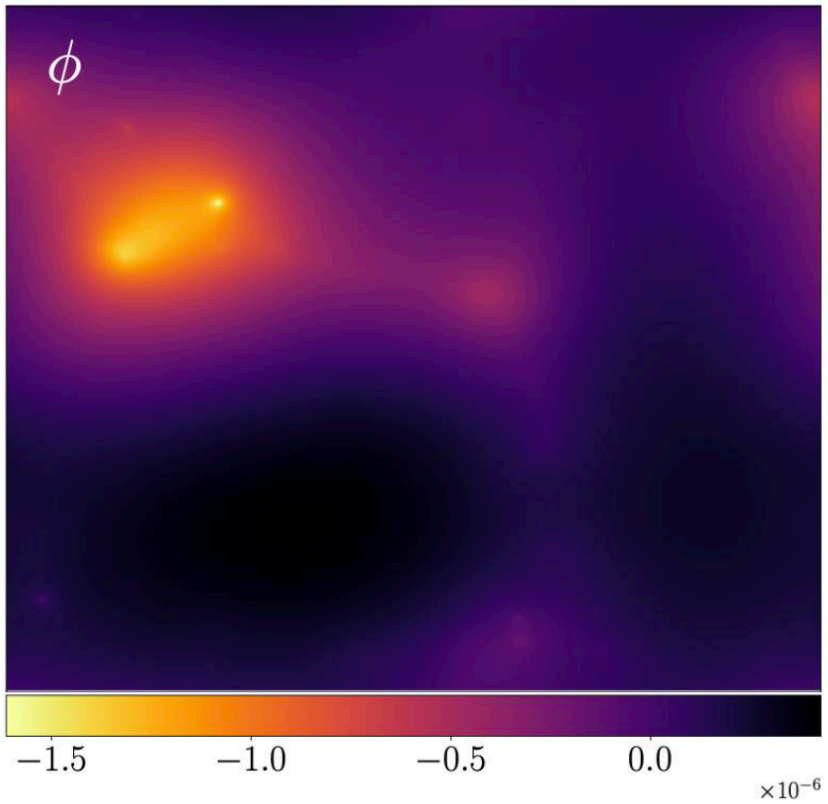

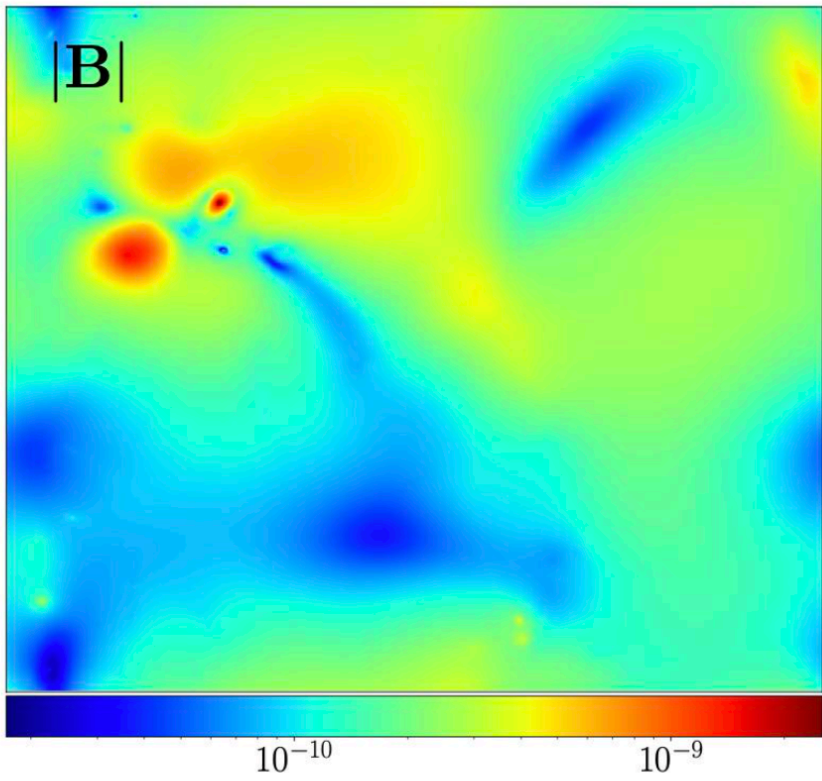

Beordo et al. in submission
W. Beordo, PhD thesis

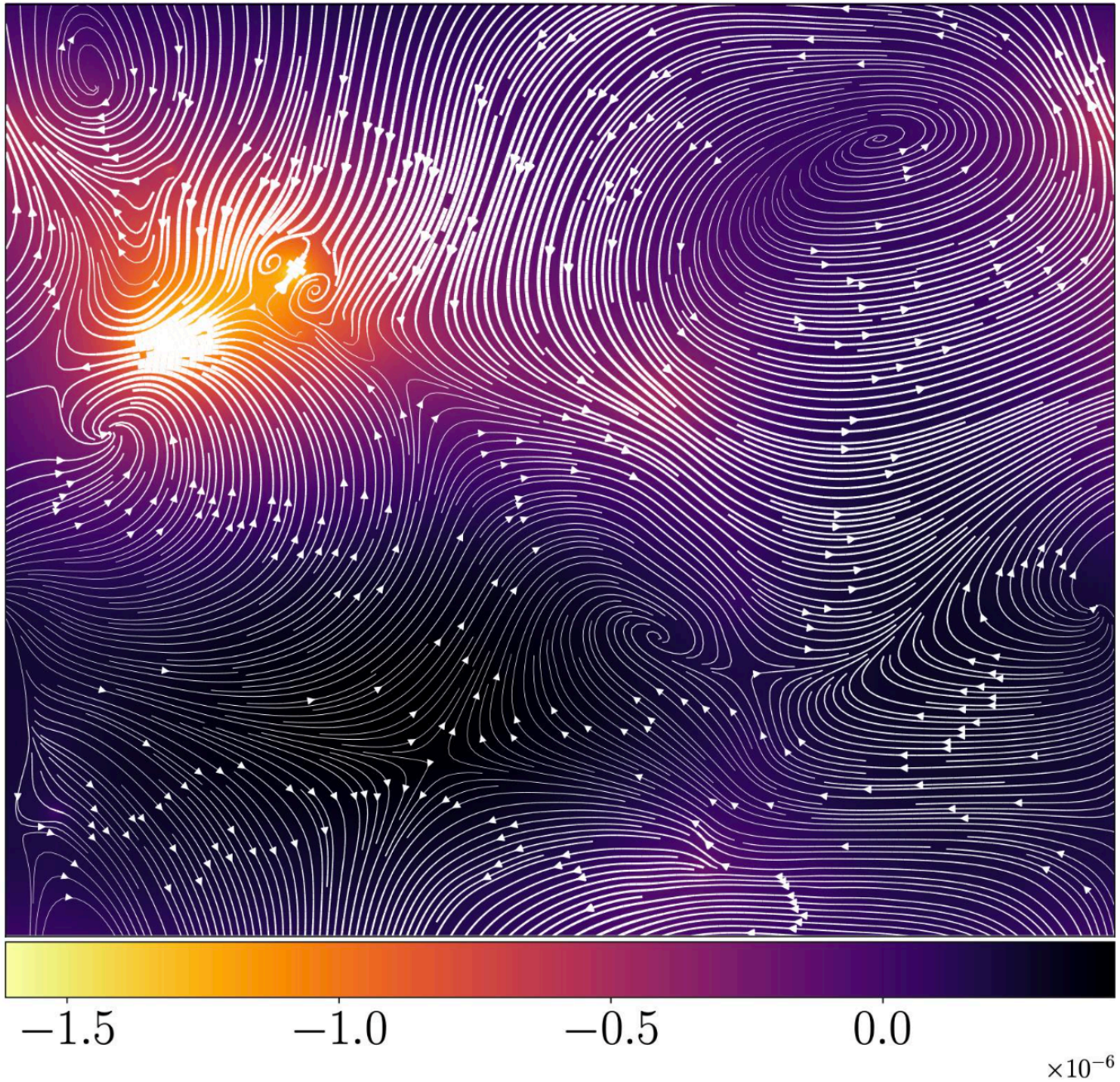

Representation of the stream lines of the vector potential, on top of the scalar potential distribution; streamlines with higher thickness represent regions where the magnitude of the vector potential is larger.

Beordo et al. in submission
W. Beordo, PhD thesis

TIME EVOLUTION

vector potential power spectrum

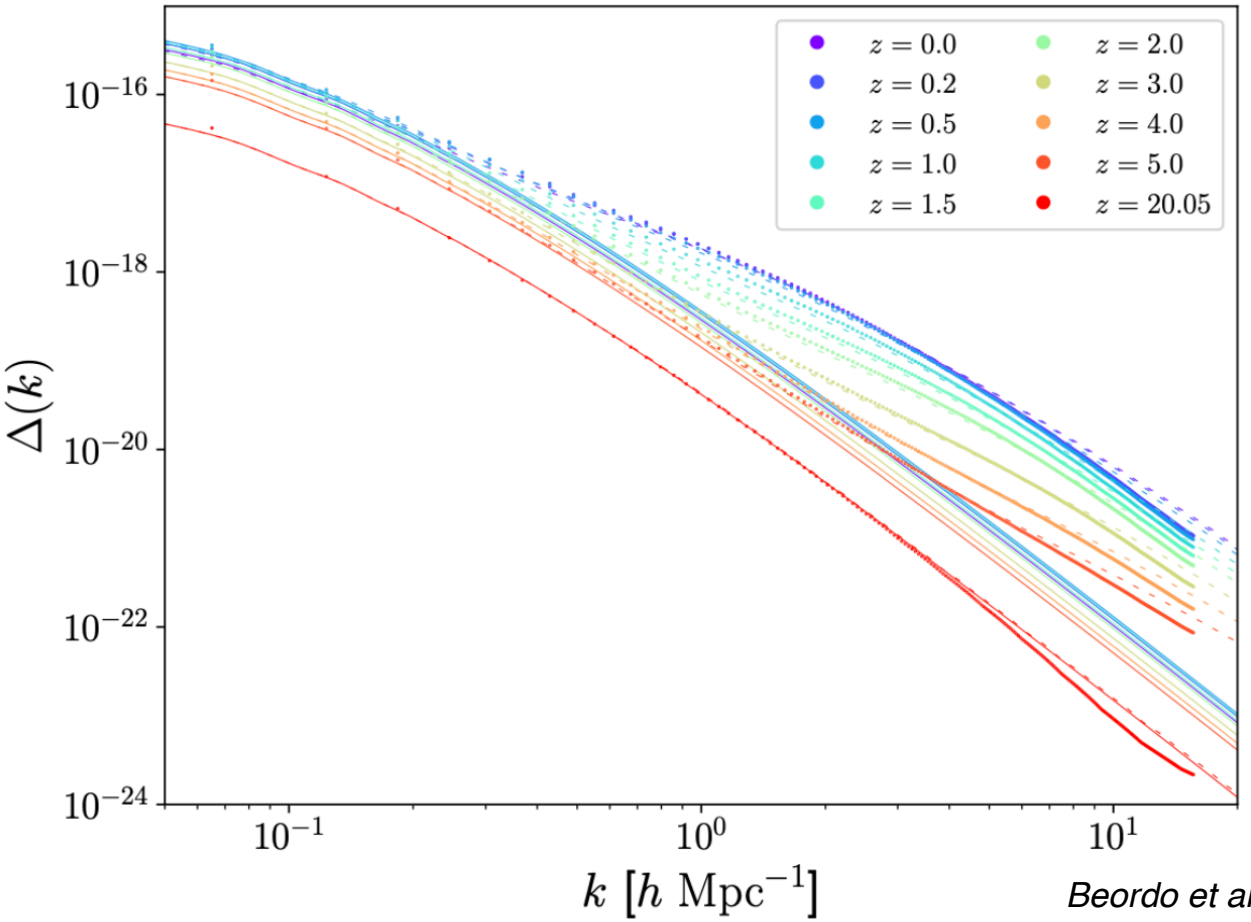

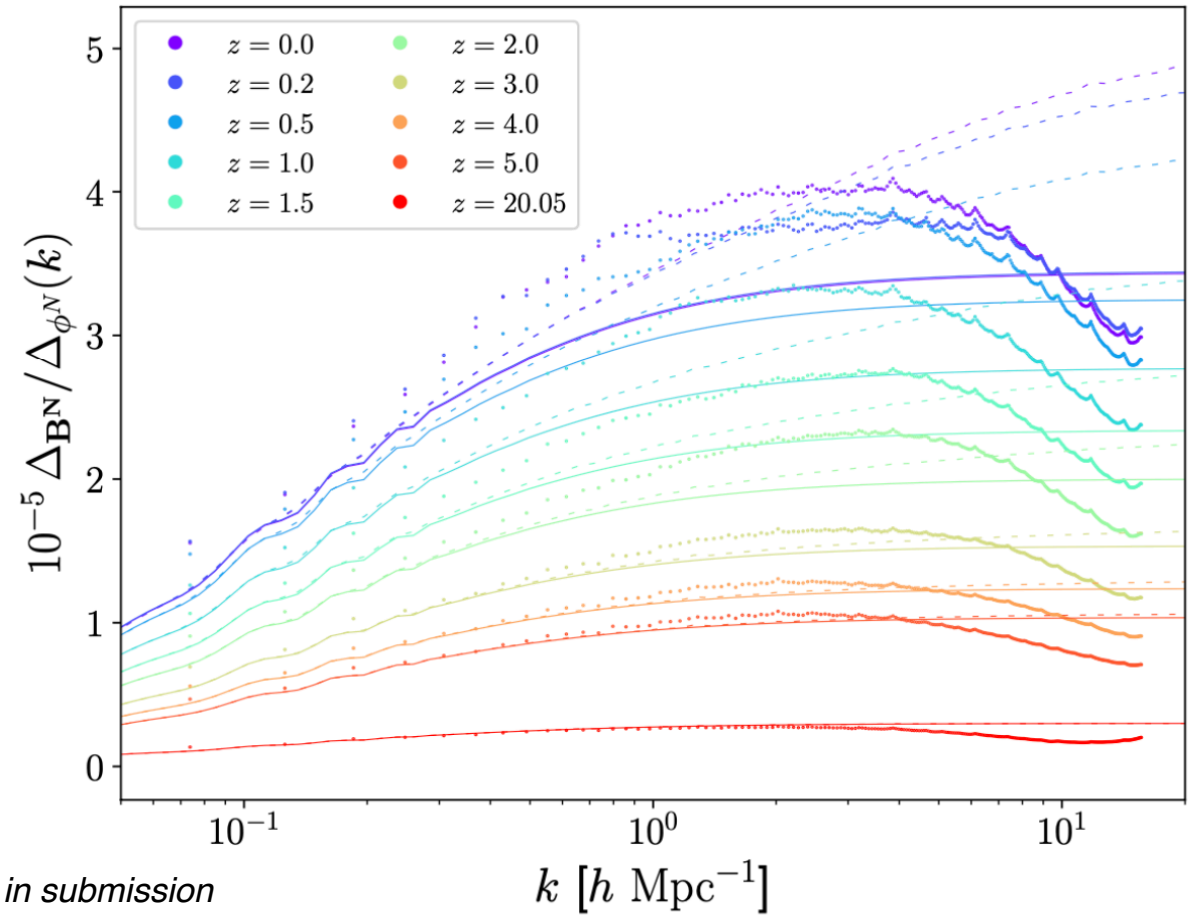

Beordo et al. in submission
W. Beordo, PhD thesis

TIME EVOLUTION

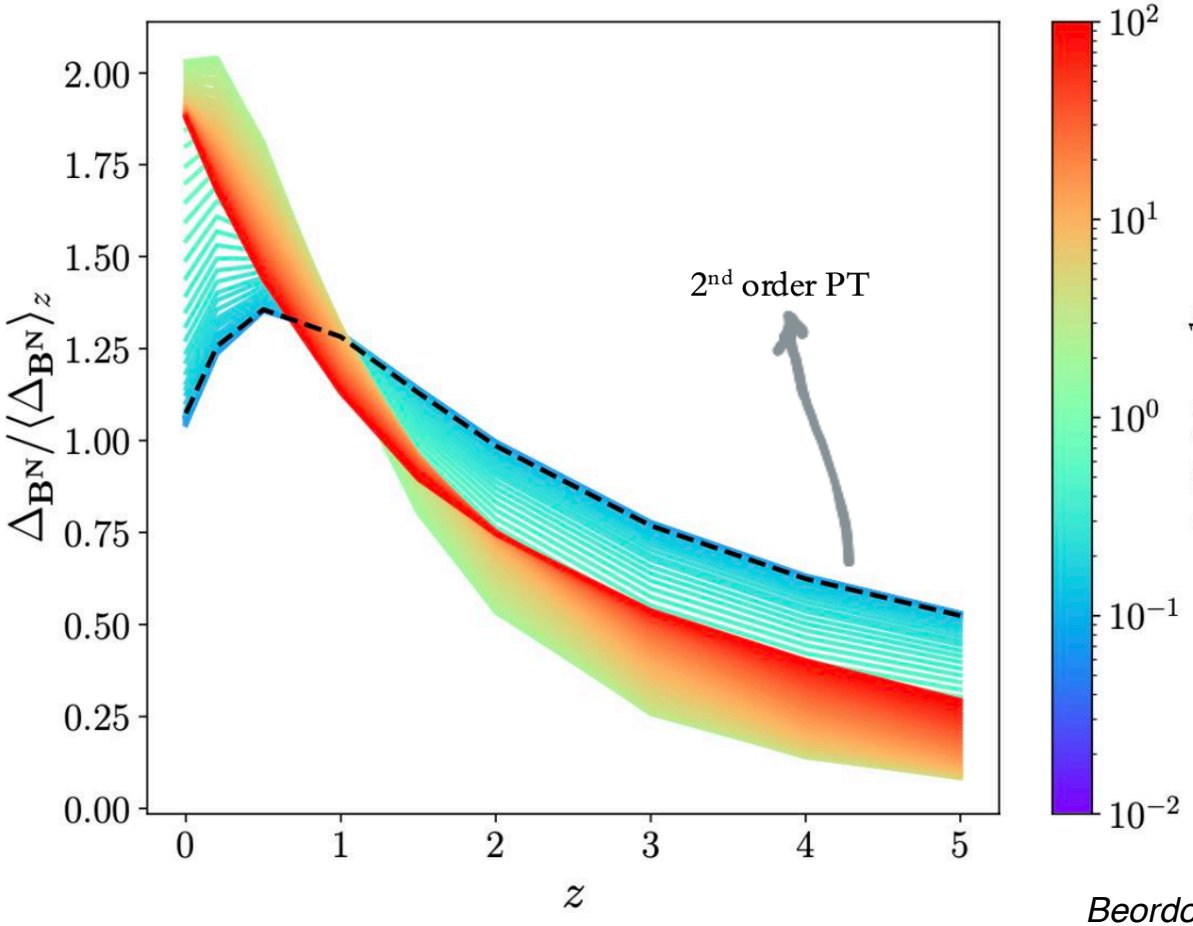

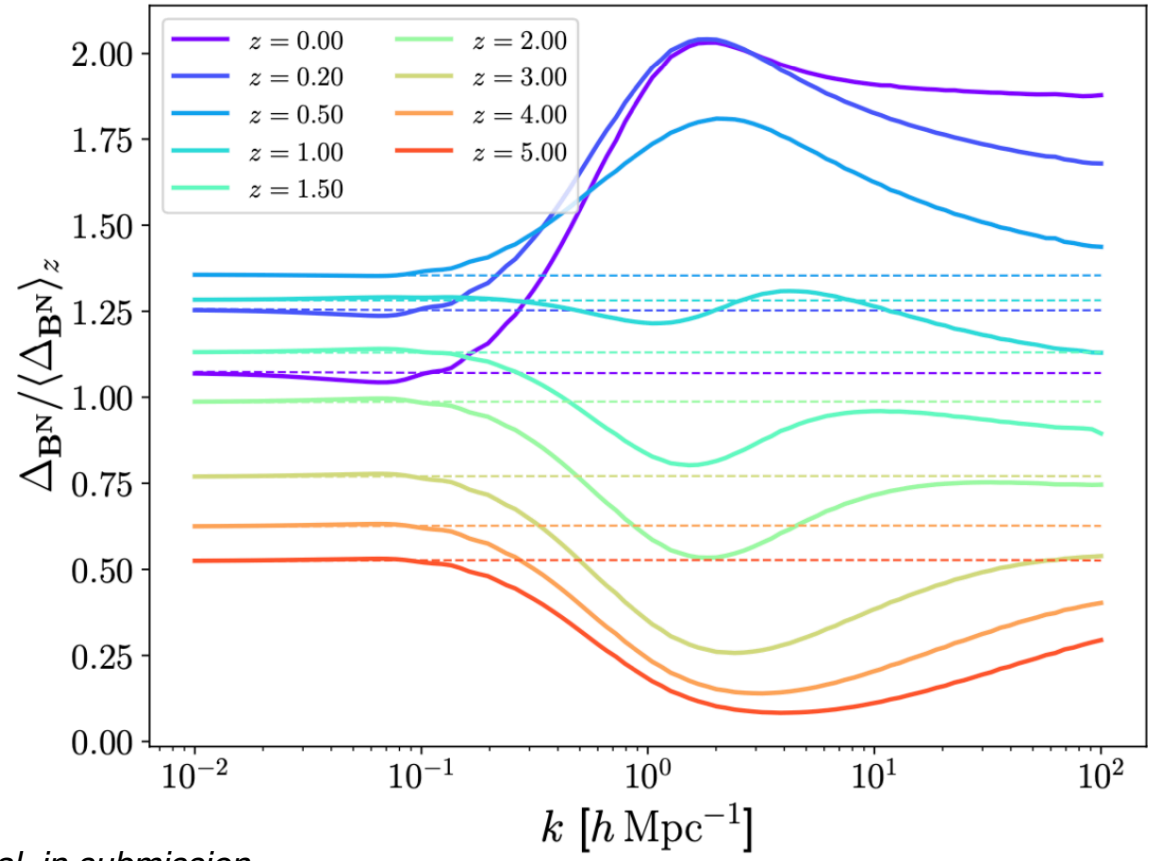

Beordo et al. in submission
W. Beordo, PhD thesis

Conclusions, the Gaia Legacy and its legacy science

- The mandatory use of GR for astrometry in space has opened new possibilities and strategies to apply Einstein's Theory in classical astronomy domain, providing new coherent methods and "laboratories" to exploit at best the standard theory of gravity and the LDCM scenario, i.e. any modification/extension of GR is done with GR as background theory

- Gravitational Astronomy in this capacity is part of Fundamental Physics and an essential tool for building up a spacetime map of our Universe

- Any GR tests performed by using Gaia @SS or @MW scale can play a reference role for other tests, much like the Sun for the stars, the Earth/ Jupiter for exoplanets, our Galaxy for other galaxies, and so on..

- For the first time, there was quantitative evidence of the differences between the Newtonian and GR approaches to MW dynamics pushing towards more mathematical solutions of Einstein's equations. Working out such solutions will imply to analyse the exchange of energy-momentum between matter and gravitational fields, including the role of the rotational energy, and to what extent it shaped the formation and evolution of our present Galaxy.

From Relativistic astrometry

the "ether" was cured by a new kinematics (i.e. special relativity) instead of "new" dynamic as inspired by the FitzGerald-Lorentz contraction phenomena ("extra molecular force")

"*We know that electric forces are affected by the motion of the electrified bodies relative to the ether and it seems a not improbable supposition that the molecular forces are affected by the motion and that the size of the body alters consequently.*" FitzGerald, Science, 1889

From Gravitational astrometry

"*One day, our actual knowledge of the composition of the fixed stars sky, the apparent motion of the fixed stars, and the position of the spectral lines as a function of the distance will probably have come far enough for us to be able to decide empirically the question whether or not Λ vanishes*" (Einstein, 1917, letter to de Sitter)